ASSESSMENT OF RELATIVE IMPORTANCE OF TOWER AND GROUND MODELS IN INSULATION CO-ORDINATION STUDIES

by

LUMINITA CURIAC

A Thesis

Submitted to the Faculty of Graduate Studies

in Partial Fulfillment of the Requirements

for Degree of

MASTER OF SCIENCE

Department of Electrical and Computer Engineering

The University of Manitoba

Winnipeg, Manitoba

June, 2007

THE UNIVERSITY OF MANITOBA

FACULTY OF GRADUATE STUDIES

*****

COPYRIGHT PERMISSION

ASSESSMENT OF RELATIVE IMPORTANCE OF TOWER AND GROUND MODELS IN INSULATION CO-ORDINATION STUDIES

BY

LUMINITA CURIAC

A Thesis/Practicum submitted to the Faculty of Graduate Studies of The University of Manitoba in partial fulfillment of the requirement of the degree

MASTER OF SCIENCE

Abstract

Accurate knowledge of the surge response of the transmission lightning-induced voltage magnitude and waveforms across the insulator strings in EHV Transmission lines is important in order to develop adequately protected transmission systems.

The main factors affecting this voltage are the tower and ground characteristics and their modelling. The aim of this thesis is to compare, by using PSCAD as a simulation tool, the effectiveness of different tower and ground models available in literature. The simulations have been applied to actual EHV tower geometries for which field gathered experimental data is available. Based on a comparison of simulated and experimental results a tower model which best mirrors experimental data has been selected and used to examine the effect of ground resistance. Furthermore a detailed ground model has also been considered. By combining the two models, the relative importance of tower and ground models in the calculation of lightning-induced voltage has been assessed.

Acknowledgments

I want to express my gratitude to my advisor, Dr. M. R. Raghuveer for his guidance and moral support throughout this research. I would like also to thank Dr. I.M.R. Ciric and Dr. S. Balakrishnan for serving on the committee.

Table of Contents

Abstract ii

Acknowledgments iii

Table of Contents iv

List of Figures vii

List of Tables xiv

Chapter 1 Introduction and Motivation 1

1.1 The Back-flashover phenomenon 1

1.2 Methodology 3

1.3 Outline of Thesis 5

Chapter 2 Tower and Ground Models in Transmission Lines Lightning Surge Analysis 7

2.1 Review of Tower Models 8

2.1.1 Breuer Model 8

2.1.2 Kawai Model 10

2.1.3 Sargent and Darveniza Model 11

2.1.4 Chisholm Model 14

2.1.5 Ishii Model 15

2.1.6 Hara Model 18

2.2 Review of Ground Models 22

Chapter 3 Investigation of different tower models with EMTDC Simulation 28

3.1 Investigation of a stand alone transmission tower response to double exponential surge waveform 29

3.1.1 Conical Model (Sargent and Darveniza Model) 30

3.1.2 Multi Storey Model (Ishii Model) 32

3.1.3 Distributed Constant Line Model (Hara model) 35

3.1.4 Simulation results 37

3.2 EMTDC simulation of a 'live laboratory' experiments conducted by Matsumoto and Motoyama, using different tower models 43

3.2.1 Stand alone transmission tower equipped with infinite overhead ground wire 44

3.2.2 Three transmission towers equipped with overhead ground wires and phase conductors 51

3.2.2.1 System response to a piecewise linear surge waveform 52

3.2.2.2 System response to a double exponential surge waveform 58

Chapter 4 Investigation of the dynamic model of ground 63

4.1 Algorithm description 63

4.2 Computation results 65

Chapter 5 Effect of combining the tower and ground models 73

5.1 Case 1: Stand alone transmission tower equipped with infinitely extending overhead ground wire and variable / constant ground resistance 74

5.2 Case 2: Three transmission towers equipped with overhead ground wires and phase conductors and variable / constant ground resistance 82

Chapter 6 Effect of different surge waveshapes on combined model 91

Chapter 7 Conclusions 106

References 110

APPENDIX A Derivation of impedance formula for Conical model of transmission tower proposed by Sargent and Darveniza 113

APPENDIX B Calculation of damping impedance for the multi-storey transmission tower model proposed by Ishii 118

APPENDIX C Derivation of equivalent radius formula for n parallel conductors 120

APPENDIX D Impulse surge current generation 123

APPENDIX E Simulation results of the field experiment presented by Hara in [5]....125

APPENDIX F The equivalent circuit for a transmission tower with two neighbouring towers equipped with phase and overhead ground wires 127

List of Figures

Fig. 1-1 Description of back-flashover phenomenon 2

Fig. 2-1 Measurement setup for Breuer's tests 8

Fig. 2-2 Measurement setup for Kawai's tests 10

Fig. 2-3 Simplified geometrical model 11

Fig. 2-4 Multi storey transmission tower model 17

Fig. 2-5 Schematic diagram of the transmission tower 20

Fig. 2-6 Equivalent line model of a transmission tower 20

Fig. 2-7 The approximate cylinder-hemispherical shape of the medium surrounding the ground rod with a buried length l and radius r_0, subjected to a surge current . 23

Fig. 3-1 Transmission Tower dimensions 29

Fig. 3-2 Conical approximation of a double circuit transmission tower 30

Fig. 3-3 The equivalent circuit for Conical Model in PSCad simulation 31

Fig. 3-4 The equivalent circuit for Multi Storey Model in PSCad simulation 32

Fig. 3-5 One of the four sections of the tower 33

Fig. 3-6 The equivalent circuit of Distributed Constant Line Model in PSCad simulation 35

Fig. 3-7 One of the four sections of the tower 36

Fig. 3-8. Location of the measurement points on the transmission tower, corresponding to each tower model. 38

Fig. 3-9 The response of the transmission tower to a 1.5/51.75 μsec, 50 kA impulse current, R_g=20Ω.. 39

Fig. 3-10 The response of the transmission tower to a 1.5/51.75 μsec, 50 kA impulse current, R_g=0Ω.. 40

Fig. 3-11 The response of the transmission tower to a 8/20 μsec, 50 kA impulse current, R_g=20Ω.. 41

Fig. 3-12 The response of the transmission tower to a 1.5/51.75 μsec, 50 kA impulse current, R_g=0Ω.. 42

Fig. 3-13 The equivalent circuit for Multi Storey Model in PSCad simulation, transmission tower equipped with infinite ground wires (60 km) 45

Fig. 3-14 The equivalent circuit for Distributed Constant Line Model in PSCad simulation, transmission tower equipped with infinite ground wires (60 km) 48

Fig. 3-15 The response of the transmission tower equipped with an infinite ground wire to a piecewise linear surge waveform, R_g=5Ω..... 50

Fig. 3-16 The equivalent circuit for transmission tower with two neighbouring towers, equipped with ground wires and phase conductors, subjected to a piecewise linear surge waveform in PSCad simulation..... 53

Fig. 3-17 The response of the transmission tower with two neighbouring towers equipped with ground wire and phase conductors to a piecewise linear surge waveform 57

Fig. 3-18 The response of the transmission tower with two neighbouring towers equipped with ground wire and phase conductors to a 1.5/51.75 μsec, 50 kA surge waveform..... 60

Fig. 3-19 The response of the transmission tower with two neighbouring towers equipped with ground wire and phase conductors to a 8/20 μsec, 50 kA surge waveform 61

Fig. 4-1 The geometry of the region surrounding the ground electrode. 65

Fig. 4-2 Variation of ground voltage and resistance vs. time for a given current when the rod is embedded in clay having a resistivity of 8720 Ωcm. 67

Fig. 4-3 Variation of ground resistance vs. surge current for a rod embedded in clay having a resistivity of 8720 Ωcm. 68

Fig. 4-4 Variation of ground voltage and resistance vs. time for a given current when the rod is embedded in sand having a resistivity of 15700 Ωcm. 69

Fig. 4-5 Variation of ground resistance vs. surge current when the rod is embedded in sand having a resistivity of 15700 Ωcm. 70

Fig. 4-6 Variation of ground voltage and resistance vs. time for a given current when the rod is embedded in gravel and sand mix having a resistivity of 31000 Ωcm. 71

Fig. 4-7 Variation of ground resistance vs. surge current for a rod embedded in sand and gravel mix having a resistivity of 31000 Ωcm. 72

Fig. 5-1 Variation of ground resistance vs. current injected into clay having a resistivity of 8720 Ωcm, when the tower top is subjected to 18/37 μsec with 11 kA peak value (one tower configuration) 76

Fig. 5-2 The response of the transmission tower equipped with an infinite ground wire to a 18/37 μsec (11 kA) surge waveform, non-ionized ground resistivity =8720

Ωcm (clay), Rg=var / Rg = 17.99 Ω average value of the variable ground resistance ... 77

Fig. 5-3 Variation of ground resistance vs. current injected into sand having a resistivity of 15700 Ωcm, when the tower top is subjected to 16/40 μsec with 6.6 kA peak value (one tower configuration) 78

Fig. 5-4 The response of the transmission tower equipped with an infinite ground wire to a 16/40 μsec (6.6 kA) surge waveform, non-ionized ground resistivity =15700 Ωcm (sand), Rg=var / Rg = 52.5 Ω average value of the variable ground resistance 79

Fig. 5-5 Variation of ground resistance vs. current injected into gravel and sand having a resistivity of 31000 Ωcm, when the tower top is subjected to 20/60 μsec with 5.5 kA peak value (one tower configuration) 80

Fig. 5-6 The response of the transmission tower equipped with an infinite ground wire to a 20/60 μsec (5.5 kA) surge waveform, non-ionized ground resistivity =31000 Ωcm (gravel and sand), Rg=var / Rg = 63.42 Ω average value of the variable ground resistance 81

Fig. 5-7 Variation of ground resistance vs. current injected into clay having a resistivity of 8720 Ωcm, when the tower top is subjected to 18/37 μsec with 11 kA peak value (three tower configuration) 84

Fig. 5-8 The response of the transmission tower with two neighbouring towers equipped with ground wire and phase conductors to a 18/37 μsec (11 kA) surge waveform, non-ionized ground resistivity =8720 Ωcm (clay), Rg=var / Rg = 19.56 Ω average value of the variable ground resistance 85

Fig. 5-9 Variation of ground resistance vs. current injected into sand having a resistivity of 15700 Ωcm, when the tower top is subjected to 16/40 μsec with 6.6 kA peak value (three tower configuration) 86

Fig. 5-10 The response of the transmission tower with two neighbouring towers equipped with ground wire and phase conductors to a 16/40 μsec (6.6 kA) surge waveform, non-ionized ground resistivity =15700 Ωcm (sand), Rg=var / Rg = 56 Ω average value of the variable ground resistance 87

Fig. 5-11 Variation of ground resistance vs. current injected into gravel and sand having a resistivity of 31000 Ωcm, when the tower top is subjected to 20/60 μsec with 5.5 kA peak value (three tower configuration) 88

Fig. 5-12 The response of the transmission tower with two neighbouring towers equipped with ground wire and phase conductors to a 20/60 μsec (5.5 kA) surge waveform, non-ionized ground resistivity =31000 Ωcm (gravel and sand), R_g=var / R_g = 74.3 Ω average value of the variable ground resistance. 89

Fig. 6-1 Variation of ground resistance vs. current injected into clay having a resistivity of 8720 Ωcm, when the tower top is subjected to 1.5/51.75 μsec , 50 kA 93

Fig. 6-2 The response of the transmission tower with two neighbouring towers equipped with ground wire and phase conductors to a 1.5/51.75 μsec (50 kA) surge waveform, non-ionized ground resistivity =8720 Ωcm (clay), Rg=var / Rg = 16.9 Ω average value of the variable ground resistance 94

Fig. 6-3 Variation of ground resistance vs. current injected into sand having a resistivity of 15700 Ωcm, when the tower top is subjected to 1.5/51.75 μsec , 50 kA 95

Fig. 6-4 The response of the transmission tower with two neighbouring towers equipped with ground wire and phase conductors to a 1.5/51.75 μsec (50 kA) surge waveform, non-ionized ground resistivity =15700 Ωcm (sand), R_g=var / R_g = 44 Ω average value of the variable ground resistance 96

Fig. 6-5 Variation of ground resistance vs. current injected into sand and gravel having a resistivity of 31000 Ωcm, when the tower top is subjected to 1.5/51.75 μsec, 50 kA..... 97

Fig. 6-6 The response of the transmission tower with two neighbouring towers equipped with ground wire and phase conductors to a 1.5/51.75 μsec (50 kA) surge waveform, non-ionized ground resistivity =31000 Ωcm (gravel and sand), R_g=var / R_g = 68.5Ω average value of the variable ground resistance 98

Fig. 6-7 Variation of ground resistance vs. current injected into clay having a resistivity of 8720 Ωcm, when the tower top is subjected to 8/20 μsec , 50 kA 99

Fig. 6-8 The response of the transmission tower with two neighbouring towers equipped with ground wire and phase conductors to a 8/20 μsec (50 kA) surge waveform, non-ionized ground resistivity =8720 Ωcm (clay), R_g=var / R_g = 17.3 Ω average value of the variable ground resistance 100

Fig. 6-9 Variation of ground resistance vs. current injected into sand having a resistivity of 15700 Ωcm, when the tower top is subjected to 8/20 μsec , 50 kA 101

Fig. 6-10 The response of the transmission tower with two neighbouring towers equipped with ground wire and phase conductors to a 8/20 μsec (50 kA) surge waveform, non-ionized ground resistivity =15700 Ωcm (sand), R_g=var / R_g = 45.5 Ω average value of the variable ground resistance 102

Fig. 6-11 Variation of ground resistance vs. current injected into sand and gravel having a resistivity of 31000 Ωcm, when the tower top is subjected to 8/20 μsec, 50 kA 103

Fig. 6-12 The response of the transmission tower with two neighbouring towers equipped with ground wire and phase conductors to a 8/20 μsec (50 kA) surge waveform, non-ionized ground resistivity =31000 Ωcm (gravel and sand), R_g=var / R_g = 69 Ω average value of the variable ground resistance 104

Fig. A-1 Conical tower used in field theory analyses [9]..... 114

Fig. D-1 Standard impulse current waveform..... 123

Fig. E-1 The response of a transmission tower to a 0.15 kA impulse current, with 200nsec time to crest..... 126

Fig. F-1 The equivalent circuit for transmission tower with two neighbouring towers, equipped with a ground wire and phase wires..... 127

Fig. F-2 The four section components for Multi Storey model (Ishii model) transmission tower..... 128

Fig. F-3 The four section components for Distributed Constant Line model (Hara model) transmission tower..... 130

List of Tables

Table 3-1 Multi Storey Model parameters 34

Table 3-2 Distributed Constant Line Model parameters 36

Table 3-3 Coordinates characteristics for piece wise linear surge waveform 46

Table 3-4 Multi Storey Model parameters 47

Table 3-5 Distributed Constant Line Model parameters 49

Table 3-6 Multi Storey Model parameters 54

Table 3-7 Distributed Constant Line Model parameters 55

Table 4-1 Input parameters used in computation 66

TableD-1 The impulse current waveform characteristics.....124

CHAPTER 1

INTRODUCTION AND MOTIVATION

1.1 The Back-flashover phenomenon

Lightning is the main cause of outages as well as damage to electrical transmission and distribution systems. Lightning strokes that directly contact the phase conductors, overhead ground wires or transmission towers are of great concern. In a well designed line, direct strokes, i.e. strokes to the phase conductor should occur very rarely. When the stroke contacts the ground wire or the tower, the injected current that propagates through the tower and ground impedances produces an instantaneous rise of the tower voltage. This results in an overvoltage across the insulator string whose magnitude may exceed the flashover rating of the string resulting in a back-flashover, i.e. a flashover from the tower body to the phase conductor.

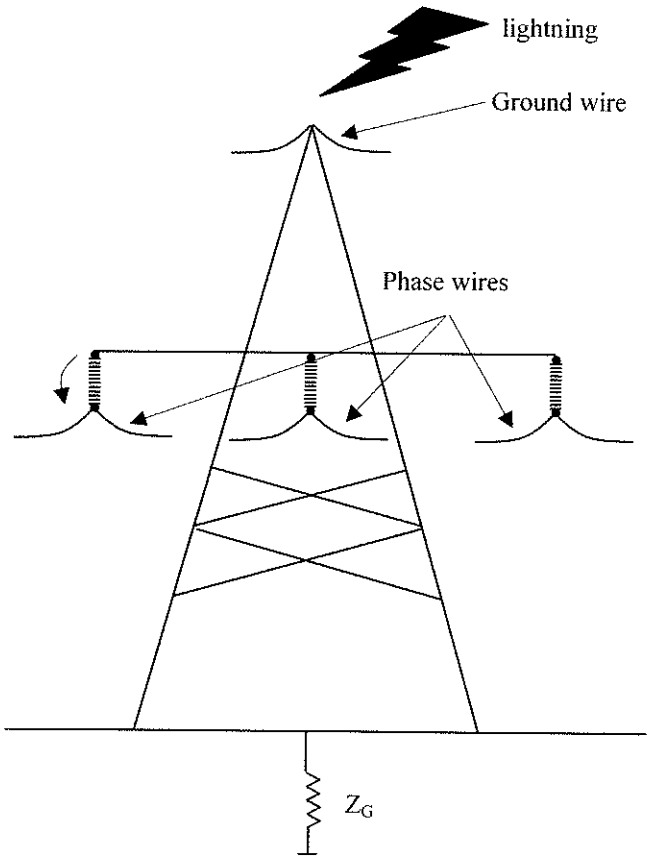

Fig. 1-1 Description of back-flashover phenomenon

An accurate prediction of the overvoltage is necessary for economical insulation co-ordination. Recognizing that the surge impedance values of the tower and ground are the main factors that influence the magnitude of this overvoltage, many researchers have considered the modeling of tower and ground separately. Early studies, based on experiments conducted on real and mock towers, showed that the tower impedance value varies with time [1], [2], [8]. Other researchers approximated the tower with a cone or an inverted cone and, based on measurements conducted on reduced-scale towers, found that the tower impedance has a constant value which is a function of the geometry of the tower [9]. Recent studies conducted on real towers lead to the

development of a tower model based on distributed parameters [6], [5]. All of these studies considered the ground resistance to be constant. No one has considered a model of ground based on the dynamic behaviour of soil resistance when it is contacted by a surge current due to the ionization process which has been proved to occur in early studies [12]. Also, no one has assessed the relative importance of modelling of tower and ground in back flash-over analysis. In this thesis, existing tower and ground models are first reviewed. Based on the review, a suitable tower and ground model has been selected and a general model which includes both tower and ground effects is presented to enable accurate prediction of overvoltages across insulator strings. A good simulation model is necessary because measurements on transmission towers are very tedious, expensive and impractical. This thesis will also examine the relative sensitivity of tower and ground models.

1.2 Methodology

Finding the most appropriate combination of the tower and ground models leads to a better determination of the magnitude and waveform of the back-flashover overvoltage. Therefore, the approach taken in this study is to investigate, at first, separately the tower and ground models found in literature, to determine which one represents more accurately the tower and ground respectively and finally to combine the selected models and to investigate the effect of the combined model of tower and ground on the back-flashover overvoltage.

Three tower models from literature are investigated by using the simulations applied to a tower which is completely geometrically described and for which

experimental data are available. The comparison between the tower models is done by injecting the tower top with the same surge current for each model and comparing the simulation results with the experimental ones reported in literature. The tower model which best mirrors the experimental data is selected. At the same time, the influence of the overhead ground wires, phase conductors, adjacent towers and ground is investigated. This is done by simulating the system in different configurations: a tower with an infinitely extending overhead ground wire and the ground resistance modelled as a constant, a tower with two neighbouring towers equipped with a ground wire and phase conductors and the ground resistance modelled as a constant but assigned different values. The systems are subjected to different types of surge current: fast and slow surge, and a piece wise linear surge current waveform that resembles a natural lightning current waveform employed in a field experiment described in literature.

The ground models found in literature are examined by simulating the dynamic behaviour of the ground when different types of soil are subjected to different types of surge current. The validity of the ground model is determined by comparing the simulation results with experimental data available.

Finally, the selected models of tower and ground are combined and the effect on the results is examined. In order to do this, the system used in the simulation has two different configurations as described above: a tower with an infinitely extending overhead wire, and a tower with two neighbouring towers equipped with a ground wire and phase conductors. For both system configurations, ground composed of three different types of soil with different non-ionized resistivities has been considered. The ground resistance has been modelled as a constant as well as being variable which

reflect its dynamic behaviour when injected with a current surge. The system is subjected to various types of slow surge currents and a fast surge current.

1.3 Outline of Thesis

In Chapter 2, a brief review of existing tower and ground models is presented. The tower models of Breuer (1958) [1], Kawai (1964) [8], Sargent and Darveniza (1969) [9], Chisolm (1983) [4], Ishii/Yamada (1991) [6], [11], Hara and Yamamoto (1996) [13] and ground models of Liew (1974) [12] and Almeida and Correia (1995) [18] are reviewed.

In Chapter 3, three tower models (the Conical, the Multi Storey and the Distributed Line Constant Model) are used in the simulation of two field experiments presented in literature. The first one is an experiment conducted by Hara on a stand alone transmission tower with neither overhead ground wires nor phase conductors; the tower is contacted by a double exponential surge current with an estimated maximum value of 0.15 kA and a 200 ns rise time. The second one is an experiment conducted by Matsumoto on an 275kV, unenergized, three phase, double circuit transmission line with three transmission towers, equipped with a ground wire and phase conductors having the center tower subjected to a piecewise linear surge waveform. The appropriate transmission tower model is selected by comparing the simulation results with the experimental ones. Also, the response of different system configurations to a fast surge current of 1.5/51.75 μse with 50 kA peak current and a slow surge current of 8/20 μse with 50 kA peak current is analyzed.

In Chapter 4, field experiments regarding the variation of resistance of different types of soil injected with different types of surge current are simulated. The types of soil and the corresponding injected currents are: clay injected with current of 11 kA peak value and waveshape 18/37 μsec, sandy soil injected with current of 6.6 kA peak value and waveshape 16/40 μsec and finally, a gravel and sand mix injected with a current of peak value 5.5 kA and waveshape 20/60 μsec. The simulation employs the Soil Ionization Dynamic Model developed by Alemeida and Correia which is based on the dynamic model of ground proposed by A.C. Liew and M. Darveniza. The validity of the model is confirmed by comparing the simulation results with the experimental data from literature.

In Chapter 5, the effect of the combined model of tower and ground on the response of two system configurations to various types of surge current is investigated. The two system configurations are a stand alone tower with a ground wire of infinite length and a tower with two neighbouring towers with ground wire and phase conductors. The types of surge current are the ones used in Chapter 4, as well as the soil parameters.

Chapter 6 analyzes the effect of a fast surge current (1.5/51.75 μsec with 50 kA crest current) and a slow surge current (8/20 μsec with 50 kA crest current) on the combined model of tower and ground. The system configuration used in this simulation consists of a tower with two neighbouring towers with a ground wire and phase conductors. The ground model uses the parameters corresponding to the three types of ground (clay, sand and a gravel and sand mix).

Finally, Chapter 7 is dedicated to conclusions.

CHAPTER 2

TOWER AND GROUND MODELS IN TRANSMISSION LINES LIGHTNING SURGE ANALYSIS

In early studies, the impedance drop along the tower structure was considered to have minimal effect on the lightning behaviour of a transmission tower. Therefore the insulator voltage was calculated simply as the product of tower footing resistance and lightning current. Field studies showed that the outage rates produced by lightning strikes exceeded by far the prediction based on this simple theory. Further experimental studies conducted both on real towers and on reduced scale-towers demonstrated that the surge response characteristics of the tower are as important as the footing response and a good approximation of these characteristics will lead to a better prediction of the tower behaviour under lightning conditions.

The two parameters describing the tower surge response are: the tower impedance and the velocity of surge propagation in tower. These two parameters are determined by measurements on full or reduced-scale towers and by theoretical studies on various kinds of models which can range from simple lumped inductances or resistances to complicated nonuniform transmission-line circuits.

2.1 Review of Tower Models

2.1.1 Breuer Model

One of the first attempts in measuring the surge characteristics of a transmission tower is attributed to Breuer (1958) [1] who used as a measurement technique the so-called reflection method. In this method, the measurements were performed by applying a surge using a voltage generator located on the ground. Connection was made to the top of the tower either through a lead perpendicular to the ground, with the generator located at the center of the base of the tower, or making an angle of 45° to the ground surface. The information about the transient impedance of the tower was derived from the reflected voltage wave.

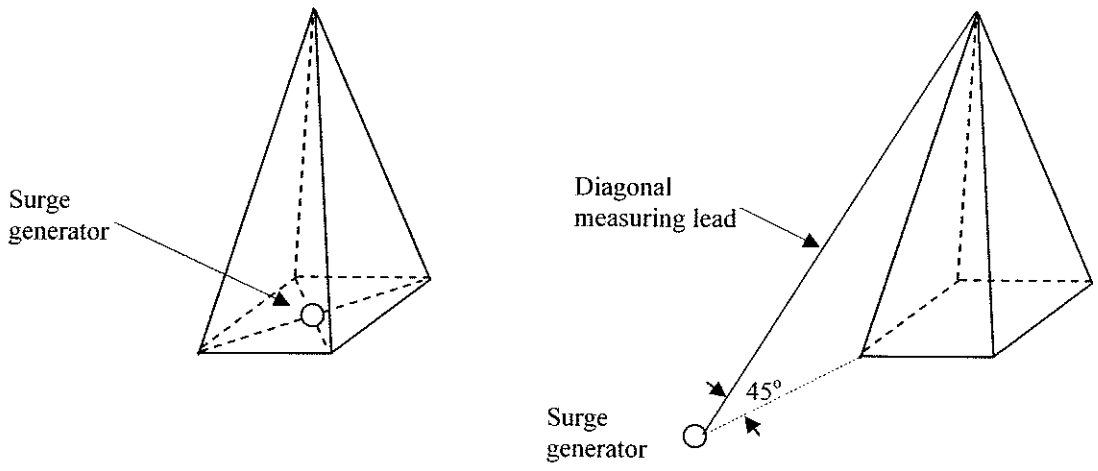

Fig. 2-1 Measurement setup for Breuer's tests

The measurements were performed both on an artificial and on an actual tower. Due to the fact that this method uses long leads, the surge impedance values for a

vertical and a diagonally placed wire were determined first as a preparation for the measurements on a full-scale tower. Having obtained these values, the surge impedance of the tower was determined from the reflected wave measured at the tower base, when the top tower was energized by a voltage surge generator located at the ground. The velocity of surge propagation was determined by dividing the length of the wire by the travel time. The reported results were obtained by experiments on a 345 kV transmission line tower, 50 m high of double circuit construction with a single ground wire isolated from the tower top, and with no insulator strings. A surge was applied through the diagonal lead to the tower top and measurements were made by means of the diagonal lead. The results were: the transient impedance at the tower top varied with time, decreasing from an initial value of 135Ω to a final value of 60Ω; the velocity of surge propagation in the tower was 282 m/μsec ~ c.

The same measurement method was also used by R.W. Caswell [2] in determining the lightning response of 38m high, 138 kV double circuit towers. The results were similar to those obtained by Breuer [1]; the impedance values were 165Ω at tower top and 50Ω at the base, and the propagation velocity was found to be equal to the velocity of light.

2.1.2 Kawai Model

Another measurement technique, called the direct method, was employed in the field tests performed by Kawai in 1964 [8]. In this method, the surge response of the tower is determined by the direct measurement of the voltage across the string insulation.

There are two cases studied by Kawai: first one – when the current flows horizontally through the overhead ground or phase wire and the second one when the current flows vertically through a conductor hanging from a balloon.

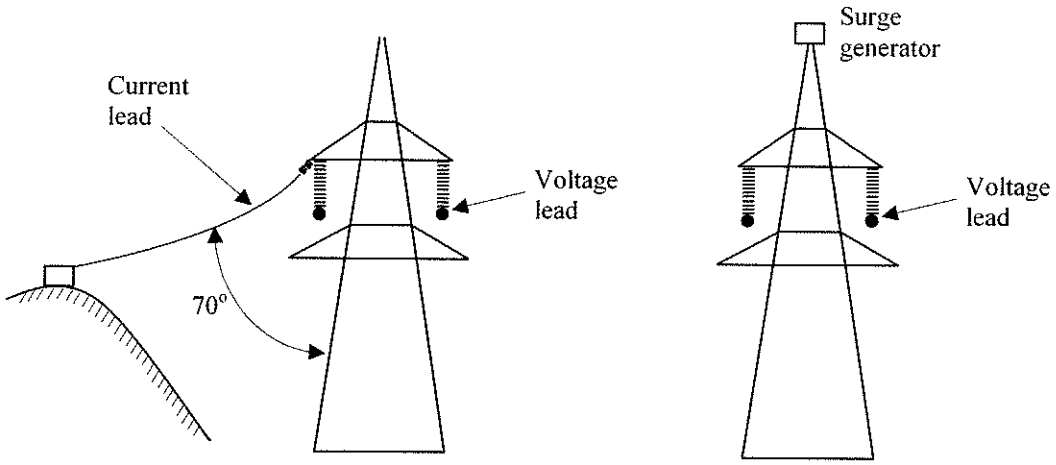

Fig. 2-2 Measurement setup for Kawai's tests

For the first case, experiments were conducted on a laboratory tower 26.5m high and on an isolated 53.3 m high tower used in a river-crossing and the current flow was injected horizontally. Also, tests were conducted on extraordinarily high tower (110m and 214m). For the second case, measurements were performed on the laboratory tower

26.5m high with vertically injected current. In both cases, the surge impedance was obtained as the ratio of voltage and current wave from oscillograms.

The results obtained from the laboratory and real tower were similar: the tower impedance was lower at the top (about 20 or 50 Ω) and increased towards the base (about 100Ω); these results are opposite to those obtained by using the reflection method. Surge velocity was 71 to 89 % of the velocity of light. Kawai pointed out that the main advantage of his method over the reflection method is that the problem regarding the distortion in the lead wires is eliminated. Another advantage is that the voltage was measured directly across the insulator string. This is the voltage of interest in insulation coordination studies.

2.1.3 Sargent and Darveniza Model

Sargent and Darveniza [9] attempted an experimental investigation of the lightning performance of transmission towers using simplified geometrical exact scale-models of the real tower, without lattice.

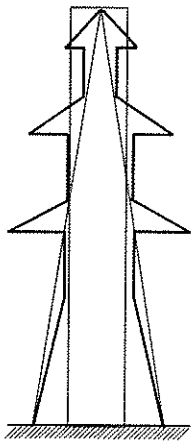

Fig. 2-3 Simplified geometrical model

The surge impedance was determined by comparing the measured tower top voltage value on the geometrical model with the one obtained by employing the traveling wave method of calculation [7]. A vertical stroke current was applied to the tower and the tower top voltage was recorded for various current wave shapes. Using an assumed value of surge impedance, the tower top voltage was calculated and was compared with the measured one. If there was no correlation between the two voltage values, the tower top voltage was calculated again for a different value of the surge impedance.

The calculated results were recorded in two ways: first as a family of curves representing the variation of tower top voltages with time for a certain current waveshape, each curve having surge impedance as parameter; and secondly as curves representing variation of tower top voltage with surge impedance for a certain current waveshape. These curves were compared with those obtained from measurements and the surge impedance was chosen.

The theoretical confirmation of the practical results was done by obtaining the surge response of a transmission tower represented as a geometrical figure using electromagnetic field theory.

Wagner and Hileman have investigated the response of a tower modelled as a cylinder to a vertical stroke of rectangular wave shape [10]. The formula obtained for surge impedance was:

$$Z = 60\ln\left[\sqrt{2}\left(ct/r\right)\right] \qquad (2.1)$$

where r is the radius of cylinder, h is the height of cylinder, c is the velocity of light and t is the time after current step reaches the tower top.

The disadvantages of this formulation pointed out by Sargent and Darveniza [9] are: the values of surge impedance calculated with this formula are higher than calculated ones; as can be noticed from the formula, the response of the cylindrical model is time-variant. This leads to the conclusion that the response to other current waveshapes might be different from the response to the rectangular one.

Sargent and Darveniza [9] concluded that, a conventional double-circuit steel lattice tower can be represented by a right cone with a surge impedance calculated with the formula (2.2) obtained by using the electromagnetic field theory. Therefore, the tower can be considered as a transmission line of constant surge impedance depending only on the geometry of the conical tower, with the velocity of surge propagation equal to the velocity of light (300m/μs) and with no attenuation. They did not present experimental results on real towers. Their formula for surge impedance was:

$$Z = 60\ln\left(\sqrt{2}/S\right) \tag{2.2}$$

where S is the sine of the half angle of the cone. The derivation of this formula is presented in Appendix A.

The conclusions derived from this formulation are: the tower can be considered as a transmission line of constant surge impedance; is time invariant, hence the response is not dependent of the current waveshape; the values of surge impedance (130-150Ω) are in agreement both in magnitude and in time invariance with the measured values.

2.1.4 Chisholm Model

Chisholm used the Time-Domain Reflectometry (TDR) in measuring the surge impedance on both reduced and full-scale towers [4]. TDR is a technique of measuring reflection coefficients. When a fast rising current surge is injected into the tower top, the incident and reflected voltages are recorded and the impedance values are determined by processing these measured values of voltage and reflection coefficients. Chisholm applied this measurement technique for obtaining the surge impedance of cylindrical, conical and inverted-cone reduced scale models due to horizontal and vertical stroke currents. The results showed that the surge response of the tower to a horizontal stroke is different from that to a vertical stroke; the tower impedance to horizontal currents is highest at the tower top and lowest at the tower base, which is similar to the result obtained by Breuer [1] using the reflection measurement method technique. The opposite is true for the tower impedance obtained by using vertically injected currents, in accordance with the results obtained with direct method by Kawai [8]. This leads to the conclusion that a conical or cylindrical theoretical model is inadequate since they provide surge impedance values that vary with the current lightning orientation.The geometrical model chosen by Chisholm is the inverted cone because this is the geometry that gives a constant value of the surge impedance in the case of the midspan stroke to the skywire, which is the most encountered situation. Based on conical antenna theory a formula for the surge impedance was found.

$$Z = 60\ln\left[\cot 1/2 \tan^{-1}(r/h)\right] \tag{2.3}$$

where r and h are the radius and height of cylinder.

If the tower shape is an inverted cone, the value of the surge impedance using the above will be a constant. If the tower shape is not an inverted cone, this formula can be used by varying the height h and the radius r for each position.

2.1.5 Ishii Model

In the models reviewed thus far, most of the field tests and the theoretical studies have reported a variation of the surge impedance with time. This variation is described also by surge impedance formulas obtained from analysis based on electromagnetic field theory on theoretical models. In this case, it is difficult to obtain numerical results considering that a significant amount of computation time would be necessary. Hence, a new model based on distributed parameters was developed by Ishii [6]. This so called Multi-Storey Model proposed by Ishii has the advantage that it can be easily interfaced with EMTP (Electromagnetic Transient Program) since the tower can be represented by an equivalent circuit. The model goal is to predict the back flashover at an individual insulator string. That is why the multi storey model is composed of four sections divided at the upper, middle and lower phase crossarm positions and is used to predict the behaviour of a double circuit tower with ground wires when the ground wires are contacted by a lightning stroke.

The results derived by use of the model were compared with those obtained from measurements conducted on a real tower of a double circuit 500kV, 62.8m high, equipped with skywires. The measurement technique used was the direct method, similar to that used by Kawai [8]. A current is injected into the tower top by a pulse generator on the ground through a 50 Ω, 300 m cable. The cable is connected to a

ground-wire crossarm of the tower through a 1kΩ resistor for wave shaping and a 0.5 Ω current shunt. The current shunt measures the injected current and a 10 kΩ resistive voltage divider measures the voltage across insulator string. All the data was transformed into light signals and are transmitted to ground through optical waveguides.

The equivalent circuit of the system consists of 4 sections. Each section is represented by a parallel circuit of a resistance and an inductance in series with a lossless transmission line. The transmission lines system that comprises eight conductors (two ground wires and six phase conductors for double circuit) is represented by the EMTP Semlyen model. The values of the tower surge impedance and of attenuation coefficients used in this model are chosen by a trial-and-error process, by adjusting the simulation results in order to match the experimental ones. Ishii selected a higher value of impedance for the tower topmost section.

Yamada [11], who used the same theoretical model in his analysis of the surge characteristics of a transmission tower, presented formulas (Eq.(2.4) to Eq.(2.7)) which may be used to obtain the parameters of the equivalent circuit. He represented the transmission line system in his model by use of EMTP J.Marti model.

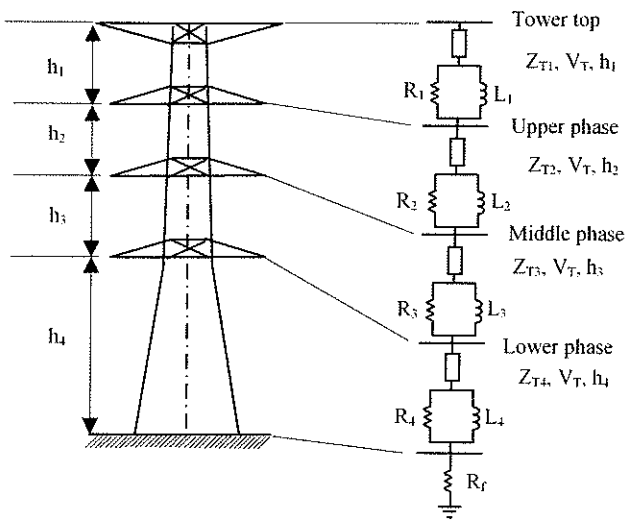

Z_T – tower surge impedance

V_T – surge propagation velocity

γ - attenuation coefficient

R_1, R_2, R_3, R_4 – damping resistance

L_1, L_2, L_3, L_4 – damping inductance

Fig. 2-4 Multi storey transmission tower model

$$R_1 = \frac{-2Z_{T1}\ln\sqrt{\gamma}}{h_1+h_2+h_3}h_1 \qquad L_1 = R_1\tau \tag{2.4}$$

$$R_2 = \frac{-2Z_{T2}\ln\sqrt{\gamma}}{h_1+h_2+h_3}h_2 \qquad L_2 = R_2\tau \tag{2.5}$$

$$R_3 = \frac{-2Z_{T3}\ln\sqrt{\gamma}}{h_1+h_2+h_3}h_3 \qquad L_3 = R_3\tau \tag{2.6}$$

$$R_4 = -2Z_{T4}\ln\sqrt{\gamma} \qquad L_4 = R_4\tau \tag{2.7}$$

$$H = h_1+h_2+h_3+h_4 \qquad \tau = 2\,H/V_T \tag{2.8}$$

The damping resistance for each section was determined from the resistance per unit length of a transmission line calculated from the surge attenuation coefficient of the tower (Appendix B). According to the calculation presented in Appendix B, the formula derived for damping resistance contains γ instead of square root of γ as was presented in [11]. In the simulation, this last version was used.

According to Yamada, the selected surge impedances of the model chosen by Ishii are higher than those measured for the tower alone (isolated from ground wires).Yamada chose, also by a trial and error process, a constant value of the surge impedance for all four sections $Z_{T1}= Z_{T2}= Z_{T3}= Z_{T4}$ with a lower value than those chosen by Ishii.

2.1.6 Hara Model

Hara and Yamamoto [5] developed a more general representation of a transmission tower model taking into account all the three parts of a transmission tower (main legs, bracings and crossarms). First, they obtained an empirical formula of the transmission tower surge impedance by measurements conducted on a cylindrical conductor (a steel pipe pole 15m in height and 51 mm in diameter). The surge response of the conductor was measured by the direct method. The injected current (10ns steep wave front) was generated by a 2kV pulse generator located on the ground through a 50m current lead. The voltage lead was perpendicular on the current lead (there was no induced voltage) and is grounded at 50m away from the conductor. The lead wires were kept horizontal to the ground by using two concrete poles that stood 20m beyond the conductors. The current at the top was measured by a pulse current transformer and the voltage by a potential probe. The measured signal was converted by an optical transducer into a light signal and transmitted to the ground. The value of surge impedance obtained was 320 Ω.

The surge impedance was measured for different sizes of vertical cylinders using the arrangement described above and an empirical formula was obtained:

$$Z_T = 60\left(\ln\frac{2\sqrt{2}h}{r} - 2\right) \tag{2.9}$$

where r and h are cylinder radius and height

Based on this empirical formula, Hara and Yamamoto developed an equivalent distributed constant line model of a transmission tower. The model consists of three parts: main legs, bracings and crossarms. The surge impedance of each part is calculated in terms of tower dimensions and geometry. Then, the calculated surge impedance is compared with the measured one (for a 500 kV tower).

The distributed constant line model was applied to a transmission tower whose geometry, presented in [13], is shown in Fig. 2-5 and is represented by the equivalent circuit shown in Fig. 2-6, presented also in [13]. The authors showed that, by modlling the tower as a one-section tower, the simulation results do not agree well with experimental ones. Therefore, they concluded that for a tower higher than 50m the tower should be divided in four sections, each section having three equivalent line models (main legs, bracings and crossarms).

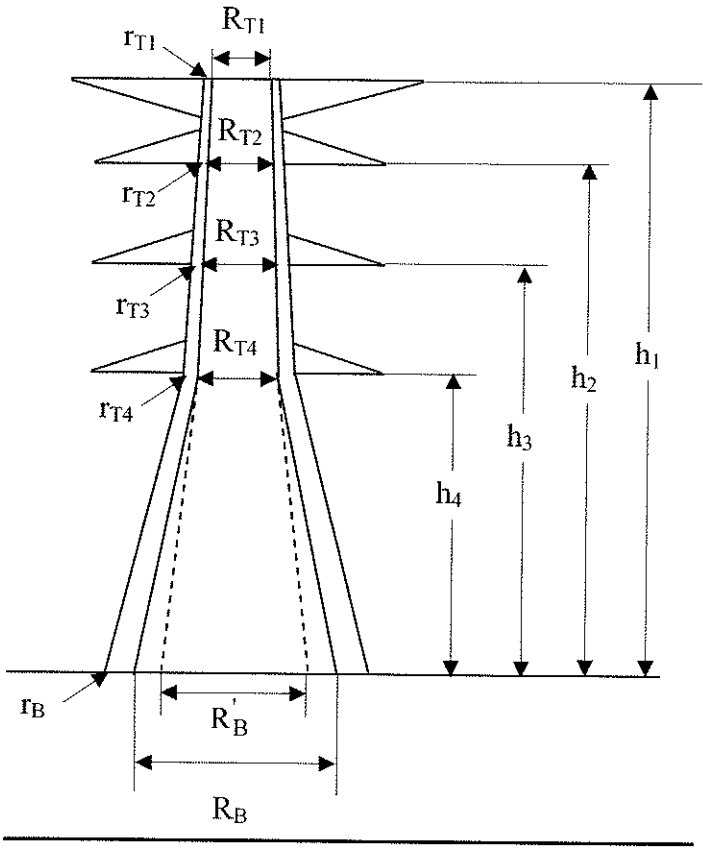

Fig. 2-5 Schematic diagram of the transmission tower

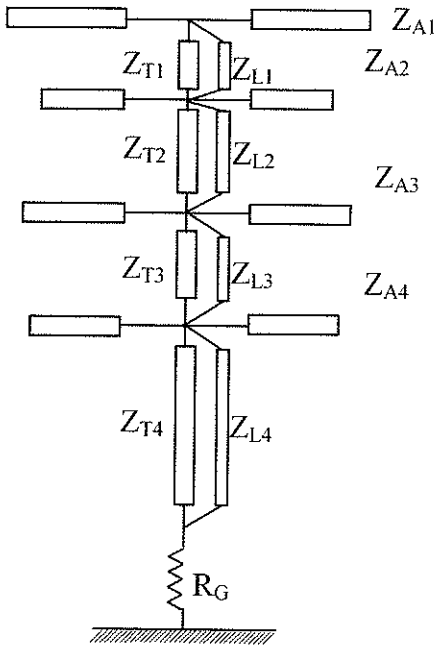

Fig. 2-6 Equivalent line model of a transmission tower

Z_T is the impedance of main legs, Z_L is the impedance of bracings and Z_A is the impedance of the crossarms.

For the model of main legs the following formula was used:

$$Z_{Tk} = 60\left(\ln\frac{2\sqrt{2}h_k}{r_{ek}} - 2\right); k = 1, 2, 3, 4 \tag{2.10}$$

$$r_{ek} = 2^{1/8}\left(r_{Tk}^{1/3} r_B^{2/3}\right)^{1/4}\left(R_{Tk}^{1/3} R_B^{2/3}\right)^{3/4}; k = 1, 2, 3, 4 \tag{2.11}$$

where r_{ek} is the equivalent radius of multiconductor systems and is derived in Appendix C.

For the model of bracings:

$$Z_{Lk} = 9Z_{Tk}; k = 1, 2, 3, 4 \tag{2.12}$$

For the model of crossarms the formula of horizontal cylinder is used:

$$Z_{Ak} = 60\ln\frac{2h_k}{r_{Ak}} \tag{2.13}$$

This formula is applicable to cylindrical shaped arms and also to the scale model arms when the equivalent radius is chosen as ¼ of the width of the arms at the junction point.

This model was applied to a 500 kV real transmission tower of certain geometry and dimensions. Hence, the surge impedance of main legs, bracing and crossarms was calculated for each of the four sections of the tower. The wave shapes of the voltages at the tip of the four arms were calculated from the tower model and compared with the measured ones. The surge characteristics of the tower were measured having an injected current of 200 ns rise time which was imposed on the top.

There is a good agreement between the measured voltage and the calculated voltage wave shapes. The surge propagation velocity along the tower was proved to be equal to the velocity of light.

2.2 Review of Ground Models

Sensitivity studies regarding the transmission line behaviour under lightning conditions [17] show that an important factor that has to be taken into account is the transmission tower footing resistance or ground resistance. The term "ground model" which is used throughout this thesis is the model of the electrode embedded in the ground used to calculate the effective resistance presented by it to the passage of surge currents.

The classification of ground models depends on how the resistance of the ground is considered when it is subjected to a surge current. The ground resistance may be a constant or variable.

A constant resistance model consists of a lumped constant resistance R_0 whose value is calculated by using the formula for a hemisphere electrode embedded in soil of uniform resistivity.

$$R_0 = \frac{\rho}{2\pi r} \tag{2.14}$$

where ρ is the resistivity of the surrounding soil and r is the radius of the ground electrode.

This model is still conveniently used for simulations when the lightning current magnitude and the soil resistivity are not too large.

A variable resistance model is more appropriate when the ground is contacted by lightning currents of high magnitude. Liew and Darveniza [12] proved experimentally and analytically that the ground resistance of a concentrated electrode drops from its initial value when it is subjected to a lightning surge current. In their publication which is titled "The Dynamic Model of Ground" they presented a model based on the hysteresis behaviour of the ground resistivity as a function of current. The medium surrounding the ground rod was considered homogeneous and isotropic, consisting of a cylindrical upper region and a hemispherical lower region as shown in Fig. 2-7.

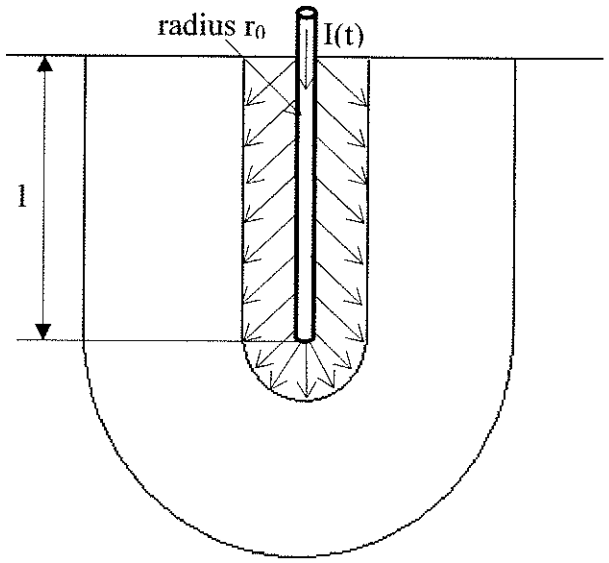

Fig. 2-7 The approximate cylinder-hemispherical shape of the medium surrounding the ground rod with a buried length l and radius r_0, subjected to a surge current

According to Liew and Darveniza [12], as the value of the current penetrating the ground increases, the current density will exceed the soil critical breakdown value in those regions which are located closer to the rod. This will trigger an ionization process and the ground resistivity decays exponentially as described by Eq. (2.15)

$$\rho = \rho_0 e^{\frac{t}{\tau_1}} \tag{2.15}$$

where ρ_0 is the non-ionized ground resistivity, τ_1 is the ionization time constant of the soil and t is the time measured from the instant of ionization.

As the current decreases from its maximum value, the resistivity recovers according to Eq. (2.16)

$$\rho = \rho_i + (\rho_0 - \rho_i)\left(1 - e^{-\frac{t}{\tau_2}}\right)\left(1 - \frac{J}{J_c}\right)^2 \tag{2.16}$$

where ρ_i is the minimum resistivity value obtained during the ionization of the ground, τ_2 is the de-ionization time constant of the soil, J is the electric current density and J_c is the critical electric current density corresponding to breakdown electric field of the soil.

The results of the analytical calculation were compared with the experimental results. The authors tested three types of soil: gritty light clay soil, soil composed of a sand and gravel mix, and loamy sand. First, they determined the resistivities of each soil by measuring its resistance and by using Dwight's formula [20]:

$$R = \frac{\rho_0}{2\pi l}\left(\ln\frac{4\pi}{r_0} - 1\right) \tag{2.17}$$

$$\Rightarrow \rho_0 = \frac{R\,2\pi l}{\left(\ln\frac{4\pi}{r_0} - 1\right)} \tag{2.18}$$

The measurements were performed on each type of soil by applying an impulse current from a surge-current generator. The input peak currents and their waveshapes were in the range of 1-20 kA and 6-16/18-54 μsec, respectively. The impulse current and voltage magnitudes and shapes across ground resistance were recorded.

The other model parameters E_c, τ_1 and τ_2 were selected by adjusting the analytical results in order to match the experimental results for a particular surge current. The values of τ_1 and τ_2 were consistently used to predict the behaviour of the soil for various experimental conditions, i.e. different impulse current and different electrode geometry. The value of E_c had to be readjusted for each electrode geometry even for the same soil.

The authors verified the validity of the model by comparing the analytical results with experimental ones for three types of soil. They concluded that their model can be successfully used to describe the surge behaviour of the first two types of ground: the gritty light clay soil with a resistivity of 5050 Ωcm, and the sand and gravel mix with a resistivity of 5000 Ωcm. For the third soil, the loamy sand, which has a higher resistivity (54000 Ωcm), the analytical results did not compare well with the experimental ones. An explanation given by the authors, is that in a high resistivity soil, high currents result in discrete breakdown paths, rather than in a diffuse growth of increasing ionization. In order to establish a resistivity range for which the model is valid, the authors simulated the test experiments conducted by Bellaschi [19] on three types of soil with higher resistivities.

The results obtained by Liew and Darveniza from the analytical calculations compared well with the experimental results obtained by Bellaschi [19]. This enabled

the authors to extend the validity of the model to soils with resistivity ranging from 5000 Ωcm to 31000 Ωcm. Once the accuracy of the model was established, the authors studied the influence of different soil resistivities and different electrode geometries (one to four rods) on ground resistance variation. Liew and Darveniza concluded that soils of higher resistivities have a greater rate of decrease. Also, the rate of decrease of ground resistance is higher for one rod than for multiple rods configuration due to the fact that the current densities in the vicinities of the rod are higher. Even though at that time there were no experimental results available for comparison, the authors declared that this model can be used in calculation of impulse resistances for surge currents up to 100 kA.

The model proposed by Almeida and Correia [18], The Soil Ionization Dynamic Model, uses the same modelling technique as the one developed by Liew and Darveniza [12]. The difference lies in the fact that the ionization process is driven by the electric field and not by the current density. The ionization process is described by Eq. (2.19)

$$\rho = \rho_0 + (\rho_c - \rho_0)\left(1 - e^{-\frac{t}{\tau_1}}\right) \tag{2.19}$$

The deionization process is described by Eq. (2.20)

$$\rho = \rho_i + (\rho_0 - \rho_i)\left(1 - e^{-\frac{t}{\tau_2}}\right)\left(1 - \frac{E}{E_c}\right)^2 \tag{2.20}$$

whith ρ_0 the non-ionized ground resistivity, ρ_c the critical value of the soil resistivity corresponding to the soil critical breakdown $\rho_c = \frac{E_c}{J}$, J the current density, ρ_i the minimum value obtained during the ionization of the ground resistivity, τ_1 / τ_2 the

ionization / deionization time constants of the soil, E the electric field, and E_c the breakdown electric field of the soil.

The simulation results compared well with the experimental results obtained by Bellaschi [19] which allowed the authors to validate this model.

CHAPTER 3

INVESTIGATION OF DIFFERENT TOWER MODELS WITH EMTDC SIMULATION

In this chapter, three tower modeling techniques reviewed in Chapter 2 are described in detail and applied for the simulation of the field experiments reported in [13] by Hara and [14] by Matsumoto. The three tower models are the Conical, Multi Storey and Distributed Constant Line models. These models were considered since they are EMTDC applicable and, according to their authors, they showed good agreement with the data generated by experimental work. The comparison between the simulation results obtained from each model with the ones obtained from the field experiments will give the grade of reproductibility of the overvoltage at the tower top and / or at the tip of the tower arms, when the system is subjected to lightning. This will enable a selection of the best model which will be used in further studies.

In order to obtain conclusive results regarding the tower behavior under lightning conditions, different cases have been investigated: Case 1: a stand alone tower with no ground wires and constant ground resistance, subjected to different double exponential surge current waveforms, Case 2: a stand alone tower with a ground wire of infinite length and lastly, Case 3: a tower with two neighbouring towers with ground wire and phase conductors, subjected to a piece wise surge current waveform and double exponential surge current waveforms.

3.1 Investigation of a stand alone transmission tower response to double exponential surge waveform

In the simulation, the tower presented in [13] will be used since it is completely geometrically described and the authors have also included experimental results. The tower geometry is shown in Fig. 3-1

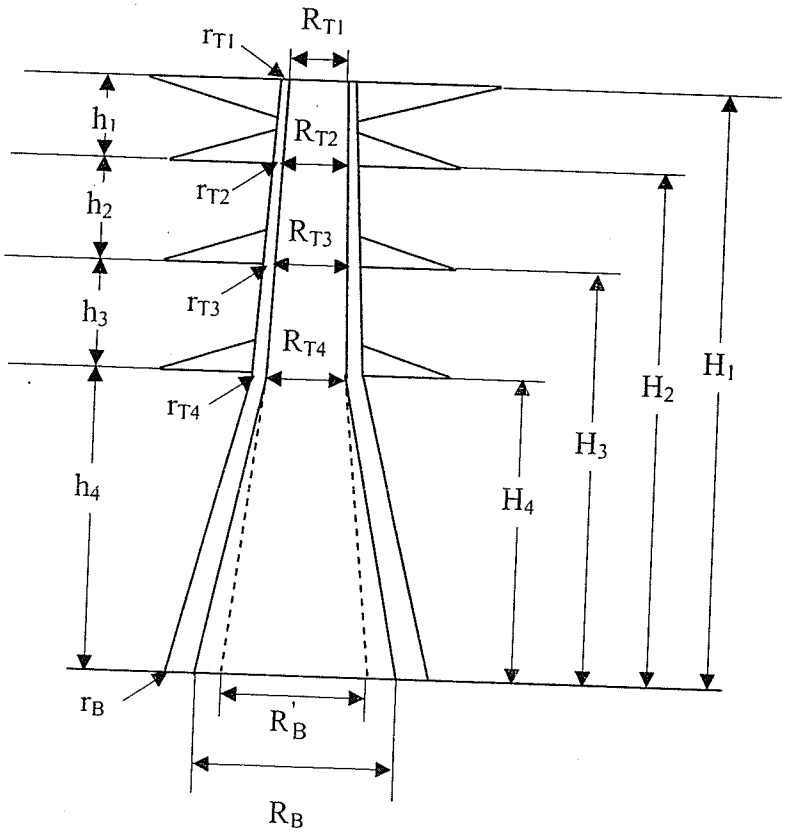

$H_1 = 59$ m
$H_2 = 47.9$ m
$H_3 = 33.6$ m
$H_4 = 22$ m
$r_{T1} = 0.07$ m
$r_{T2} = 0.08$ m
$r_{T3} = 0.16$ m
$r_{T4} = 0.178$ m
$R_{T1} = 5$ m
$R_{T2} = 5.45$ m
$R_{T3} = 6.03$ m
$R_{T4} = 6.50$ m
$r_B = 0.203$ m
$R_B = 12.55$ m
$R_B' = 7.40$ m

Fig. 3-1 Transmission Tower dimensions

3.1.1 Conical Model (Sargent and Darveniza Model)

The formula of the surge impedance of a transmission tower represented as a cone (2.2), derived by Sargent and Darveniza, was presented in the previous chapter. The transmission tower of Fig. 3-1 is approximated by a cone as shown in Fig. 3-2.

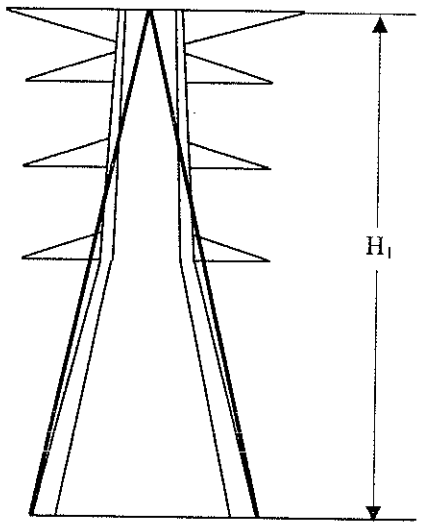

Fig. 3-2 Conical approximation of a double circuit transmission tower

In this case S will be:

$$S=\frac{\frac{R_B}{2}+r_B}{\sqrt{\left(\frac{R_B}{2}+r_B\right)^2+H_1^2}} \Rightarrow Z=150\Omega \qquad (3.1)$$

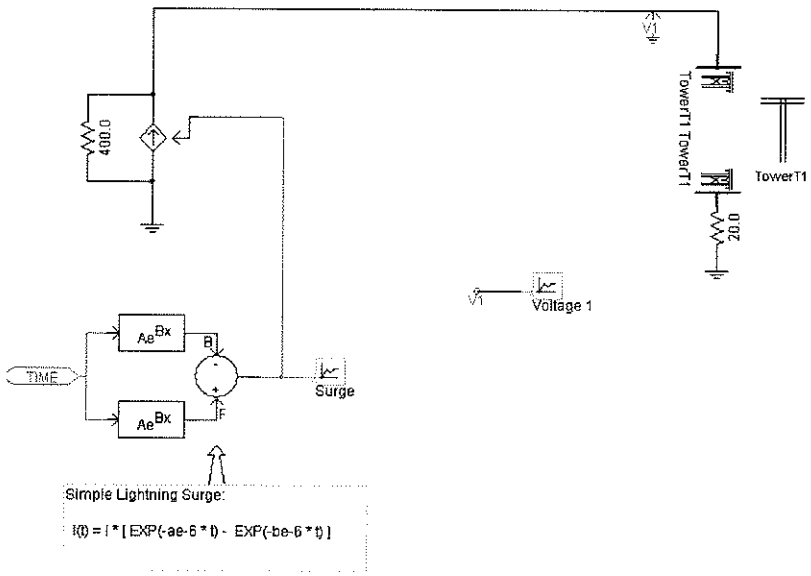

Fig. 3-3 The equivalent circuit for Conical Model in PSCad simulation

Fig. 3-3 shows the equivalent circuit of the system simulated in PSCad which is used to describe the lightning response of a stand alone tower. The transmission tower was represented by a lossless transmission line, using the Bergeron model available in PSCad library. This model is based on a distributed L-C parameter traveling wave line, having a lumped resistance and a constant surge impedance. The input data were: the surge impedance calculated by formula (3.1), the propagation time, which was calculated by assuming a propagation speed equal to that of light, and the length of the line denoted by H_1 (see Fig. 3-2). The lightning was modeled as a current source, generating a double exponential wave form, in parallel with a lightning discharge impedance of 400 Ω. Generation of a double exponential waveform is explained in Appendix D.

3.1.2 Multi Storey Model (Ishii Model)

As mentioned in Chapter 2, the Multi Storey model proposed by Ishii consists of four sections. Each section is represented by a parallel circuit consisting of one resistance and one inductance in series with a lossless transmission line.

The parameters of the equivalent circuit are obtained by use of Eqs (2.4) - (2.8).

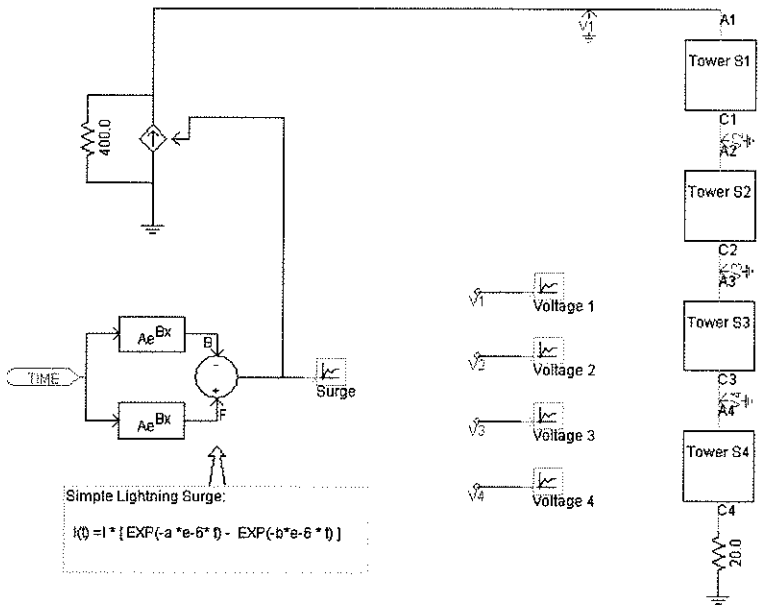

Fig. 3-4 The equivalent circuit for Multi Storey Model in PSCad simulation

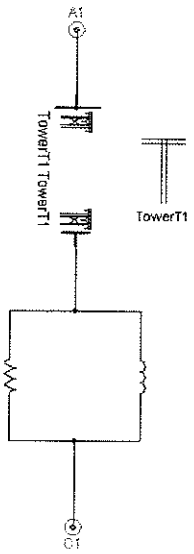

Fig. 3-5 One of the four sections of the tower

As shown in Fig. 3-4, the tower was divided into 4 sections (Tower S1 – S4), each section being represented by the circuit shown in Fig. 3-5. The model parameters are presented in Table 3-1.

Table 3-1 Multi Storey Model parameters

Section	Attenuation coefficient γ	Impedance Z	Resistance R	Inductance L	Tower dimensions L_T
		[Ω]	[Ω]	[μsec]	[m]
I	0.8	120	8.03	2.92	11.1
II		120	10.35	3.77	14.3
III		120	8.4	3.05	11.6
IV		120	26.78	9.7	17.6

The attenuation coefficient γ and the impedance corresponding to each section were chosen according to [14]. The rest of the parameters were calculated according to the formulas (2.4) - (2.8).

3.1.3 Distributed Constant Line Model (Hara model)

The model proposed by Hara and Yamamoto consists of four sections, similar to the Multi Storey model. The difference between the two models is the following: in the case of a distributed constant line model, all the tower components (main legs, bracing and crossarms) are taken into consideration and the surge impedance corresponding to each component is calculated as a function of the dimensions and geometry of the tower (as shown in Fig. 2-5).

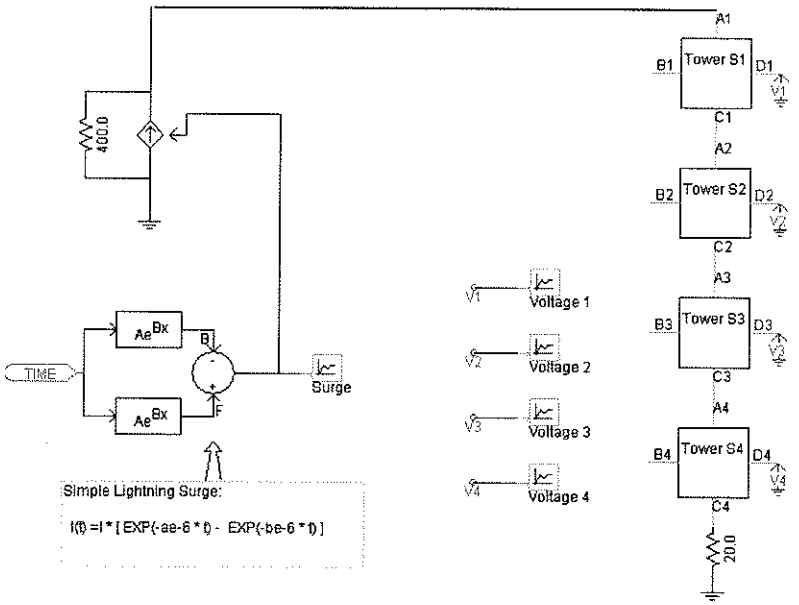

Fig. 3-6 The equivalent circuit of Distributed Constant Line Model in PSCad simulation

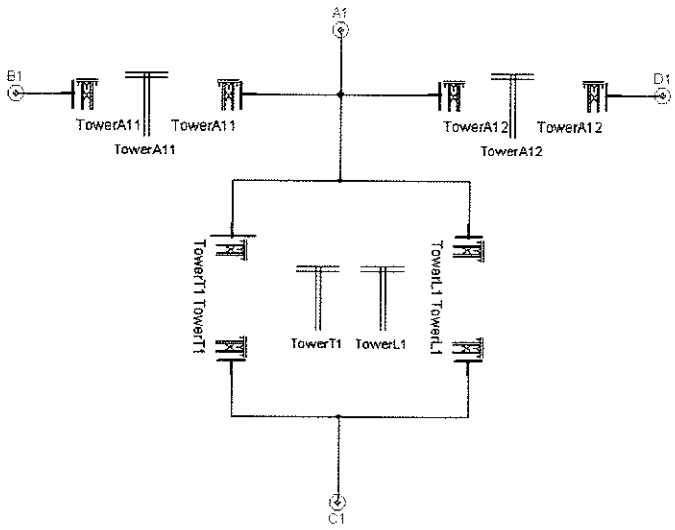

Fig. 3-7 One of the four sections of the tower

Table 3-2 Distributed Constant Line Model parameters

Section	Impedance			Tower dimensions L		
	Main legs Z_T	Bracings $Z_L=9*Z_T$	Crossarms Z_A	Main legs L_T	Bracings $L_L=1.5*L_T$	Crossarms L_A
	[Ω]	[Ω]	[Ω]	[m]	[m]	[m]
I	127	1143	221	11.1	16.5	18.5
II	112	1008	215	14.3	21.45	11.8
III	86	774	195	11.6	17.4	16.3
IV	43	384	178	17.6	26.4	13.5

The parameters presented in Table 3-2 were calculated using equations (2.10) - (2.13).

3.1.4 Simulation results

A preliminary step in the PSCad simulation process was to verify the accuracy of the simulation program by implementing the exact data presented by Hara and Yamamoto in [13]. Therefore, the transmission tower was subjected to an impulse current of 0.15 kA (the estimated maximum value) with a 200 ns rise time. These results which are shown in Appendix E are in good agreement with the ones obtained by the authors.

The transmission tower was subjected to double exponential fast surge current of 1.5/51.75 μsec, 50 kA peak value, and double exponential slow surge current of 8/20 μsec (standard lightning current impulse), 50 kA peak value. The fast surge current characteristics (front time / tail time) were chosen from [22]. The peak value of 50 kA was considered because, according to IEC standards, peak impulse currents greater than 50 kA can not be expected from lightning events [23]. The ground resistance R_g is modelled as a constant but assigned subsequently different values (20 Ω and 0 Ω).

The simulation results are shown in Fig. 3-8, Fig. 3-9, Fig. 3-10 and Fig. 3-11. The surge current is shown in Plot 1 of each figure. The voltages recorded at the tower top for the Conical model (Sargent and Darveniza model), at the topmost section for the Multi Storey model (Ishii model) and at the tip of the topmost crossarm for the Distributed Constant Line model (Hara model) are shown in Plot 2 of each figure. The voltages corresponding to Ishii and Hara models recorded at the second, third and fourth section (Ihii model) / tip of the crossarm (Hara model) are shown in Plot 3, Plot 4 and Plot 5 of each figure. In Plot 2 the blue curve represents the voltage corresponding to

Ishii model, the green curve to Hara model, and the grey curve to Sargent and Darveniza model. In Plot 3, Plot 4 and Plot 5 the blue curve is the voltage corresponding to Ishii model and the green curve is the voltage corresponding to Hara model.

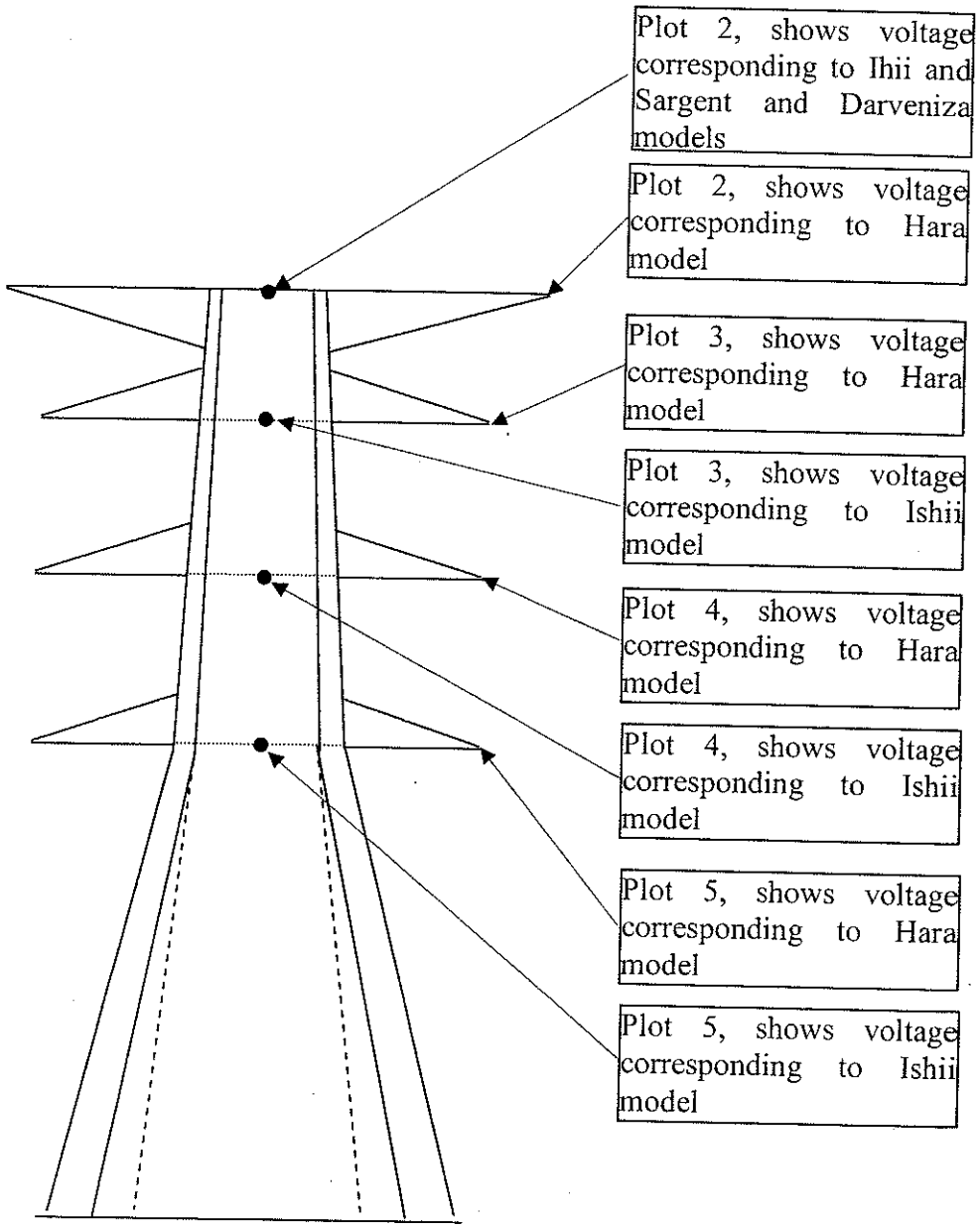

Fig. 3-8. Location of the measurement points on the transmission tower, corresponding to each tower model.

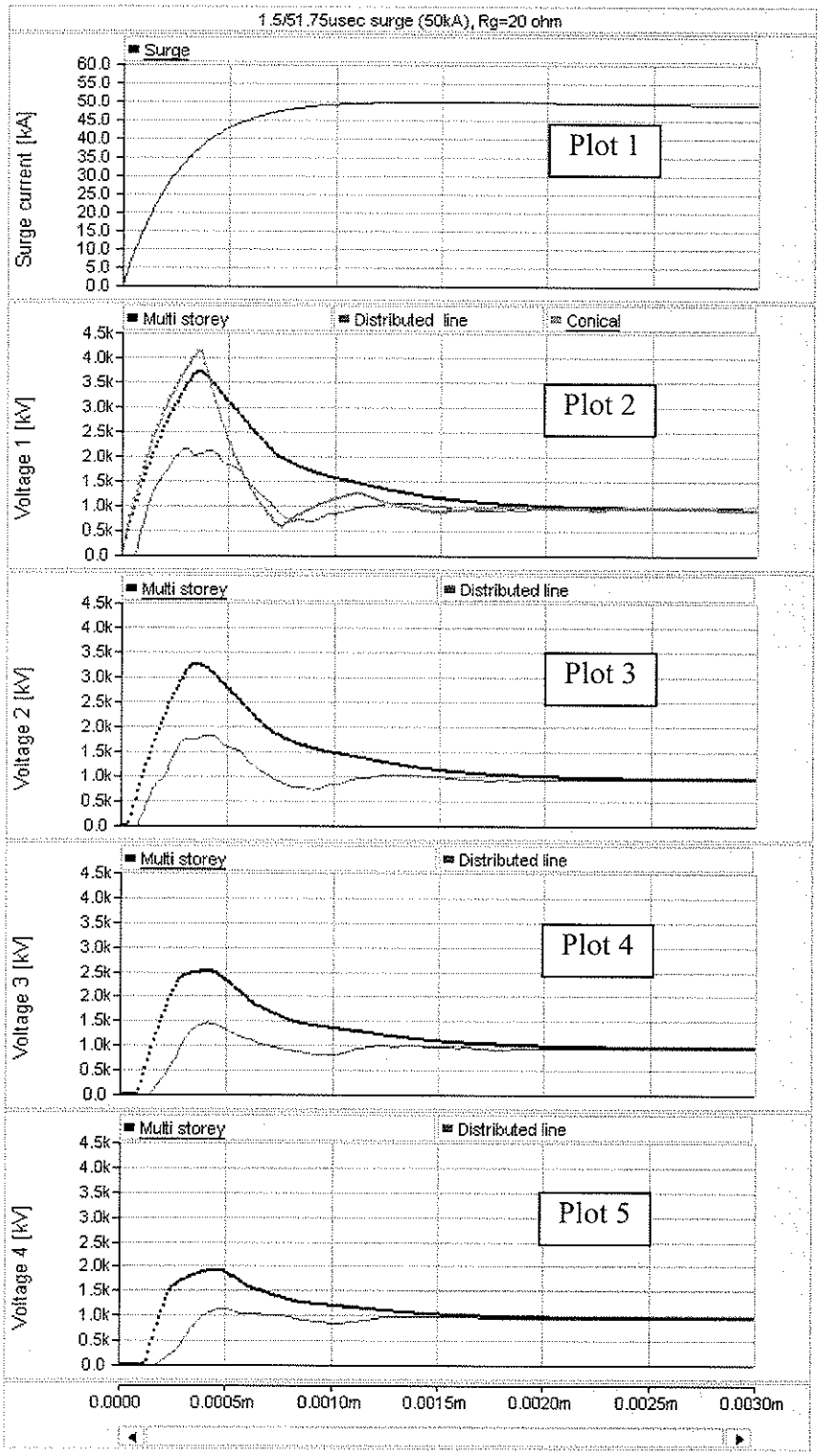

Fig. 3-9 The response of the transmission tower to a 1.5/51.75 µsec, 50 kA impulse current, R_g=20Ω. See Fig. 3-8 for explanation of Plots 2 to 5.

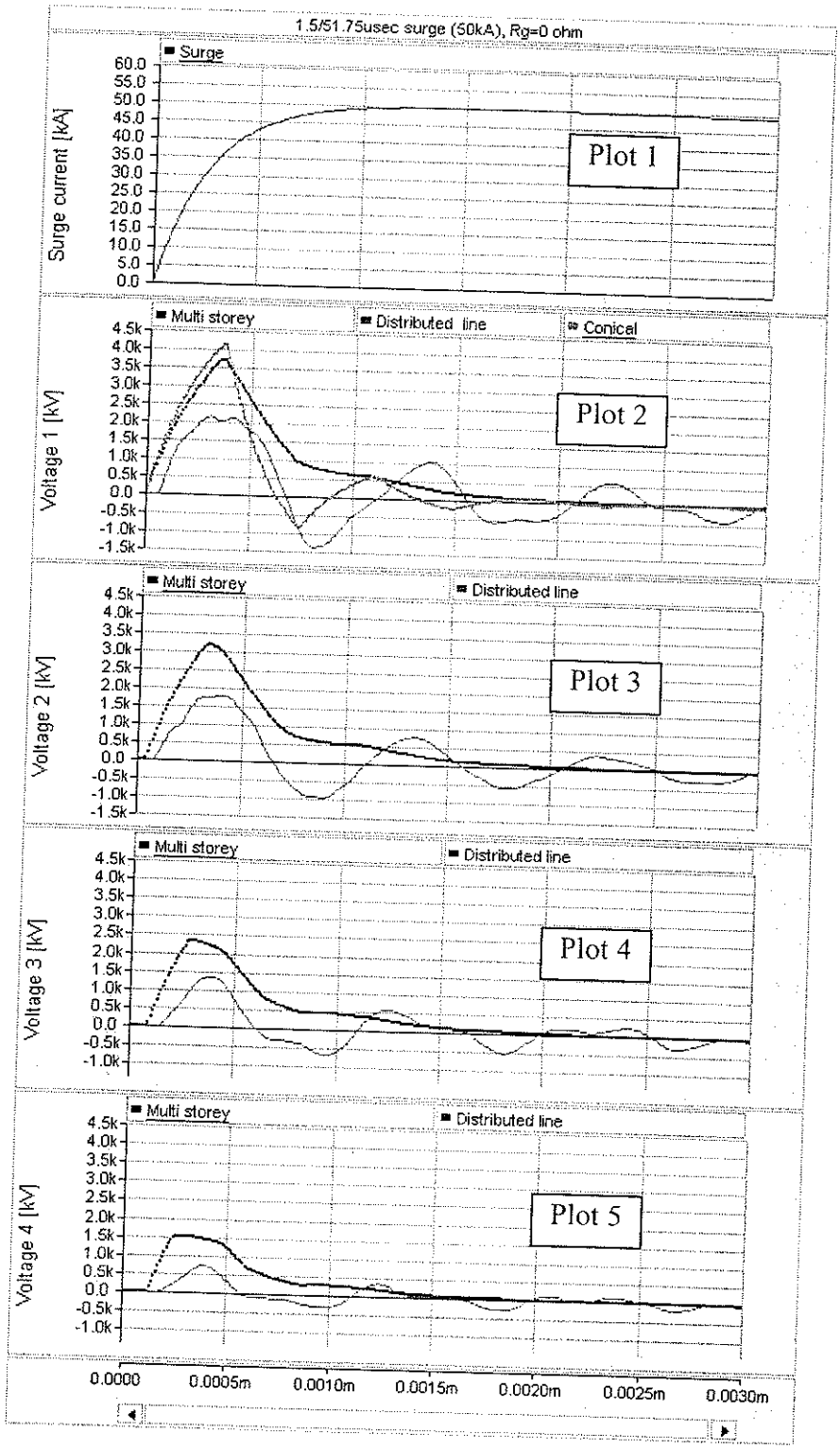

Fig. 3-10 The response of the transmission tower to a 1.5/51.75 µsec, 50 kA impulse current, R_g=0Ω. See Fig. 3-8 for explanation of Plots 2 to 5.

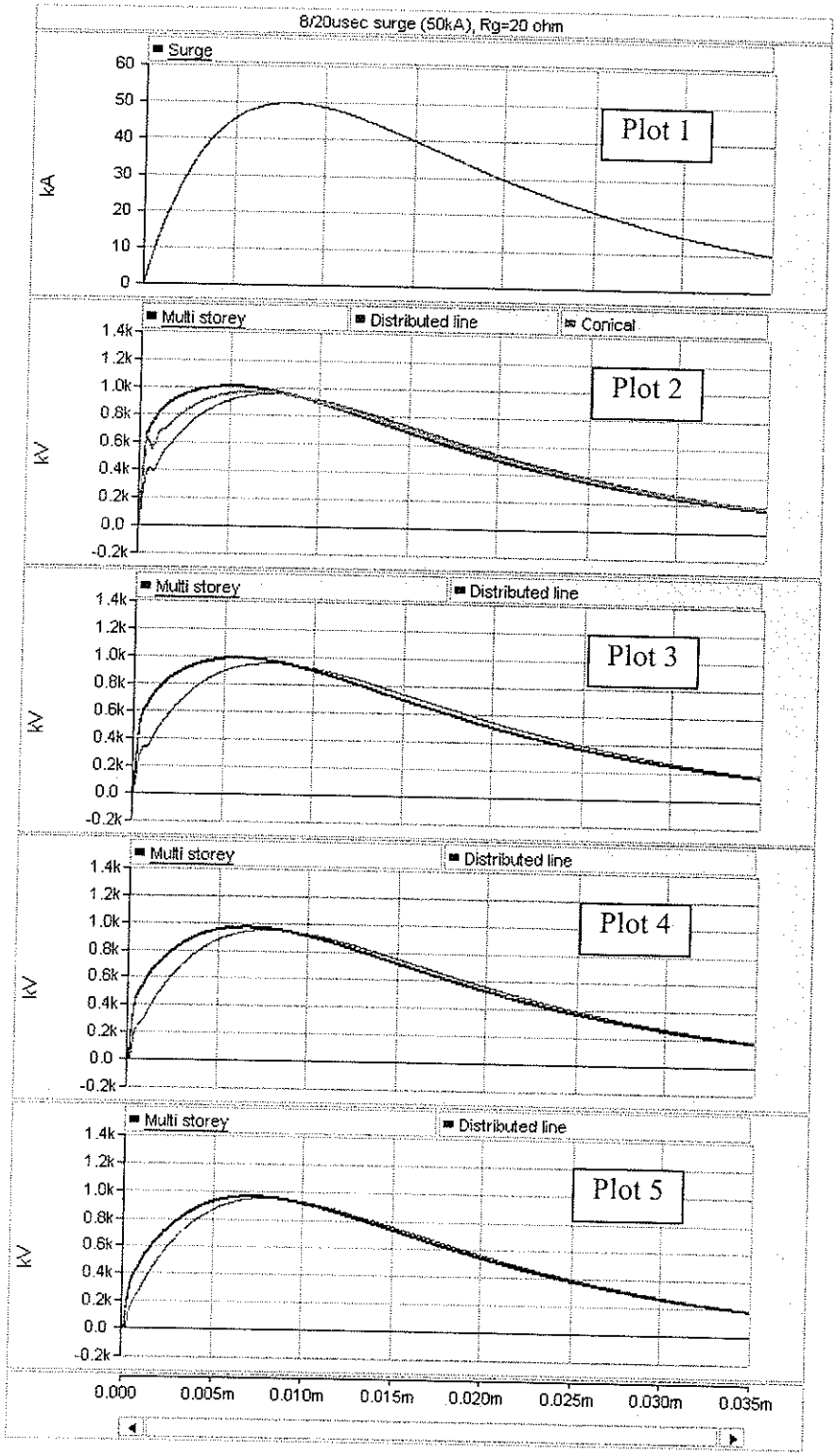

Fig. 3-11 The response of the transmission tower to a 8/20 μsec, 50 kA impulse current, R_g=20Ω. See Fig. 3-8 for explanation of Plots 2 to 5.

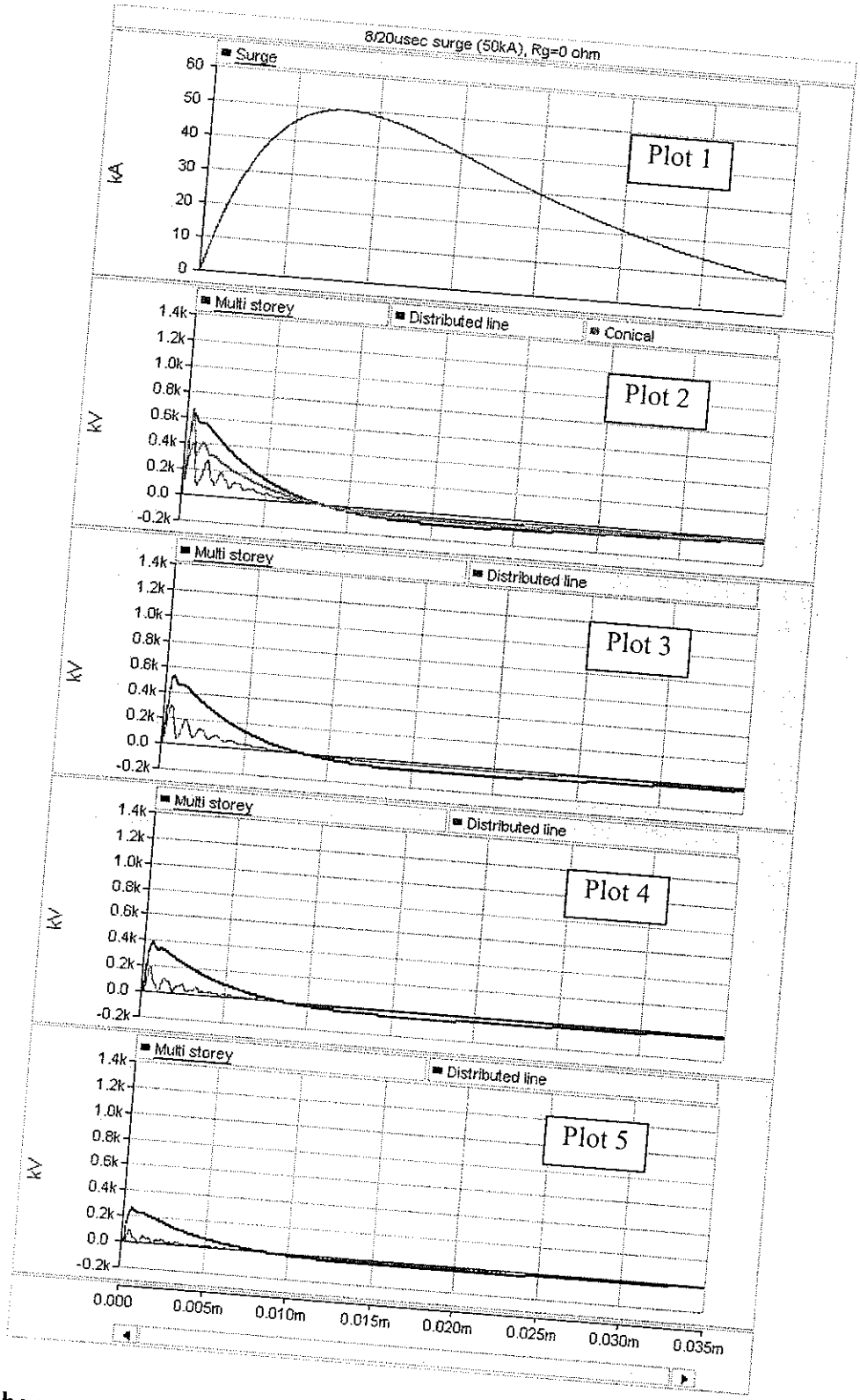

Fig. 3-12 The response of the transmission tower to a 1.5/51.75 μsec, 50 kA impulse current, R_g=0Ω. See Fig. 3-8 for explanation of Plots 2 to 5.

It can be seen from Fig. 3-9 and Fig. 3-10 that there is a significant difference between the voltage magnitudes corresponding to the three models when the tower is subjected to a fast surge waveform. The voltages corresponding to Conical and Multi Storey models are much higher than those corresponding to the Distributed Constant Line model. Therefore, at this point, a conclusion regarding the selection of the best model cannot yet be reached. In the case of a slow surge, the difference between the voltages is not significant, which implies that in this case the tower modeling technique does not have much of an effect on the results. From the same plots, one can notice that the variation of ground resistance does not play an important role in the fast surge case, and the values of the induced voltages are not affected. An explanation would be that for a slow impulse, the reflected waves from the tower footing will have a higher impact over the voltage values recorded at the tower top or at the tip of the tower arms.

3.2 EMTDC simulation of a 'live laboratory' experiments conducted by Matsumoto and Motoyama, using different tower models

In this section, the field experiment presented in [14] and [15] by Mastumoto and Motoyama will be analyzed. In their experiment they investigated the response of an unenergized 275 kV double circuit test transmission line, equipped with a single ground wire, to natural lightning which was approximated, for simulation purposes, as a piecewise linear surge waveform. The transmission line system was composed of seven

transmission towers (No. 28 to No. 34) and had a total length of 2.15 Km. The transmission tower under observation was tower No. 30, equipped with a lightning rod. The response of the tower to lightning surge was evaluated by comparing the overvoltage magnitudes and waveforms measured across the insulator strings with the calculated ones resulted from EMTP simulation in which the Multi Storey tower model (Ishii model) was used.

In the present study, the accuracy of the Multi Storey (Ishii) and Distributed Constant Line (Hara) models will be tested by analyzing the tower No. 30 response to different surge waveforms, in different configurations.

The experimental results consist in voltages across the insulator strings. By using the Conical model in the simulation, only the voltage at the tower top can be determined; therefore, in this case it would not be possible to compare simulation results with the experimental ones. That is why the Conical model has been discarded.

3.2.1 Stand alone transmission tower equipped with infinite overhead ground wire

The equivalent circuits for the Multi Storey model and respective Distributed Constant line model are shown in Fig. 3-13 and Fig. 3-14 respectively. The tower equipped with infinite ground wires is subjected to a piecewise linear surge waveform whose coordinates characteristics are shown in Table 3-3. The Multi Storey model parameters as in [15] are shown in Table 3-4 and they are different from the ones presented in [14], since some calculation errors were found in [14] and were corrected

later in [15]. The Distributed Constant Line model parameters are shown in Table 3-5 and were calculated using equations (2.10) - (2.13). Simulation results are shown in Fig. 3-15.

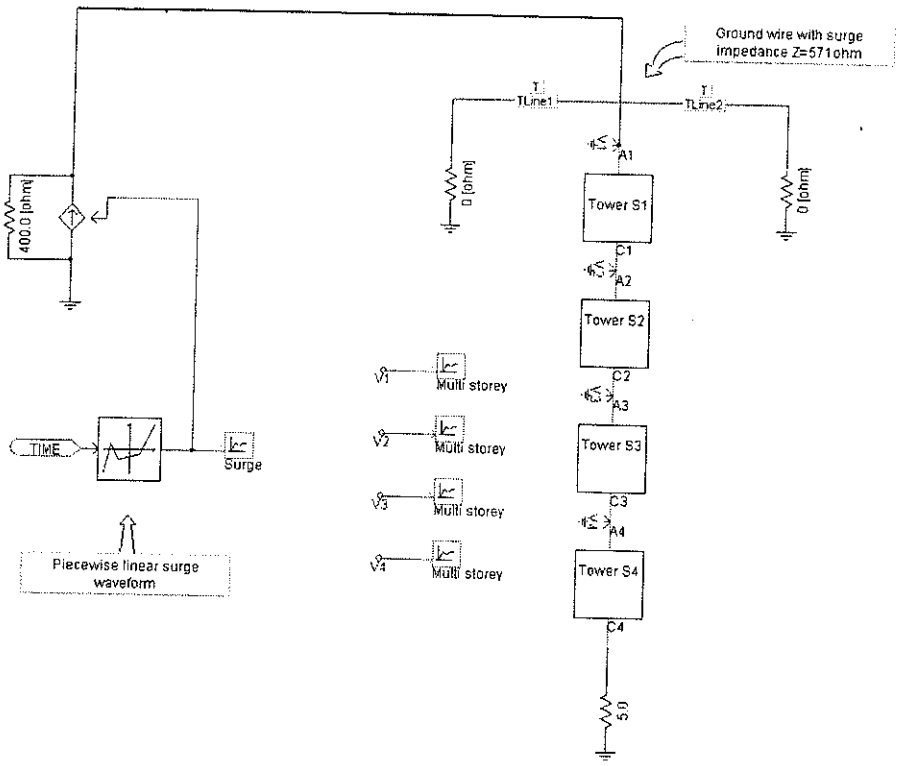

Fig. 3-13 The equivalent circuit for Multi Storey Model in PSCad simulation, transmission tower equipped with infinite ground wires (60 km)

Table 3-3 Coordinates characteristics for piece wise linear surge waveform

Time [μsec]	I [kA]
100	0
110	0
127	90
128	132
140	106
150	0
157	-50
170	0
180	20
200	0

Table 3-4 Multi Storey Model parameters

Section	Tower #30				
	Attenuation coefficient γ	**Impedance** **Z**	**Resistance** **R**	**Inductance** **L**	**Length** **l**
		[Ω]	**[Ω]**	**[μsec]**	**[m]**
I	0.8	120	5.83	2.3	5
II		120	11.7	4.61	10
III		120	9.37	3.69	8
IV		120	26.8	10.60	36.4

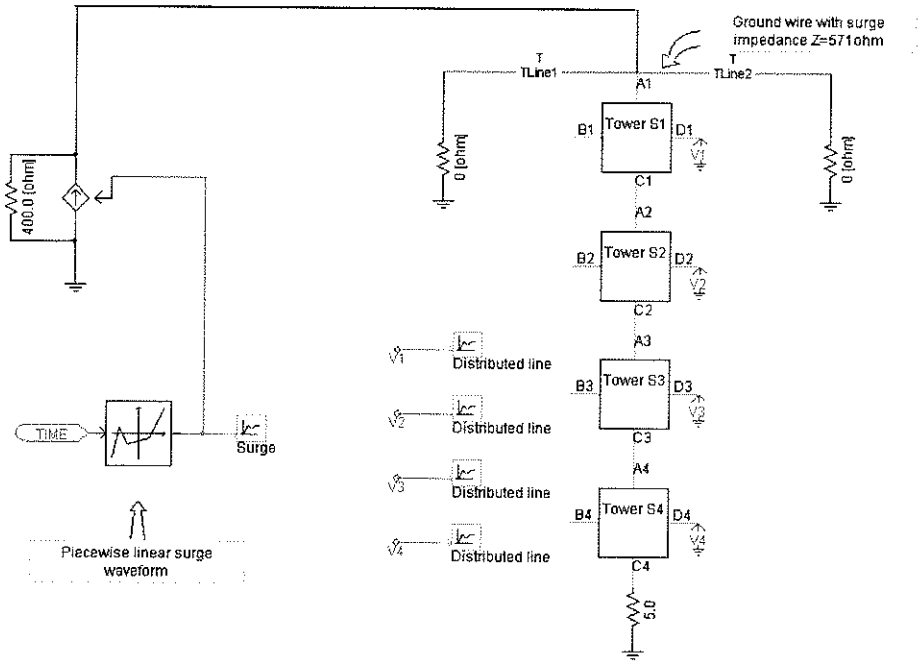

Fig. 3-13 The equivalent circuit for Distributed Constant Line Model in PSCad simulation, transmission tower equipped with infinite ground wires (60 km)

Table 3-5 Distributed Constant Line Model parameters

Section	Tower #30					
	Impedance			Length		
	Main legs Z_T	Bracings $Z_L=9*Z_T$	Crossarms Z_A	Main legs L_T	Bracings $L_L=1.5*L_T$	Crossarms L_A
	[Ω]	[Ω]	[Ω]	[m]	[m]	[m]
I	108	968	222	5	7.5	6
II	100	903	222	10	15	8.3
III	83	748	212	8	12	10.7
IV	73	661	209	36.4	54.6	9.5

In Fig. 3-15 the surge current imposed on the top of the transmission tower is shown in Plot 1. The voltages corresponding to section 1 to section 4 of Ishii model, starting with the topmost section, are shown in Plot 2 to Plot 5 (the blue curve). For Hara model, the voltages recorded at the tip of the tower crossarms, starting with the one holding the ground wire, are also shown in Plot 2 to Plot 5 (the green curve).

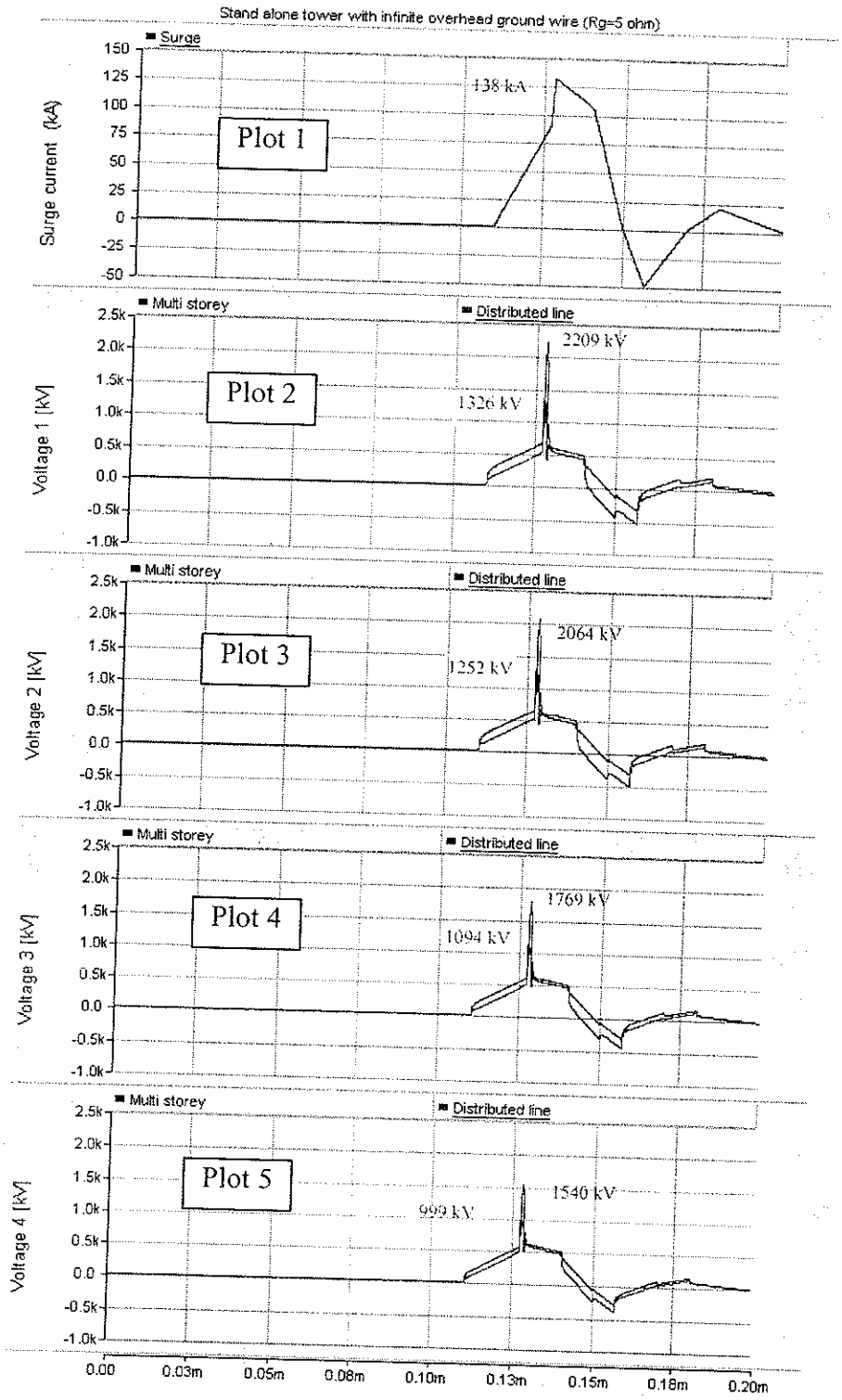

Fig. 3-15 The response of the transmission tower equipped with an infinite ground wire to a piecewise linear surge waveform, R_g=5Ω. See Fig. 3-8 for explanation of Plots 2 to 5.

It can be seen from the Fig. 3-15 that despite the fact that the voltage waveforms corresponding to the two models are almost similar, the peak voltage values are different.

3.2.2 Three transmission towers equipped with overhead ground wires and phase conductors

The simulation of the field experiment described in [14], which employs both transmission tower modeling techniques, offers the opportunity of comparing the simulation results with the experimental data in order to determine which one of the two models provides the most accurate representation of the transmission tower. In PSCad simulation only three of the towers were used instead of seven as in the field experiment. This was due to the limitation of the software edition that was available for this study and due to the fact that the results would not have been significantly different had the seven tower configuration been used. After choosing the model, the system response to two different types of double exponential surge waveforms for several ground resistance values will be analyzed.

3.2.2.1 System response to a piecewise linear surge waveform

Fig. 3-16 shows the equivalent circuit for the Multi Storey model and the Distributed Constant Line model equivalent circuit for transmission tower with two neighbouring towers, equipped with ground wires and phase conductors, subjected to a piecewise linear surge waveform whose characteristics are presented in Table 3-3. This equivalent circuit is explained in detail in Appendix F. The Multi Storey model parameters for the three towers as described in [15] are shown in Table 3-6. The Distributed Constant Line model parameters for the three towers are presented in Table 3-7 and were calculated using equations (2.10) - (2.13).

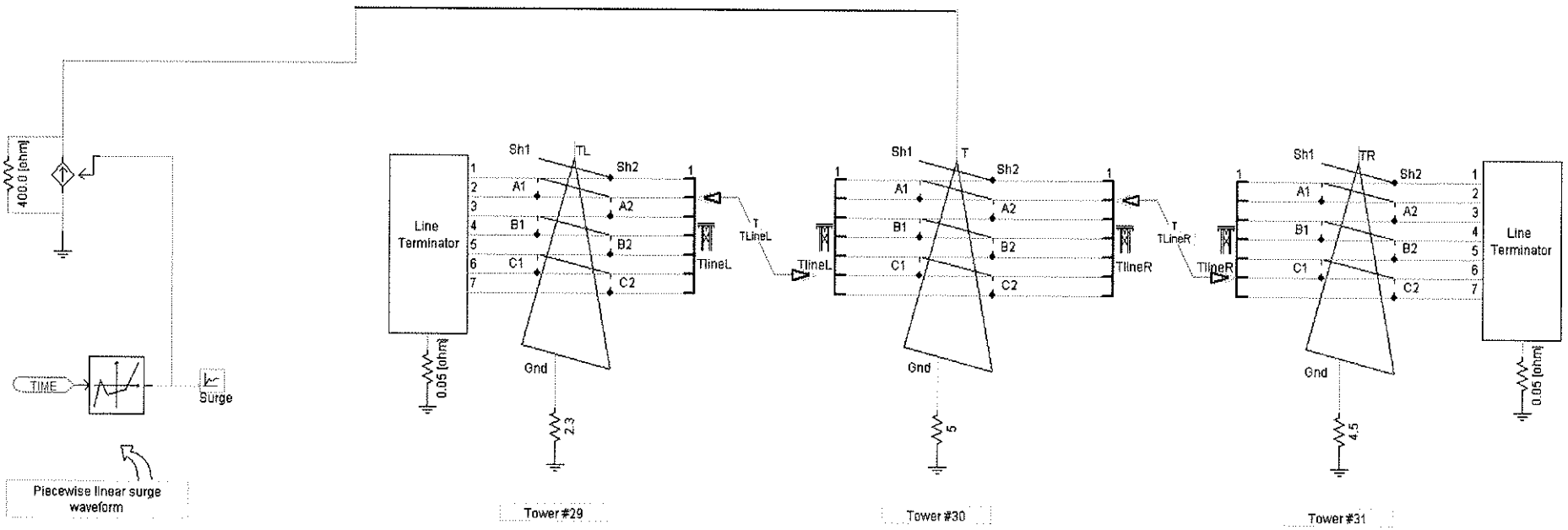

Fig. 3-15 The equivalent circuit for transmission tower with two neighbouring towers, equipped with ground wires and phase conductors, subjected to a piecewise linear surge waveform in PSCad simulation

Table 3-6 Multi Storey Model parameters

Section	Tower #29				Tower #30				Tower #31			
	Imped. Z	Resist. R	Induct. L	Length l	Imped. Z	Resist. R	Induct. L	Length l	Imped. Z	Resist. R	Induct. L	Length l
	[Ω]	[Ω]	[μsec]	[m]	[Ω]	[Ω]	[μsec]	[m]	[Ω]	[Ω]	[μsec]	[m]
I	120	9.3	3.68	13	120	5.83	2.3	5	120	9.3	3.68	13
II	120	9.45	3.74	13.2	120	11.7	4.61	10	120	9.45	3.74	13.2
III	120	8.02	3.17	11.2	120	9.37	3.69	8	120	8.02	3.17	11.2
IV	120	26.78	10.6	22	120	26.8	10.60	36.4	120	26.78	10.6	22
Span length [m]	182				437							

Table 3-7 Distributed Constant Line Model parameters

Section	Tower #29						Tower #30						Tower #31					
	Impedance			Length			Impedance			Length			Impedance			Length		
	Main legs Z_T	Bracings $Z_L=9*Z_T$	Crossarms Z_A	Main legs L_T	Bracings $L_L=15*L_T$	Crossarms L_A	Main legs Z_T	Bracings $Z_L=9*Z_T$	Crossarms Z_A	Main legs L_T	Bracings $L_L=15*L_T$	Crossarms L_A	Main legs Z_T	Bracings $Z_L=9*Z_T$	Crossarms Z_A	Main legs L_T	Bracings $L_L=15*L_T$	Crossarms L_A
	[Ω]	[Ω]	[Ω]	[m]	[m]	[m]	[Ω]	[Ω]	[Ω]	[m]	[m]	[m]	[Ω]	[Ω]	[Ω]	[m]	[m]	[m]
I	116	1048	222	13	19.5	8	108	968	222	5	7.5	6	116	1048	222	13	19.5	8
II	100	898	213	13.2	19.8	9.5	100	903	222	10	15	8.3	100	898	213	13.2	19.8	9.5
III	75	672	194	11.2	16.8	15	83	748	212	8	12	10.7	75	672	194	11.2	16.8	15
IV	43	389	178	22	33	10.6	73	661	209	36.4	54.6	9.5	43	389	178	22	33	10.6
Span length [m]	182						437											

The simulation results are shown in Fig. 3-17. The surge current injected on the top of the central transmission tower is shown in Plot 1. The voltages corresponding to section 1 to section 4 of Ishii model, starting with the topmost section, are shown in Plot 2 to Plot 5 (the blue curve). For Hara model, the voltages recorded at the tip of the tower crossarms, starting with the one holding the ground wire, are also shown in Plot 2 to Plot 5 (the green curve).

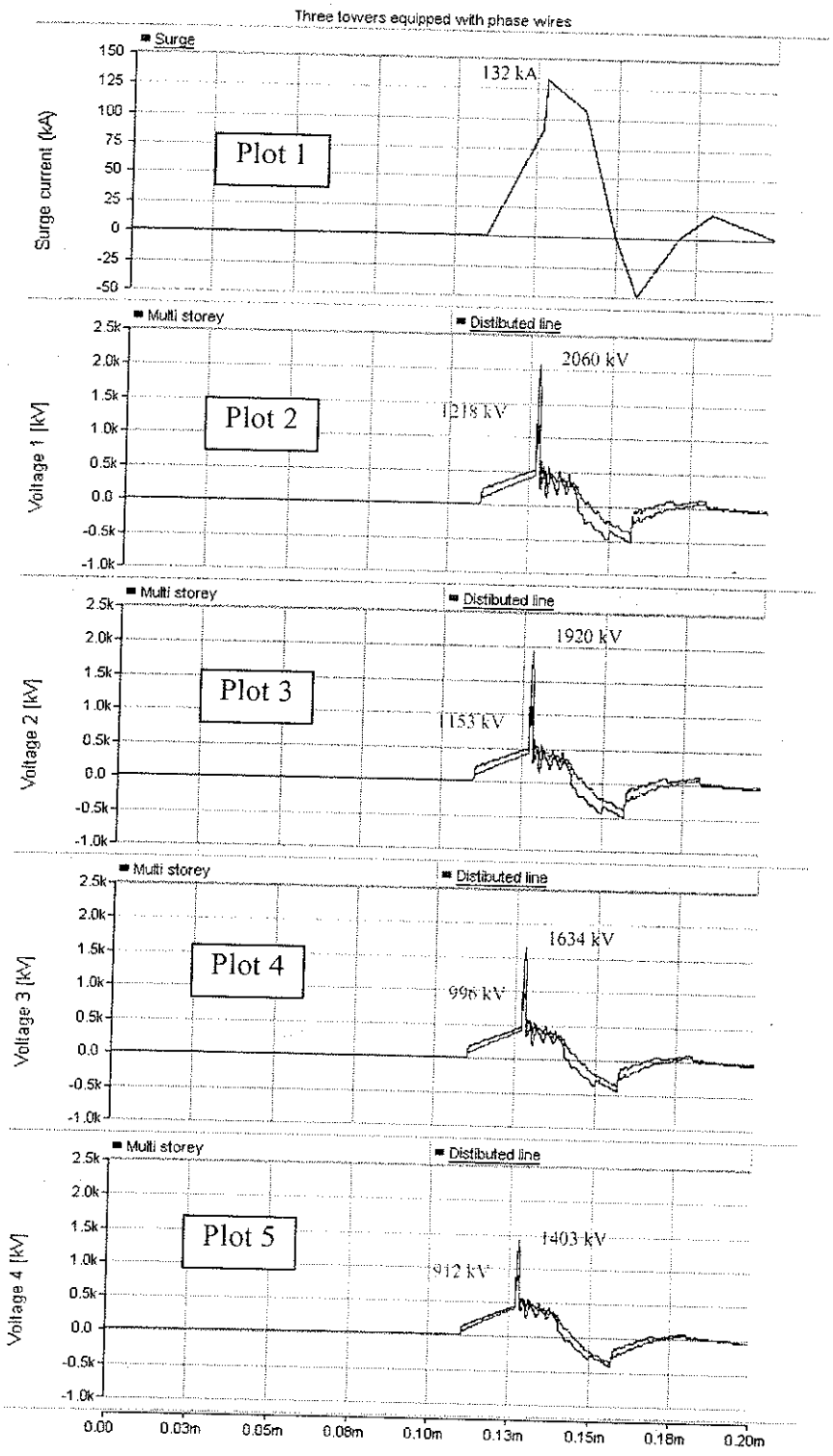

Fig. 3-17 The response of the transmission tower with two neighbouring towers equipped with ground wire and phase conductors to a piecewise linear surge waveform. See Fig. 3-8 for explanation of Plots 2 to 5.

According to the authors in [14], the calculated peak values of the induced voltage across each insulator string were in agreement with the measured ones: at the first insulator string V=1174 kV, at the second insulator string V=1061 kV and at the third insulator string V=932 kV. In Fig. 3-15 it can be noticed that the voltage peak values corresponding to the Distributed Constant Line model (Hara model) are similar to those presented in [14]: at the first insulator string V=1153 kV, at the second insulator string V=996 kV and at the third insulator string V=912 kV. The voltages corresponding to the Multi Storey model (Ishii model) are much higher. Since the Distributed Constant Line model (Hara model) represents the transmission tower most accurately, it will be used in further studies in this thesis. Also, by comparing the plots from Fig. 3-15 and Fig. 3-17 it can be noticed that in the case of a transmission tower with two neighboring towers equipped with phase and overhead ground wires, the peak values of the induced voltages recorded on the middle tower are approximate 100 kV lower than in the case of a stand alone tower equipped with infinite overhead ground wires.

3.2.2.2 System response to a double exponential surge waveform

In this section, the effect of ground resistance variation on induced voltage magnitudes and waveforms when the system is contacted by a fast and a slow surge current is investigated.

The three tower system described in 3.2.2.1 is subjected to a 1.5/51.75 μsec, 50 kA and 8/20 75 μsec, 50 kA double exponential waveforms. The towers are modeled using the Distributed Constant Line modeling technique (Hara model). The ground

resistances are equal for each tower and are assigned subsequently three values: 0, 50 and 100 Ω. Simulation results are shown in Fig. 3-18 and Fig. 3-19.

The surge current is shown in Plot 1 of each figure. The voltages corresponding to the three resistance values, recorded at the tip of the tower crossarm holding the ground wire, are shown in Plot 2 of each figure. Also, the voltages corresponding to the three resistance values, recorded at the tip of the tower crossarm holding the phase wires are shown in Plot 3, Plot 4 and Plot 5 (the blue curve corresponds to R_g =0 Ω, the green curve corresponds to R_g =50 Ω and the red curve corresponds to R_g =100 Ω).

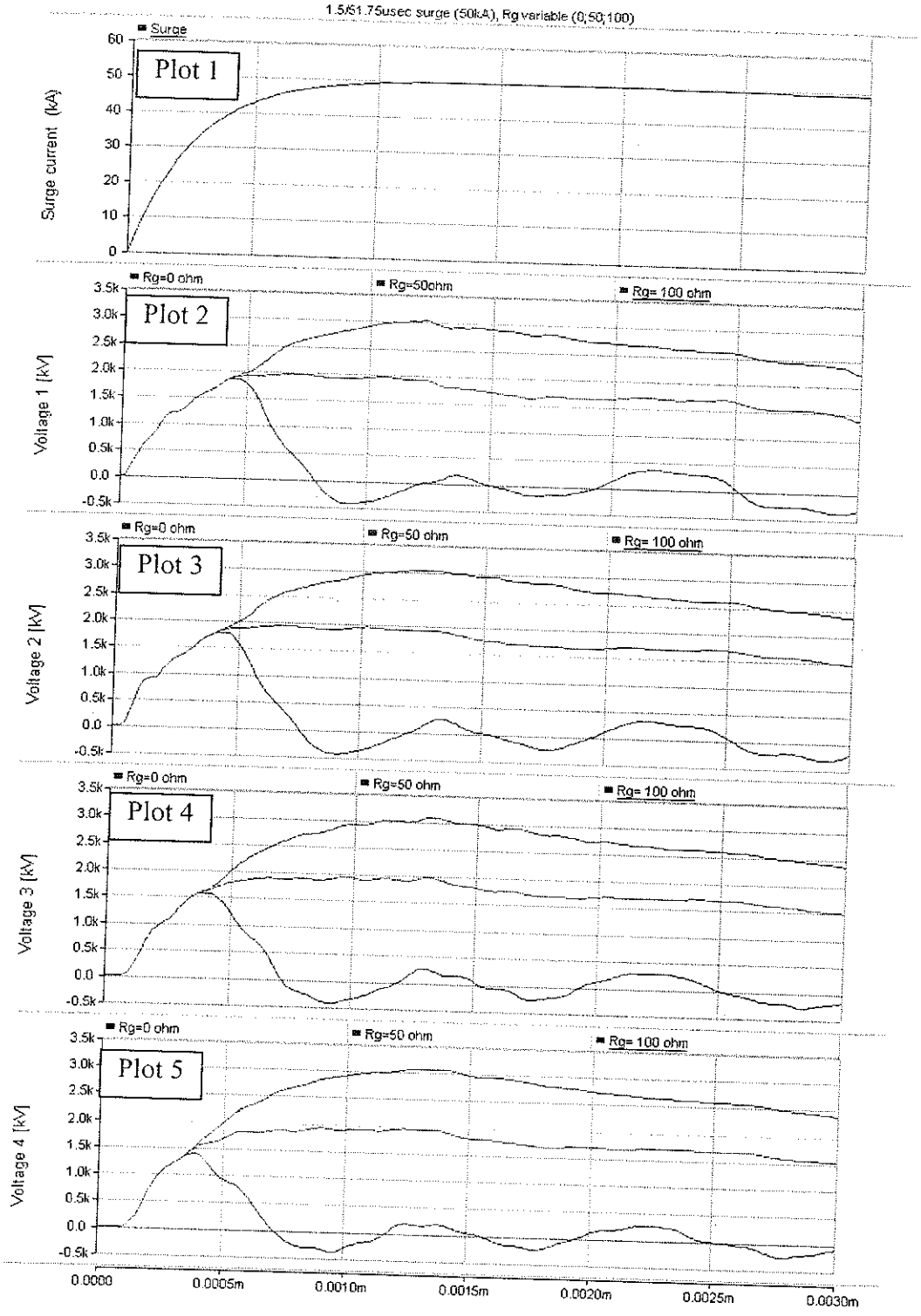

Fig. 3-18 The response of the transmission tower with two neighbouring towers equipped with ground wire and phase conductors to a 1.5/51.75 μsec, 50 kA surge waveform. See Fig. 3-8 for explanation of Plots 2 to 5.

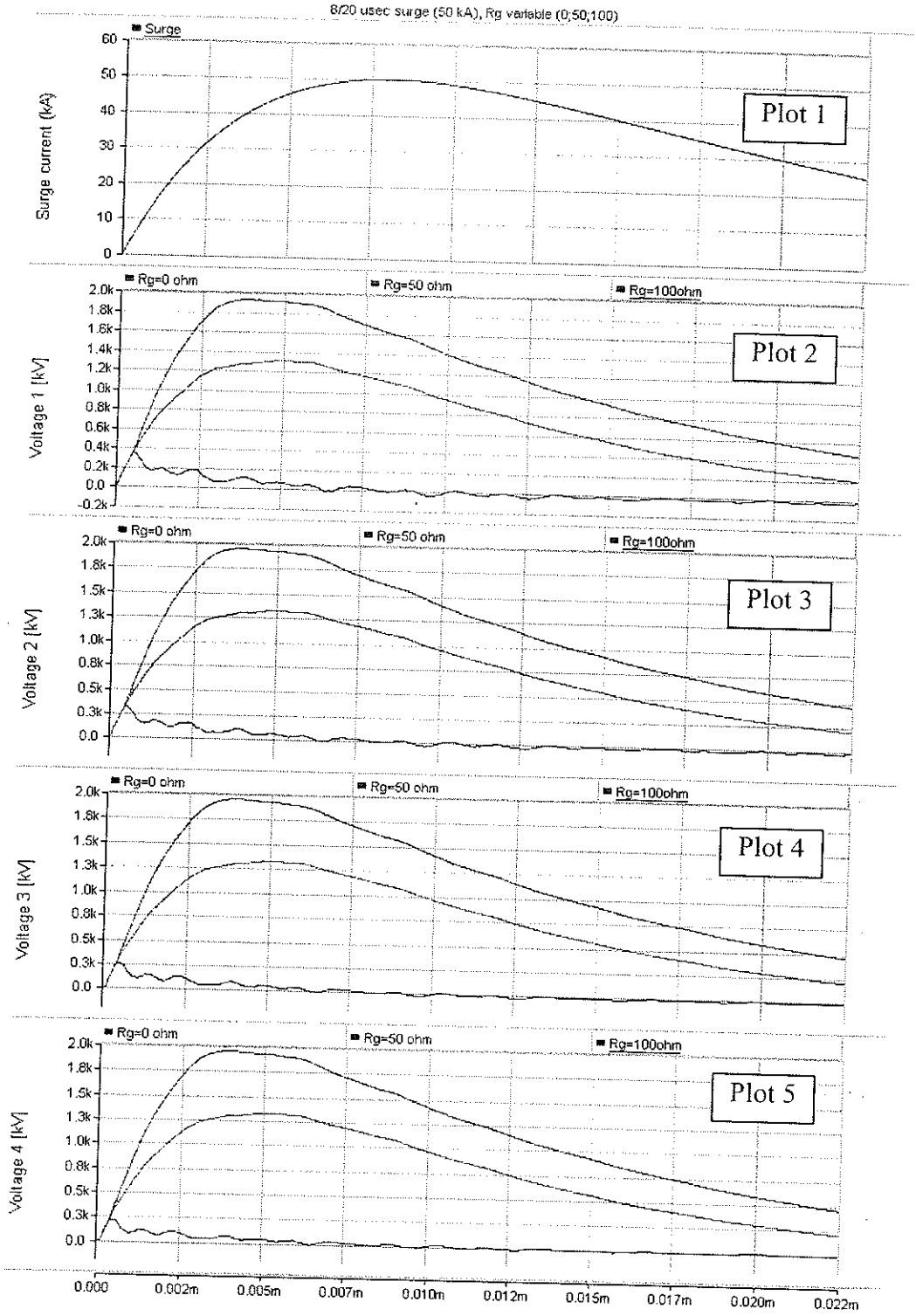

Fig. 3-19 The response of the transmission tower with two neighbouring towers equipped with ground wire and phase conductors to a 8/20 μsec, 50 kA surge waveform. See Fig. 3-8 for explanation of Plots 2 to 5.

It may be seen from Fig. 3-18 and Fig. 3-19 that the magnitude and the waveform of the induced voltage developed at each tower arm tip are more sensitive to the variation of ground resistance when the tower is contacted by a slow surge waveform. In the case of a fast surge waveform, the effect of variation of ground resistance on the induced voltages can be neglected for lower resistance values.

CHAPTER 4

INVESTIGATION OF THE DYNAMIC MODEL OF GROUND

The ground model considered for this study is the Soil Ionization Dynamic Model developed by Alemeida and Correia [18], presented in section 2.2. The model is based on the "Dynamic Model of Ground" proposed by A.C. Liew and M. Darveniza [12] which describes the variation of ground resistance with the impulse current. The model proposed by Alemeida and Correia was also chosen due to the fact that the authors presented also a numerical algorithm. This model will be used to reproduce the experimental results obtained by Bellaschi [19] and presented also by Liew and Darveniza in [12].

4.1 Algorithm description

A Matlab code was written based on the algorithm presented in [18]. The cylinder – hemisphere concept described by Liew and Daveniza is used for modelling the region surrounding the ground electrode of radius r_0 and length l Fig. 4-1. This area is discretized into n number of shells, having equipotential surfaces.

$$n = \frac{r_M - r_0}{\Delta r} \tag{4.1}$$

where r_M is the maximum distance around the rod and Δr the discretization step.

Each shell element is subjected to the impulse current. As the current increases, the electric field intensity will reach at one point the critical value E_c. The area A_k corresponding to an elemental shell *k* is calculated as

$$A_k = 2\pi r_k l + 2\pi r_k^2 \tag{4.2}$$

The time interval for which the simulation is performed is divided into small time steps Δt. At each time step, the electric field is calculated as

$$E_k = \rho_{0k}\, I(t)/A_k \tag{4.3}$$

where $\rho_{0k} = \rho_0$, ρ_0 being the initial value of resistivity , for $E_k < E_c$. For the case when $E_k > E_c$, the resistivity is given by

$$\rho_k = \rho_{ik} + (\rho_{0k} - \rho_{ik})\left(1 - e^{-\frac{t_k}{\tau_2}}\right) \tag{4.4}$$

where ρ_{ik} is the value of the resistivity evaluated at a previous time step.

As the current decreases from its maximum value, the resistivity is obtained as

$$\rho_k = \rho_{lk} + (\rho_0 - \rho_{lk})\left(1 - e^{-\frac{t_{lk}}{\tau_2}}\right)\left(1 - \frac{E_k}{E_c}\right)^2 \tag{4.5}$$

where ρ_{lk} is the lowest value of the resistivity reached by the elemental shell k during ionization at t_{lk}. Finally, the total resistance calculated at each time step, is the summation of the resistances of all shells, each shell resistance being calculated as

$$R_k = \frac{\rho_k}{A_k}\Delta r \tag{4.6}$$

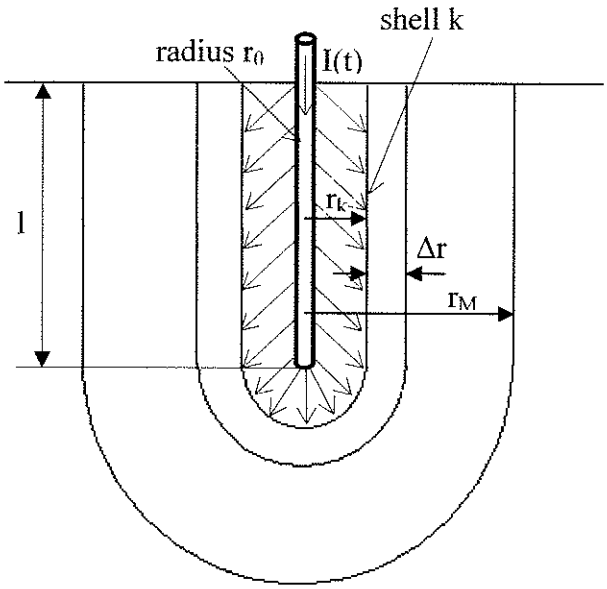

Fig. 4-1 The geometry of the region surrounding the ground electrode.

4.2 Computation results

The input parameters are shown in Table 4-1 and they are the same as the ones corresponding to the three types of soil used for the experimental tests in [12]. The double exponential waveforms and the peak values of the surge current were determined from the plots describing the experimental results conducted by Bellaschi. The computation results representing the variation of ground voltage and resistance vs. time as well as the hysteresis variation of ground resistance vs. surge current are shown in Fig. 4-2 to Fig. 4-7.

Table 4-1 Input parameters used in computation

Ground type		Clay	Sand	Gravel and sand
Soil parameters	Resistivity ρ_0 [Ωcm]	8720	15700	31000
	Breakdown gradient E_c [kV/cm]	1.27	2	0.7
	Ionization time constant τ_1 [μsec]	1.5	2	2
	Deionization time constant τ_2 [μsec]	0.5	0.5	2
Electrode parameters	Radius of the rod r_0 [mm]	12.7	7.94	12.7
	Depth buried l [m]	3.05	2.16	2.44
Surge current	Peak value [kA]	11	6.6	5.5
	Front time/tail time [μsec]	18/37	16/40	20/60

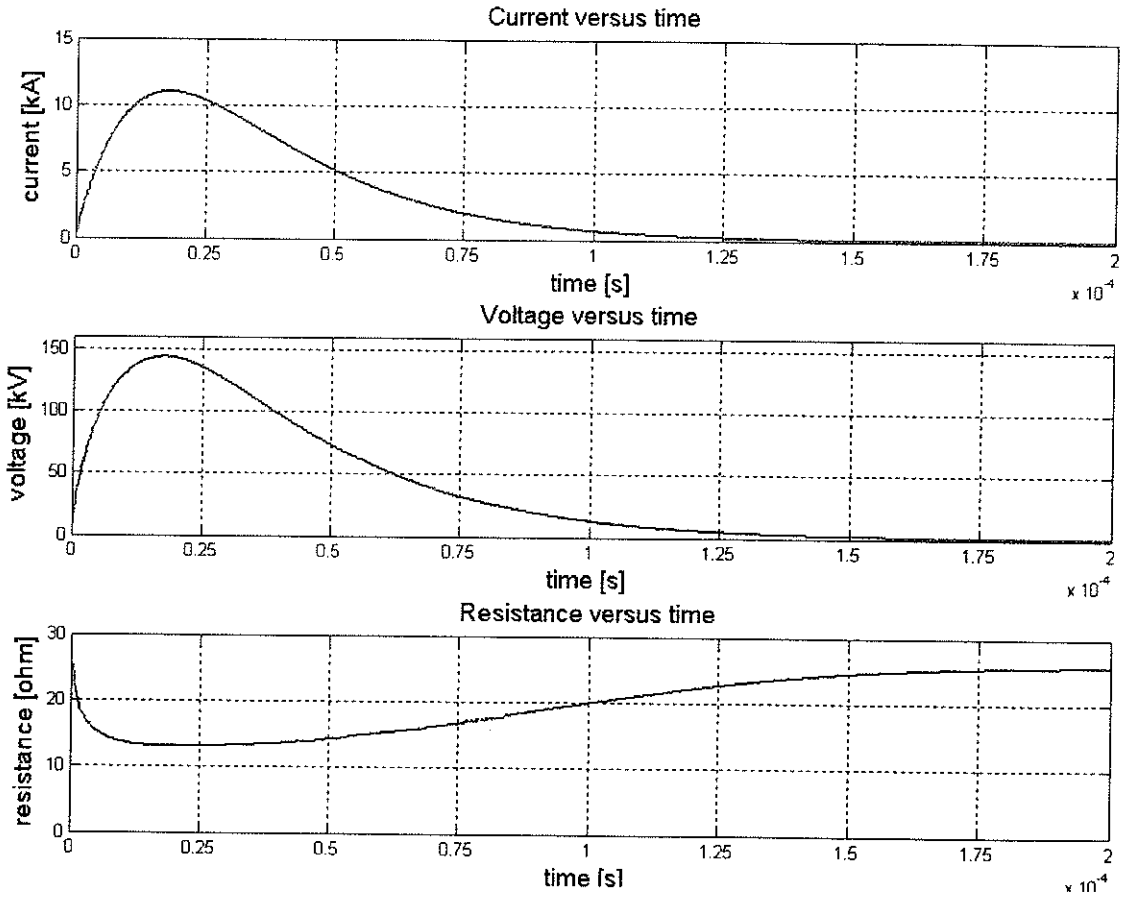

Fig. 4-2 Variation of ground voltage and resistance vs. time for a given current when the rod is embedded in clay having a resistivity of 8720 Ωcm.

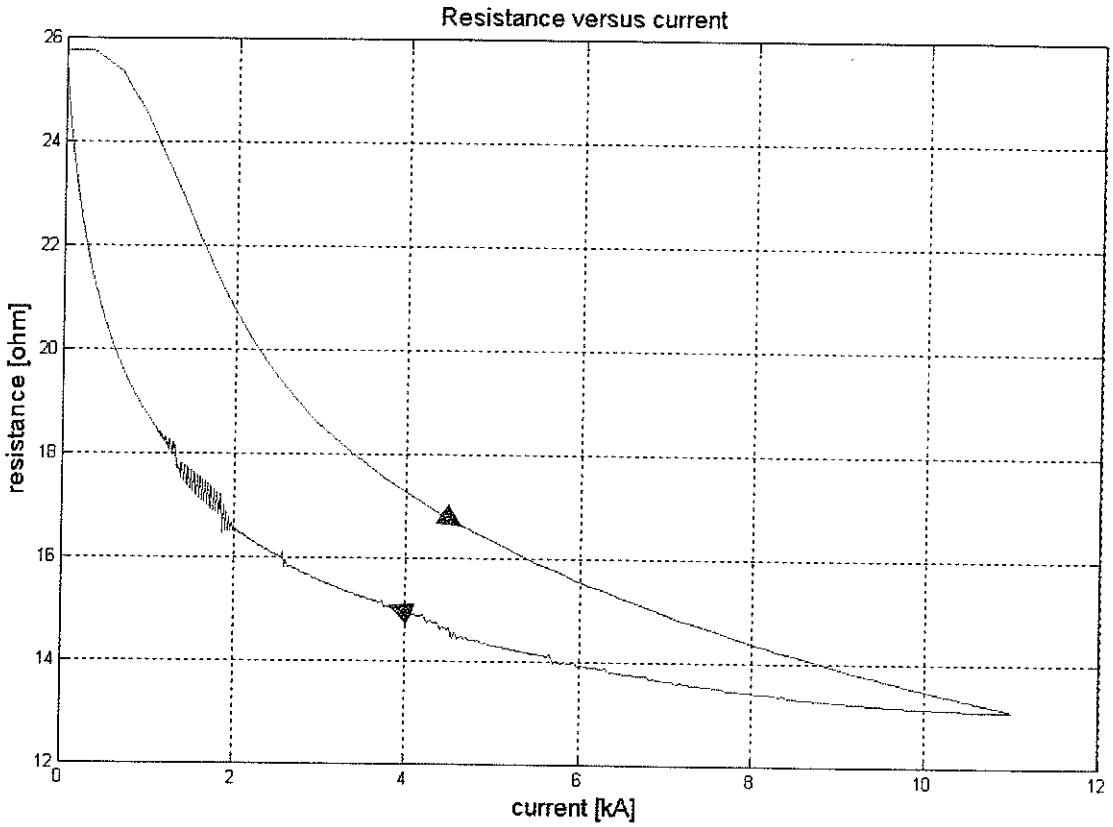

Fig. 4-3 Variation of ground resistance vs. surge current for a rod embedded in clay having a resistivity of 8720 Ωcm.

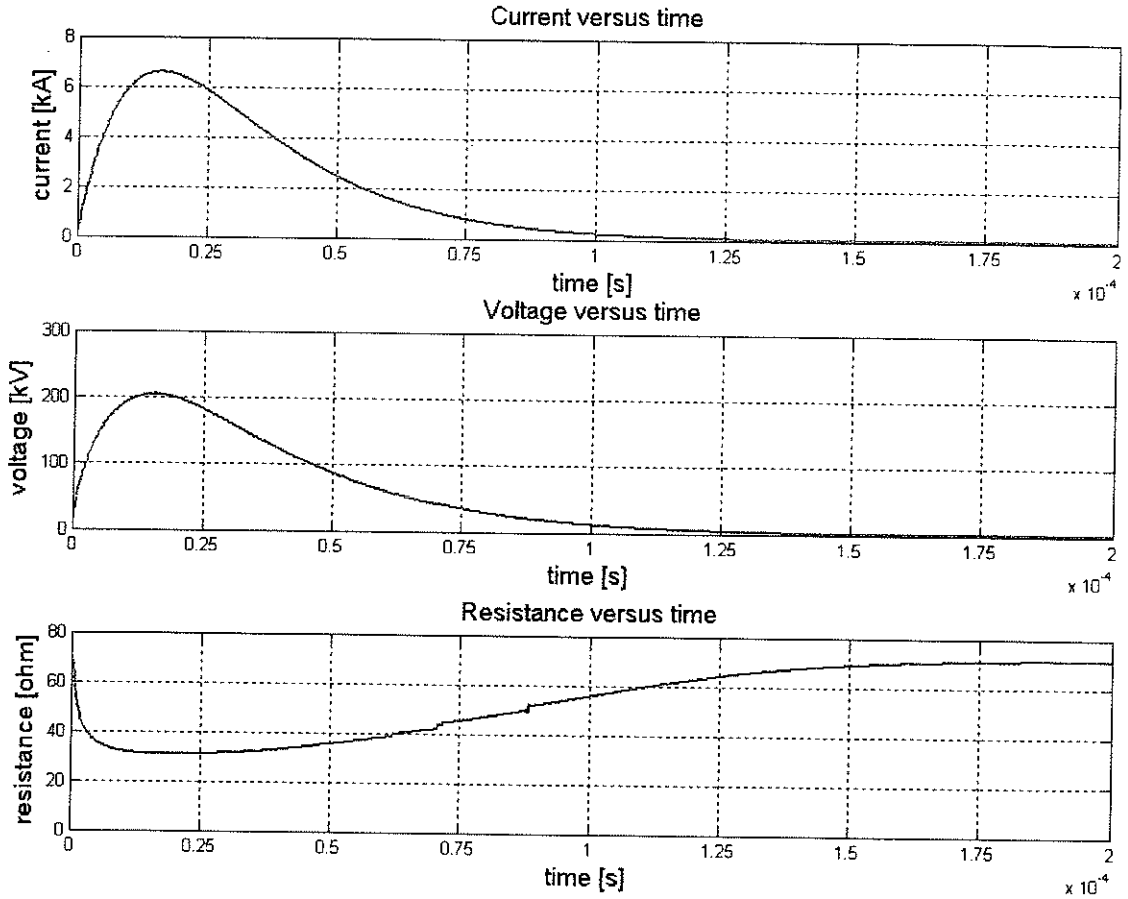

Fig. 4-4 Variation of ground voltage and resistance vs. time for a given current when the rod is embedded in sand having a resistivity of 15700 Ωcm.

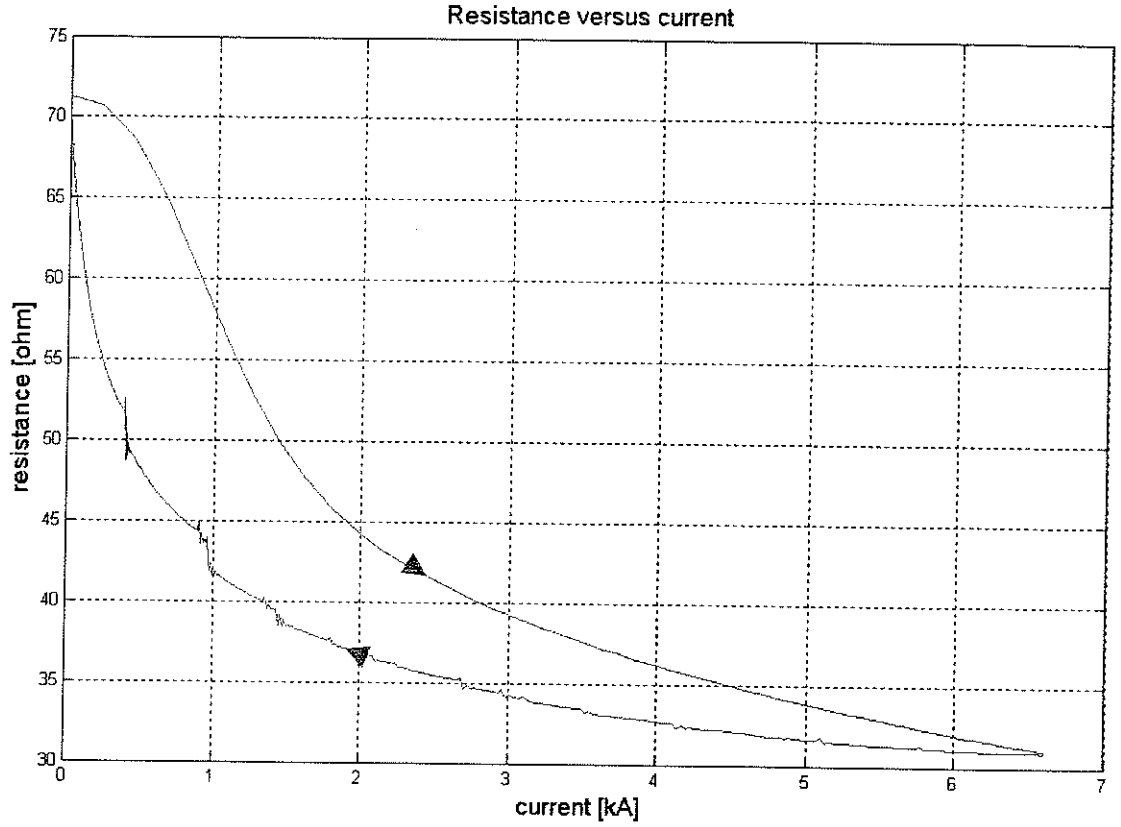

Fig. 4-5 Variation of ground resistance vs. surge current when the rod is embedded in sand having a resistivity of 15700 Ωcm.

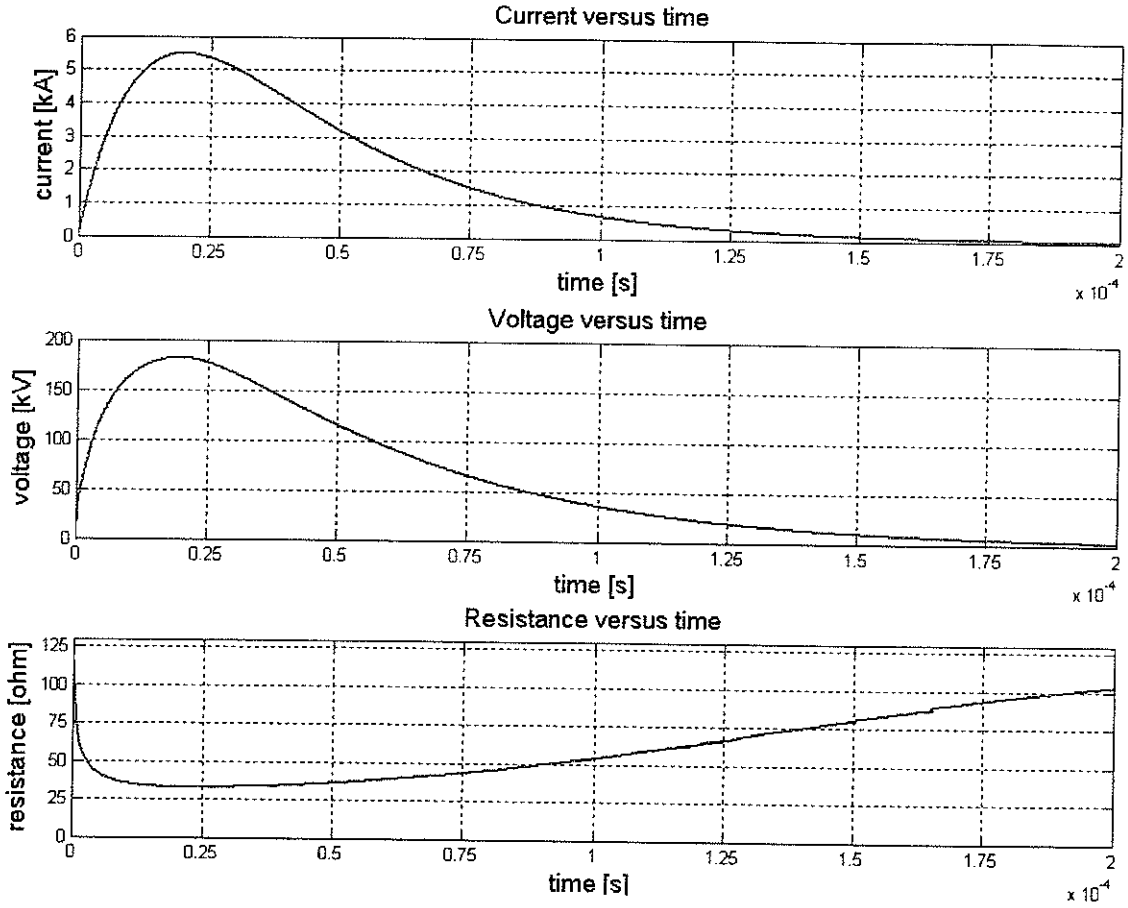

Fig. 4-6 Variation of ground voltage and resistance vs. time for a given current when the rod is embedded in gravel and sand mix having a resistivity of 31000 Ωcm.

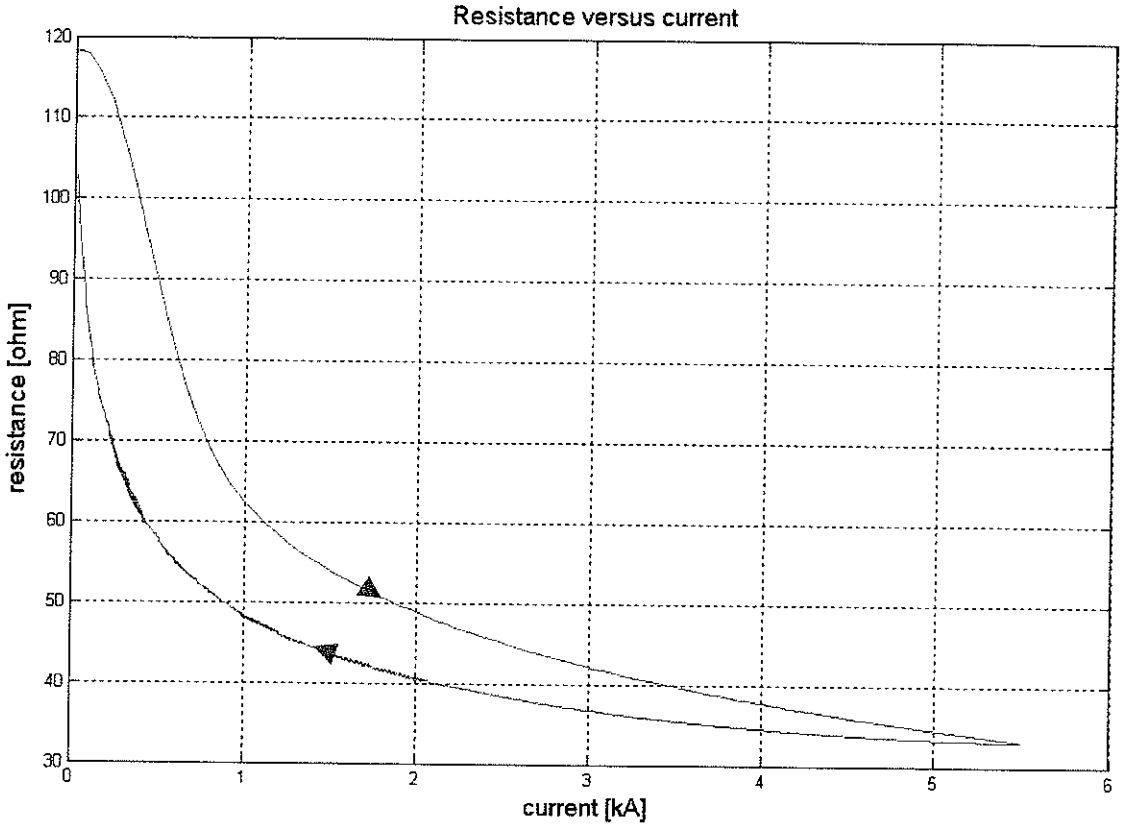

Fig. 4-7 Variation of ground resistance vs. surge current for a rod embedded in sand and gravel mix having a resistivity of 31000 Ωcm.

The simulation results are in good agreement with the experimental results obtained by Bellaschi, and with the simulation results obtained by Liew and Darveniza, Almeida and Correia. Therefore, this model will be used in further study in the following chapters.

CHAPTER 5

EFFECT OF COMBINING THE TOWER AND GROUND MODELS

In this chapter, the relative sensitivity of tower and ground models is examined by combining the Distributed Constant Line transmission tower model (Hara model) with the Soil Ionization Dynamic ground model (Almeida and Correia model). The behaviour of the combined model of tower and ground in various cases has been simulated using PSCad. Two cases have been considered: Case 1: a stand alone tower without phase wires, with an infinitely extending ground wire connected at one of the ends of the topmost crossarm of the tower, and variable/constant ground resistance, Case 2: an unenergized, three phase, double circuit transmission line in three tower configuration equipped with phase wires and a ground wire connected at one end of the topmost crossarm of each tower, and variable/constant ground resistance. In both cases, the ground model uses the parameters corresponding to the three types of soil (clay, sand and sand and gravel mix) employed in the experimental tests [12] which were discussed in the previous chapter. The combined model of tower and ground has been subjected to three types of surge currents (18/37 μsec with 11 kA peak value for clay, 16/40 μsec with 6.6 kA peak value for sand and 20/60 μsec with 5.5 kA peak value for gravel and sand) used also in the experimental tests referred to in Chapter 4 . The ground resistance corresponding to each type of soil has been modeled as function of the current appearing at the base of the tower which is injected into ground.

In the PSCad simulation, the dynamic behaviour of the ground resistance was represented by a variable resistor controlled by a non-linear transfer characteristic component found in the PSCad library. The current – ground resistance transfer characteristics used in the PSCad simulation were determined from Fig. 5-1, Fig. 5-3, Fig. 5-5, Fig. 5-7, Fig. 5-9, Fig. 5-11. The simulation results obtained by employing a variable ground resistance were compared with the ones using a constant ground resistance. The constant resistance was calculated as the average of two ground resistances, one corresponding to zero current and the other corresponding to the crest value of current.

5.1 Case 1: Stand alone transmission tower equipped with infinitely extending overhead ground wire and variable / constant ground resistance

The equivalent circuit for the transmission tower is similar to the one shown in Fig. 3-12. The tower equipped with infinitely extending ground wires is subjected to double exponential surge waveforms whose characteristics are shown in Table 4-1 along with the ground model parameters. Simulation results are shown in Fig. 5-2, Fig. 5-4 and Fig. 5-6. The surge current along with the current appearing at the base of the tower are shown in Plot 1 of each figure (the blue curve is the surge current at the top of the tower and the green curve is the current at the base of the tower). The simulation results

consist in the voltages recorded at the tip of each of the four crossarms of the transmission tower. These voltages are shown in Plot 2 to Plot 5 of Fig. 5-2, Fig. 5-4 and Fig. 5-6 (the blue curve represents the voltage corresponding to a variable ground resistance, and the green curve represents the voltage corresponding to a constant ground resistance). The voltages shown in Plot 2 of each figure were recorded at the connection with the ground wire and the following voltages shown in Plot 3, Plot 4 and Plot 5 were recorded at the connection with the high voltage insulators.

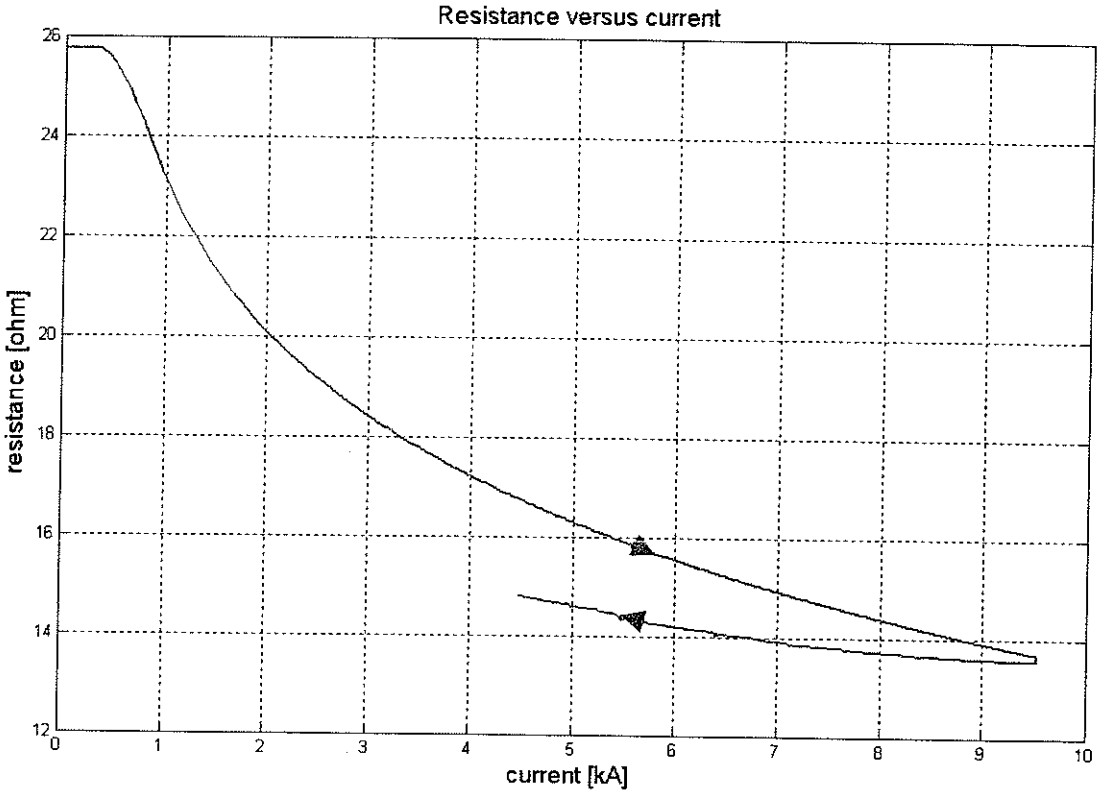

Fig. 5-1 Variation of ground resistance vs. current injected into clay having a resistivity of 8720 Ωcm, when the tower top is subjected to 18/37 μsec with 11 kA peak value (one tower configuration)

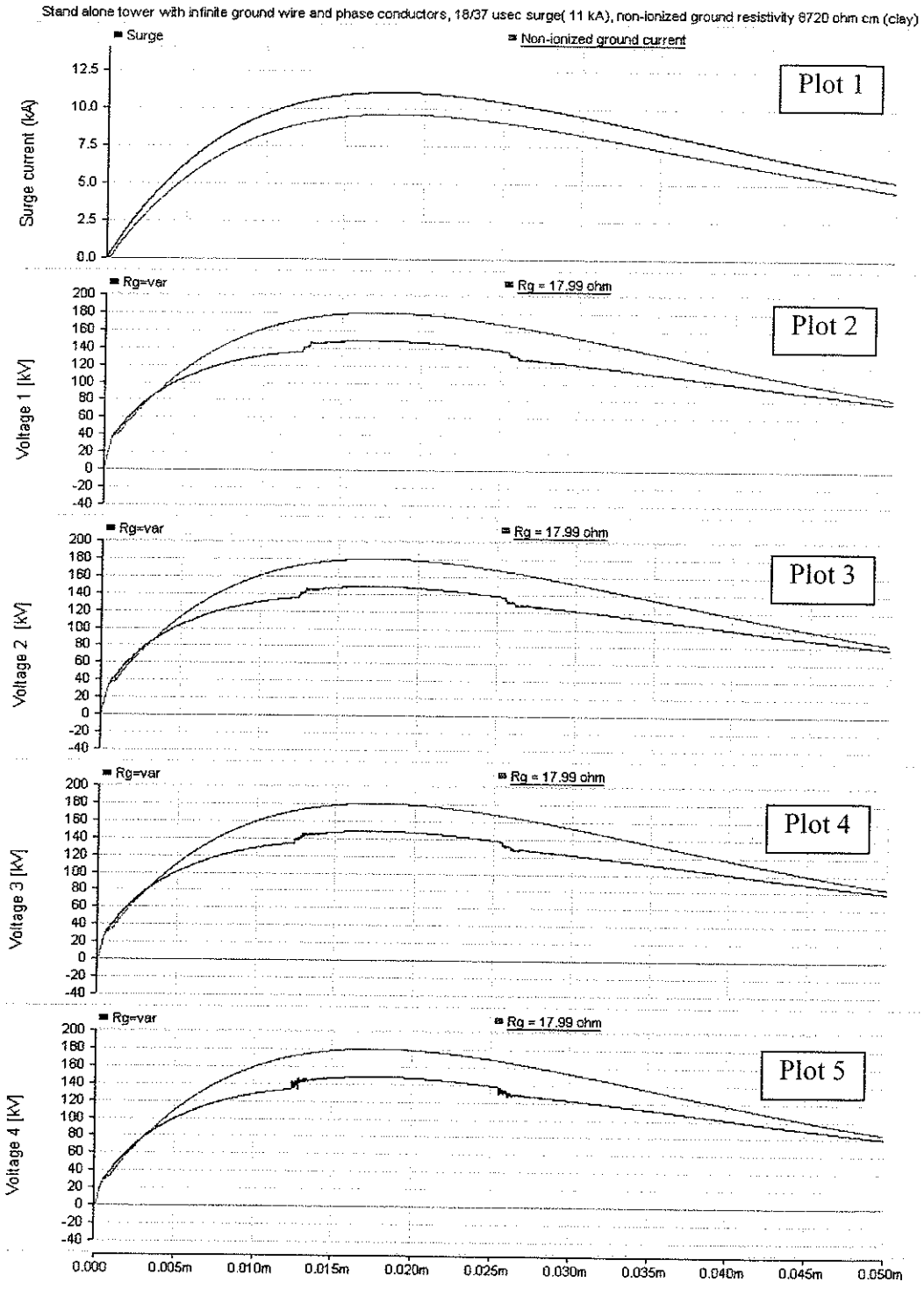

Fig. 5-2 The response of the transmission tower equipped with an infinite ground wire to a 18/37 μsec (11 kA) surge waveform, non-ionized ground resistivity =8720 Ωcm (clay), Rg=var / Rg = 17.99 Ω average value of the variable ground resistance

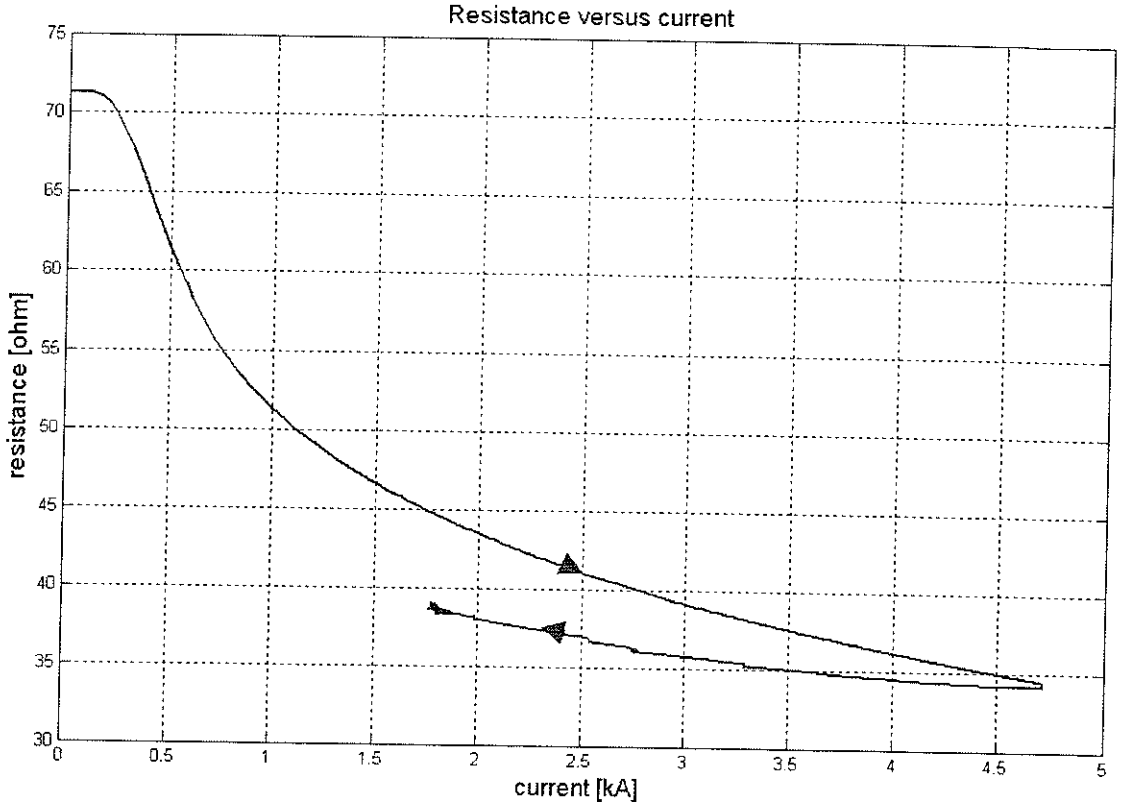

Fig. 5-3 Variation of ground resistance vs. current injected into sand having a resistivity of 15700 Ωcm, when the tower top is subjected to 16/40 μsec with 6.6 kA peak value (one tower configuration)

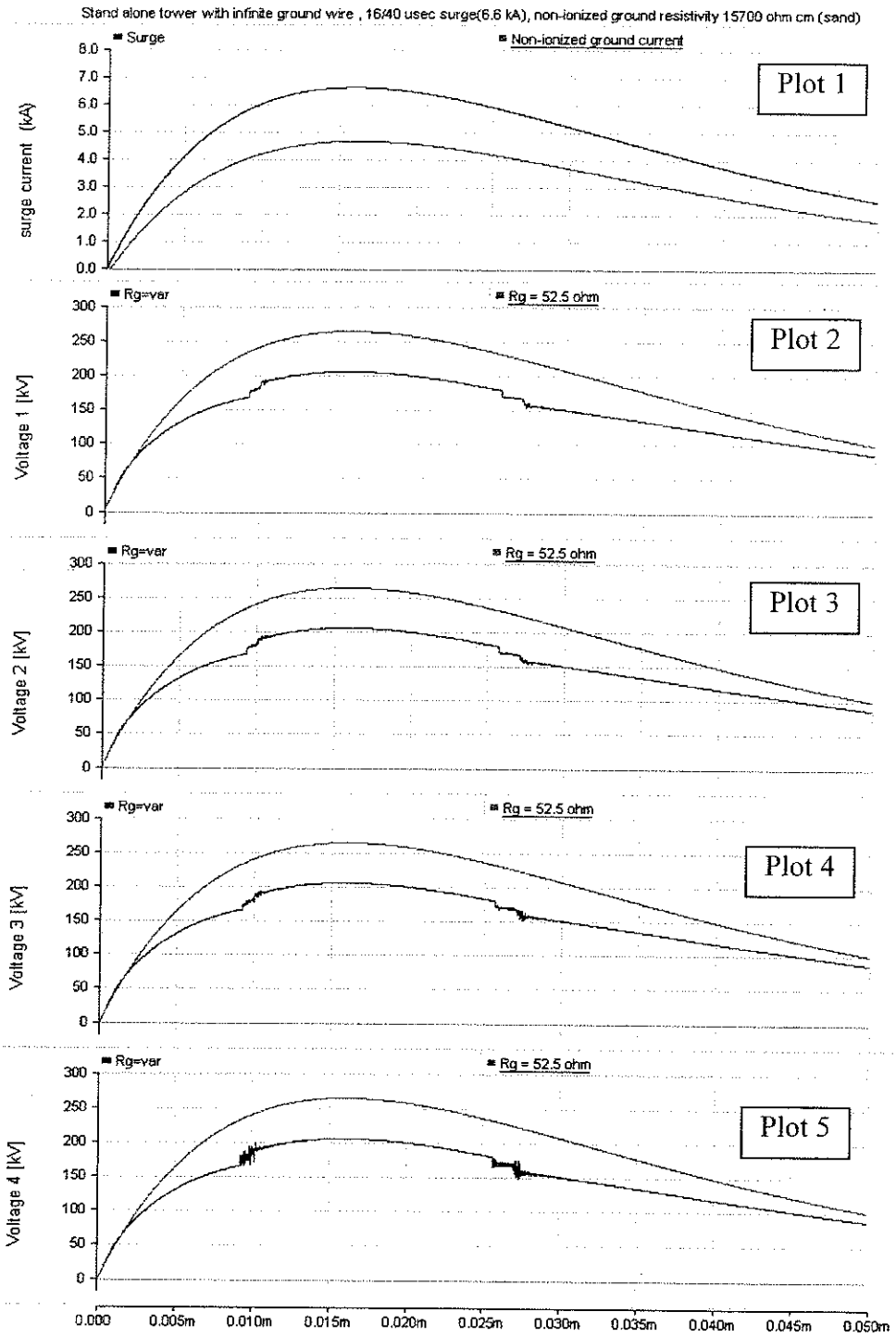

Fig. 5-4 The response of the transmission tower equipped with an infinite ground wire to a 16/40 μsec (6.6 kA) surge waveform, non-ionized ground resistivity =15700 Ωcm (sand), Rg=var / Rg = 52.5 Ω average value of the variable ground resistance

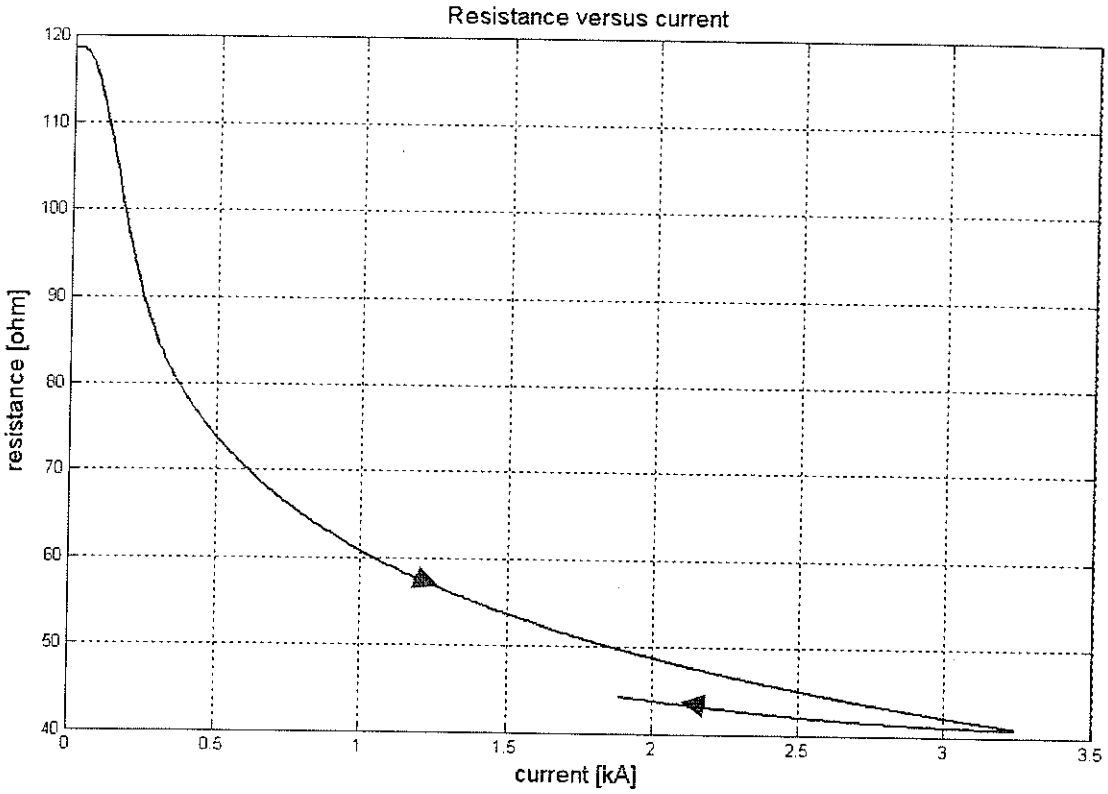

Fig. 5-5 Variation of ground resistance vs. current injected into gravel and sand having a resistivity of 31000 Ωcm, when the tower top is subjected to 20/60 μsec with 5.5 kA peak value (one tower configuration)

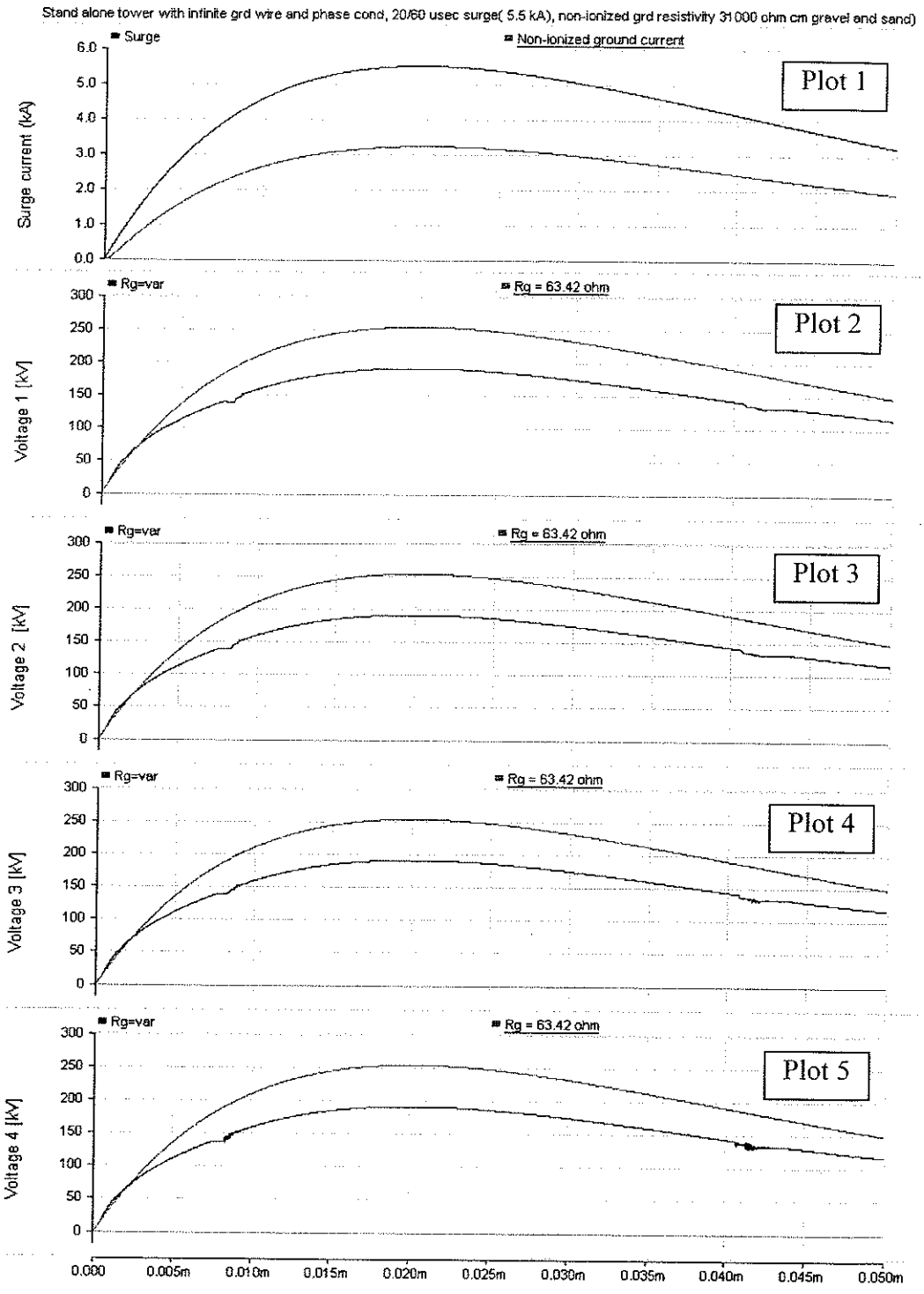

Fig. 5-6 The response of the transmission tower equipped with an infinite ground wire to a 20/60 μsec (5.5 kA) surge waveform, non-ionized ground resistivity =31000 Ωcm (clay), Rg=var / Rg = 63.42 Ω average value of the variable ground resistance

It may be seen from Fig. 5-2, Fig. 5-4 and Fig. 5-6 that the voltage magnitudes at the tip of the tower crossarms depend on how the ground is modeled, as a constant or variable value. This leads to the conclusion that the dynamic behaviour of the ground resistance as a function of surge current has an impact over the voltage values recorded at the tip of the tower crossarms. Also, one can notice the similitude of the magnitudes and waveshapes of these voltages with the voltages across ground resistance recorded when the ground electrodes are subjected to the same surge currents (Fig. 4-2, Fig. 4-4 and Fig. 4-6).The simulation results in the case of a stand alone transmission tower equipped with infinitely extending ground wire and a variable ground resistance which is subjected to various slow surge currents, showed similarities with the ones for which the same slow surge currents are injected directly into the ground, described in Chapter 4.

5.2 Case 2: Three transmission towers equipped with overhead ground wires and phase conductors and variable / constant ground resistance

Fig. 3-15 shows the equivalent circuit for the transmission tower with two neighboring towers, equipped with ground wires and phase conductors. The model parameters for the three towers are shown in Table 3-7. The central tower is subjected to double exponential surge waveform whose characteristics are shown in Table 4-1

along with the ground model parameters. Simulation results are shown in Fig. 5-8, Fig. 5-10 and Fig. 5-12. The surge current along with the current appearing at the base of the tower are shown in Plot 1 of each figure (the blue curve is the surge current at the top of the tower and the green curve is the current at the base of the tower). The simulation results consist in the voltages recorded at the tip of each of the four crossarms of the central transmission tower. These voltages are shown in Plot 2 to Plot 5 of Fig. 5-8, Fig. 5-10, Fig. 5-12 (the blue curve represents the voltage corresponding to a variable ground resistance and the green curve represents the voltage corresponding to a constant ground resistance). The voltages shown in Plot 2 of each figure were recorded at the connection with the ground wire and the following voltages shown in Plot 3, Plot 4 and Plot 5 were recorded at the connection with the high voltage insulators connected to the phase wires.

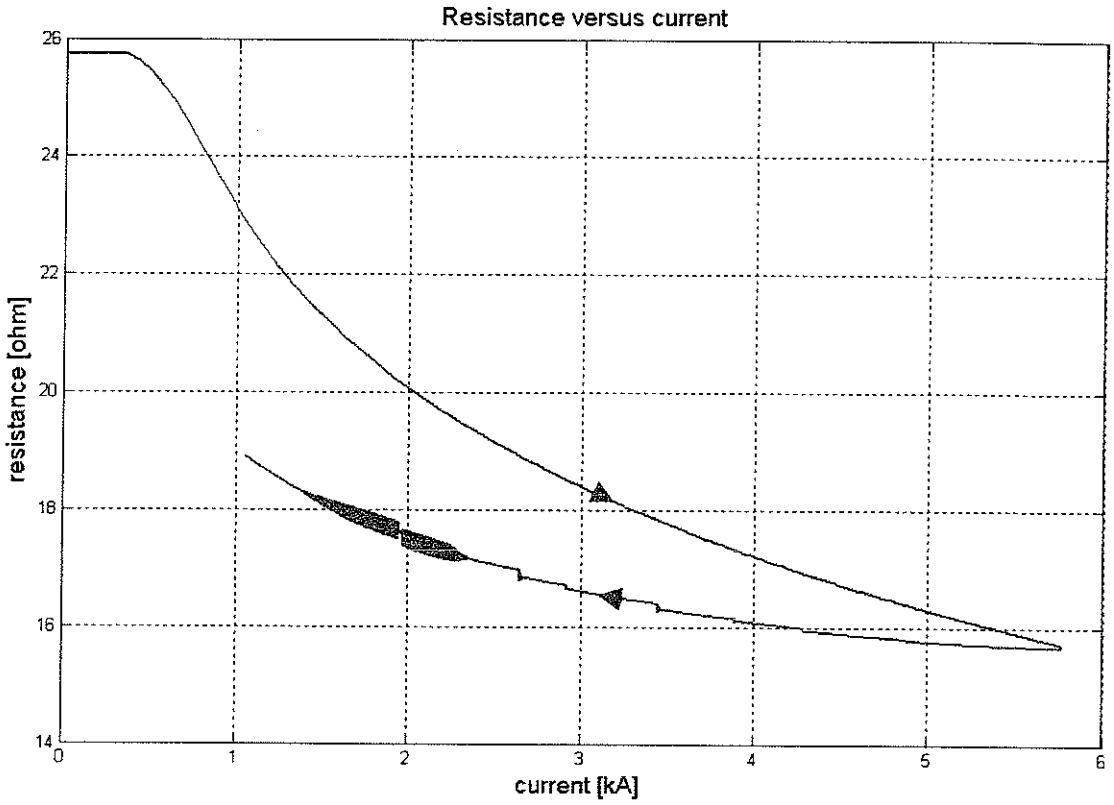

Fig. 5-7 Variation of ground resistance vs. current injected into clay having a resistivity of 8720 Ωcm, when the tower top is subjected to 18/37 μsec with 11 kA peak value (three tower configuration)

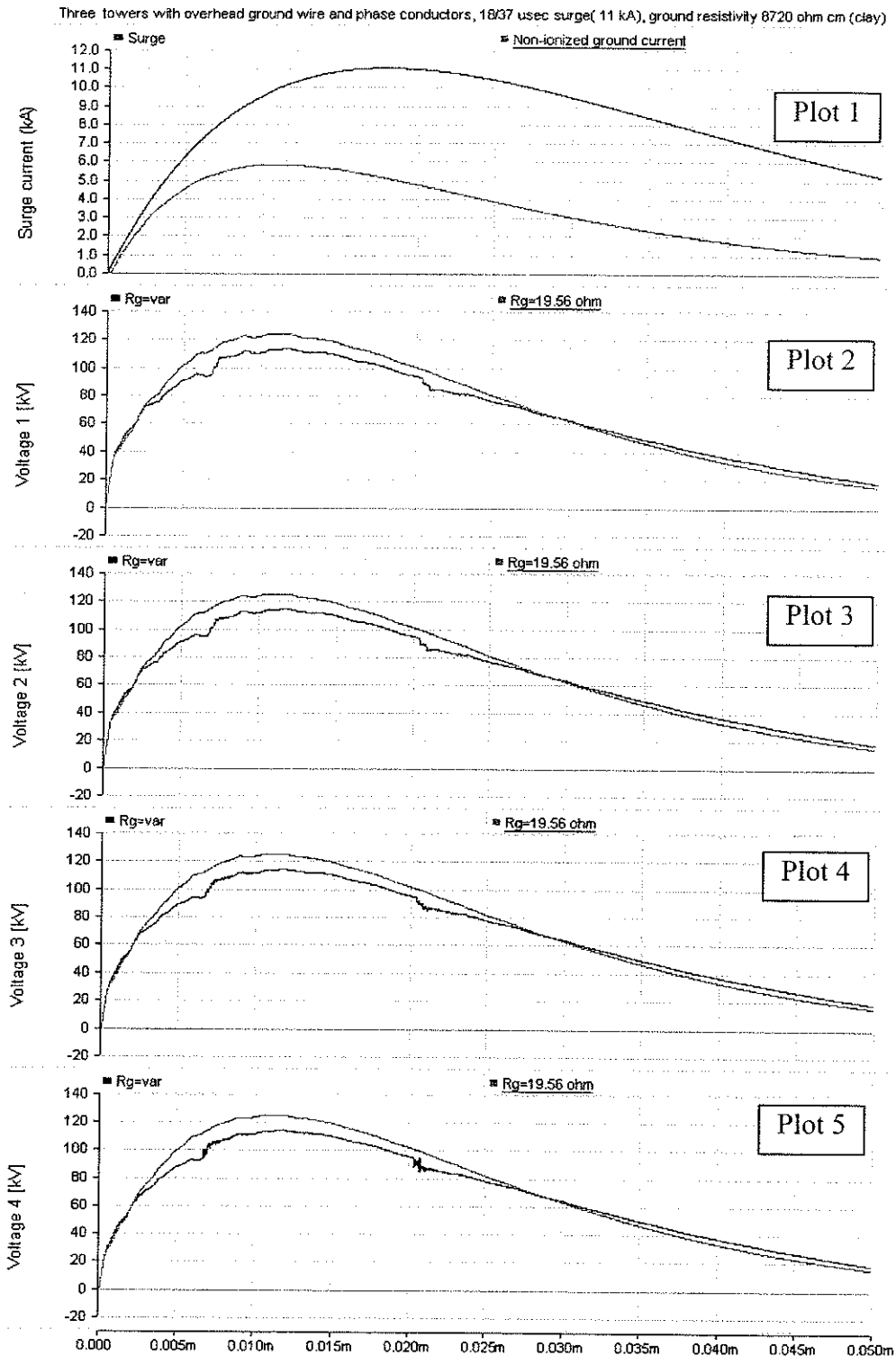

Fig. 5-8 The response of the transmission tower with two neighbouring towers equipped with ground wire and phase conductors to a 18/37 μsec (11 kA) surge waveform, non-ionized ground resistivity =8720 Ωcm (clay), Rg=var / Rg = 19.56 Ω average value of the variable ground resistance

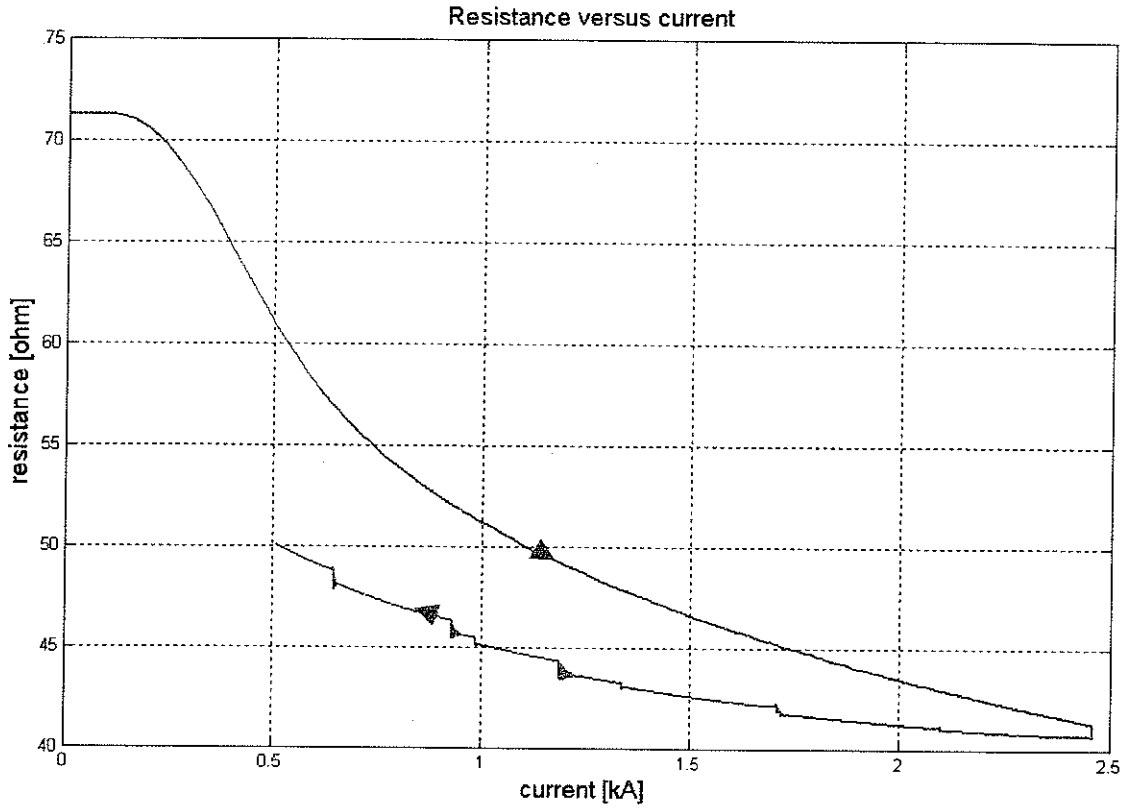

Fig. 5-9 Variation of ground resistance vs. current injected into clay having a resistivity of 15700 Ωcm, when the tower top is subjected to 16/40 μsec with 6.6 kA peak value (three tower configuration)

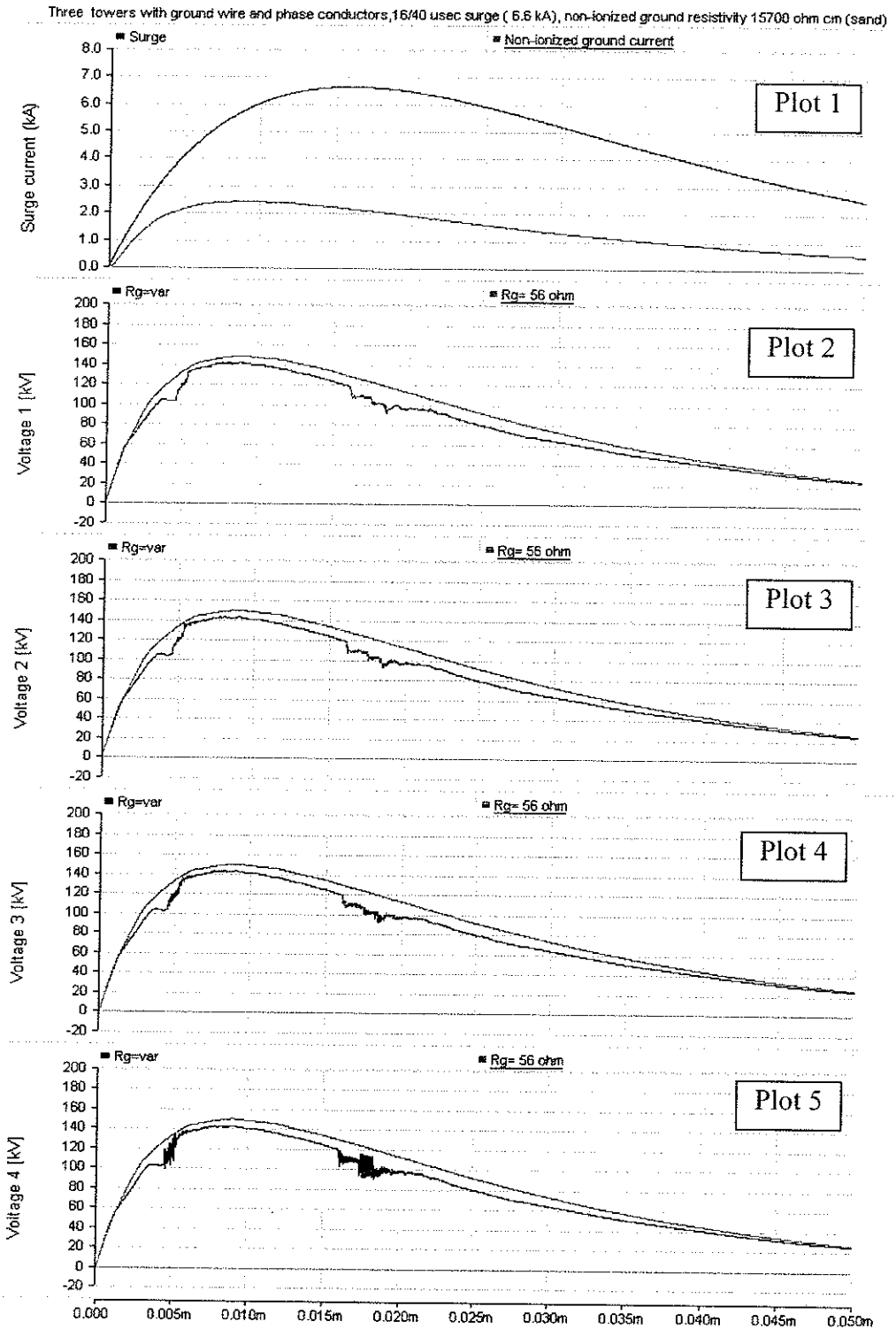

Fig. 5-10 The response of the transmission tower with two neighbouring towers equipped with ground wire and phase conductors to a 16/40 μsec (6.6 kA) surge waveform, non-ionized ground resistivity =15700 Ωcm (sand), Rg=var / Rg = 56 Ω average value of the variable ground resistance

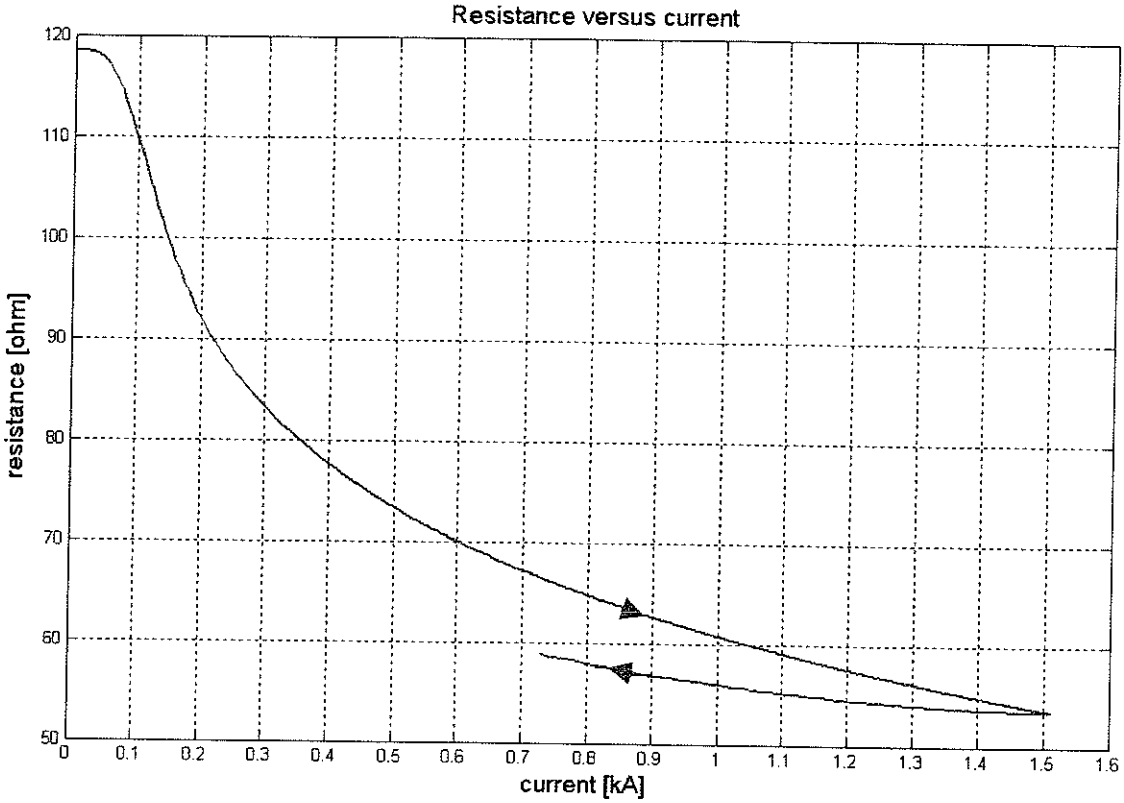

Fig. 5-11 Variation of ground resistance vs. current injected into clay having a resistivity of 31000 Ωcm, when the tower top is subjected to 20/60 μsec with 5.5 kA peak value (one tower configuration)

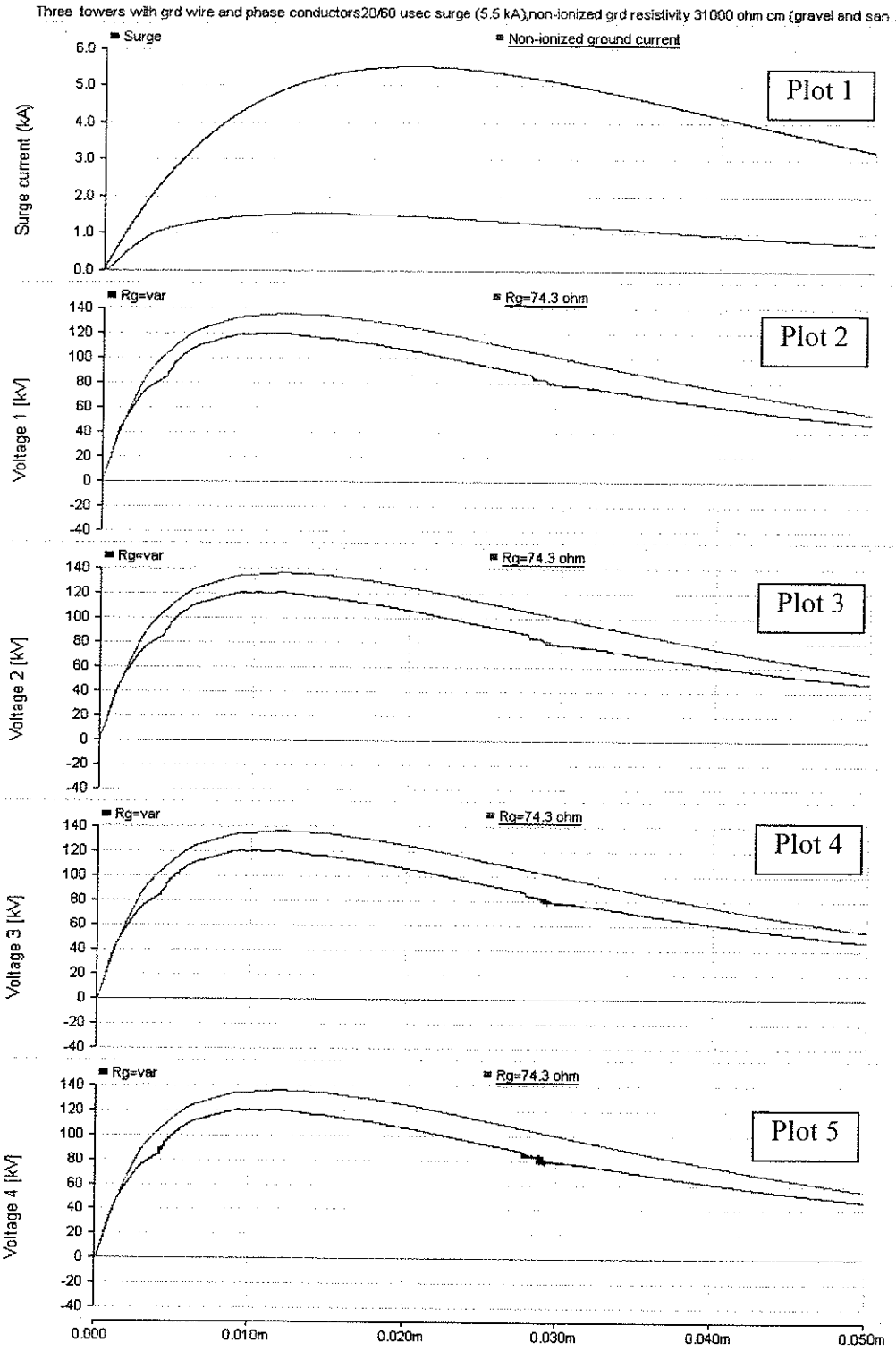

Fig. 5-12 The response of the transmission tower with two neighbouring towers equipped with ground wire and phase conductors to a 20/60 μsec (5.5 kA) surge waveform, non-ionized ground resistivity =31000 Ωcm (gravel and sand), R_g=var / R_g = 74.3 Ω average value of the variable ground resistance

As in the case of the stand alone transmission tower considered in section 5.1, one can notice that the voltage magnitudes depend on the ground modeling technique for all three types of soil (see Fig. 5-8, Fig. 5-10 and Fig. 5-12).

CHAPTER 6

EFFECT OF DIFFERENT SURGE WAVESHAPES ON COMBINED MODEL

In this chapter, the response of the combined model of tower and ground to a fast (1.5/51.75μsec with a 50 kA crest value) and a slow (8/20μsec with a 20 kA crest value) surge current is investigated.

For PSCad simulation, it has been considered as an unenergized, three phase, double circuit transmission line in three tower configuration, equipped with phase wires and a ground wire connected at one end of the topmost cross-arm of the tower. Their resitance of ground was modelled as either a variable resistance or a constant. The equivalent circuit and the model parameters of the transmission line are shown in Fig. 3-16 and Table 3-7 respectively. The ground model uses the parameters corresponding to the three types of soil (clay, sand and sand and gravel), shown in Table 4-1. For each type of soil, the center tower has been subjected subsequently to a 1.5/51.75 μsec, 50 kA and a 8/20μsec, 50 kA surge current, which is shown in Plot 1 of Fig. 6-2, Fig. 6-4, Fig. 6-6, Fig. 6-8, Fig. 6-10 and Fig. 6-12 (the blue curve). The ground resistance corresponding to each type of soil has been modeled as function of the current appearing at the base of the tower which is injected into ground. This current is shown in addition to the current injected at the tower top in Plot 1 of Fig. 6-2, Fig. 6-4, Fig. 6-6, Fig. 6-8, Fig. 6-10, Fig. 6-12 (the green curve). The variation of ground resistance with this current for each type of soil and for the two types of injected current at the top of the

6-1, Fig. 6-3, Fig. 6-5, Fig. 6-7, Fig. 6-9, and Fig. 6-11. The constant resistance represents the average of the two ground resistances, one corresponding to zero current and the other corresponding to the crest value of current.

The simulation results obtained by employing a variable ground resistance were compared with the ones using constant ground resistance. The simulation results consist of the voltages recorded at the tip of each of the four arms of the central transmission tower. These voltages are shown in Plot 2 to Plot 5 of Fig. 6-2, Fig. 6-4, Fig. 6-6, Fig. 6-8, Fig. 6-10 and Fig. 6-12 (the blue curve represents the voltage corresponding to a variable ground resistance, and the green curve represents the voltage corresponding to a constant ground resistance). The voltages shown in Plot 2 of each figure were recorded at the connection with the ground wire and the following voltages shown in Plot 3, Plot 4 and Plot 5 were recorded at the connection with the high voltage insulators, connected to the phase wires.

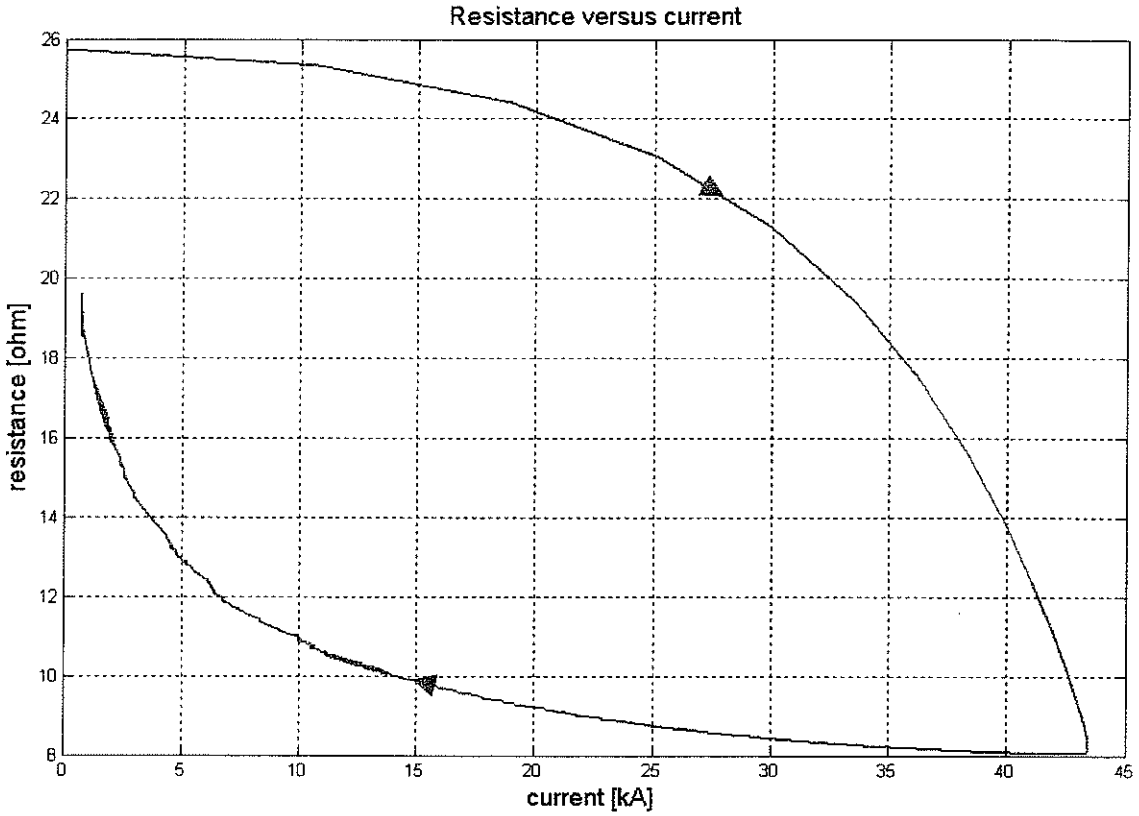

Fig. 6-1 Variation of ground resistance vs. current injected into clay having a resistivity of 8720 Ωcm, when the tower top is subjected to 1.5/51.75 μsec , 50 kA

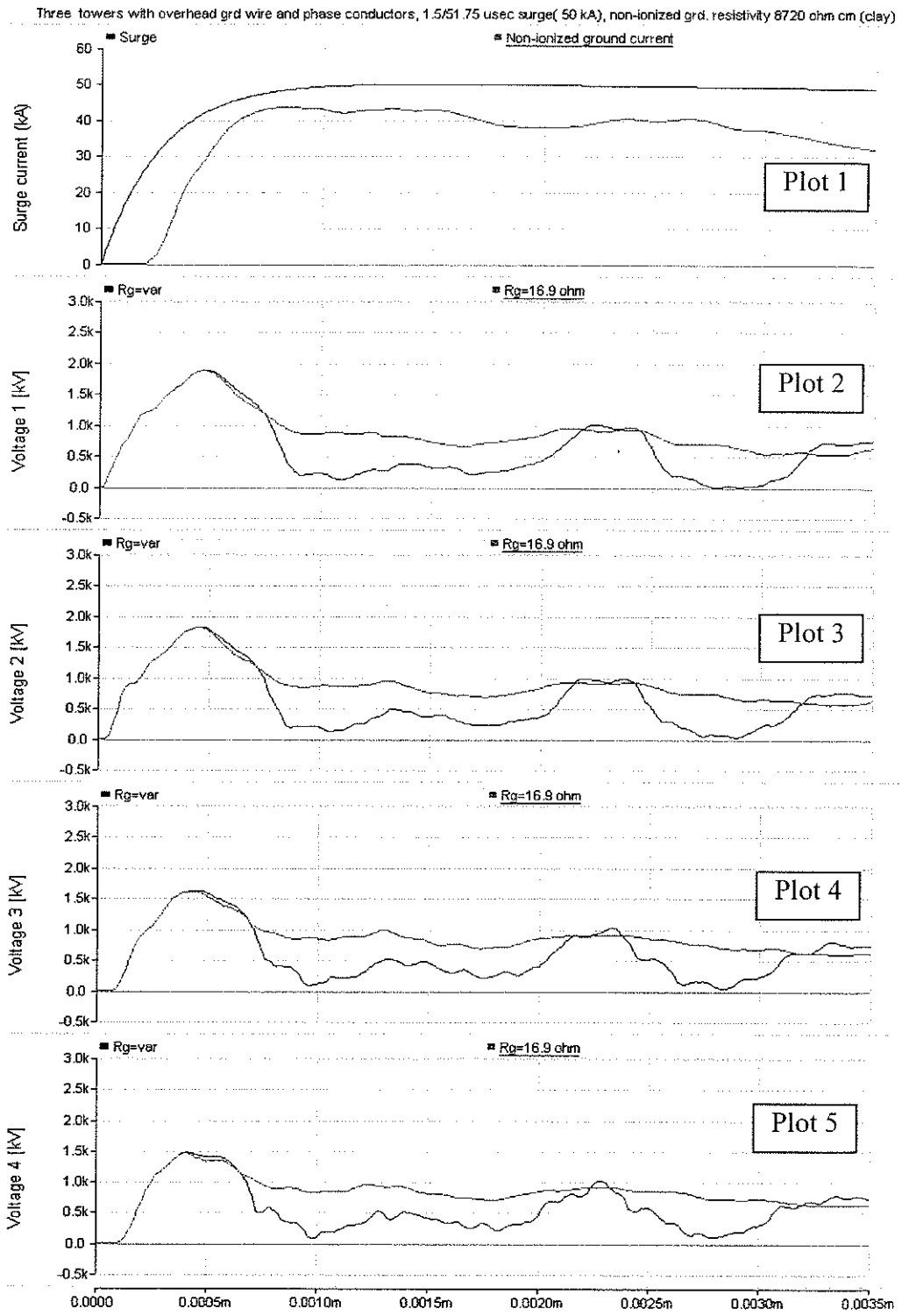

Fig. 6-2 The response of the transmission tower with two neighbouring towers equipped with ground wire and phase conductors to a 1.5/51.75 μsec (50 kA) surge waveform, non-ionized ground resistivity =8720 Ωcm (clay), Rg=var / Rg = 16.9 Ω average value of the variable ground resistance

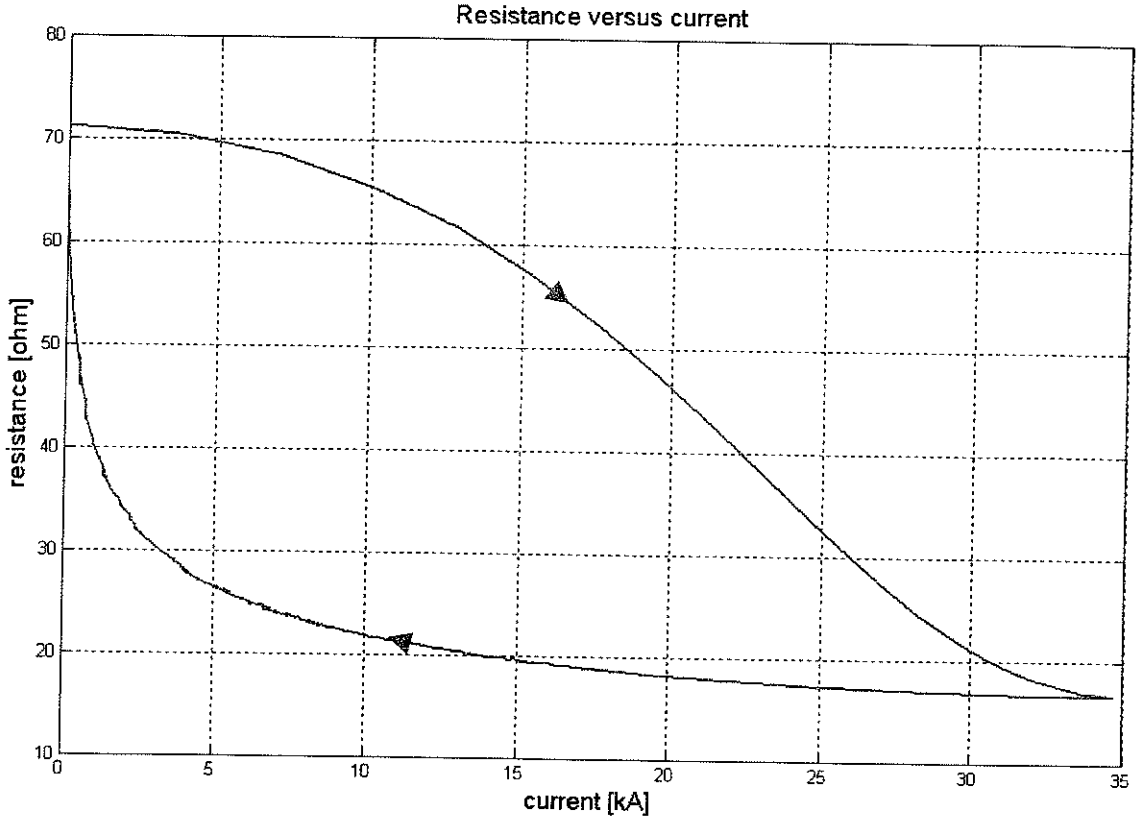

Fig. 6-3 Variation of ground resistance vs. current injected into sand having a resistivity of 15700 Ωcm, when the tower top is subjected to 1.5/51.75 μsec , 50 kA

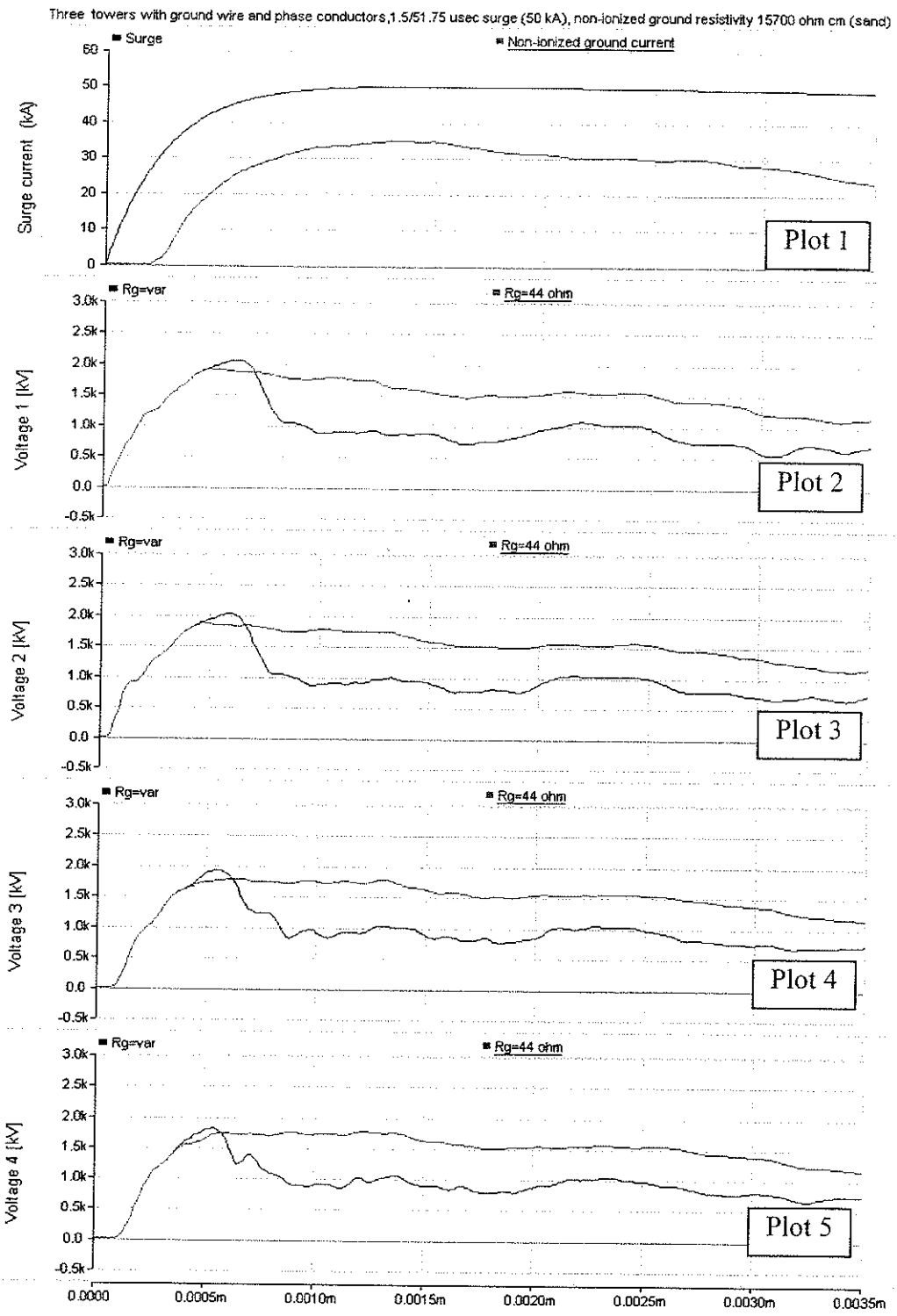

Fig. 6-4 The response of the transmission tower with two neighbouring towers equipped with ground wire and phase conductors to a 1.5/51.75 μsec (50 kA) surge waveform, non-ionized ground resistivity =15700 Ωcm (sand), R_g=var / R_g = 44 Ω average value of the variable ground resistance

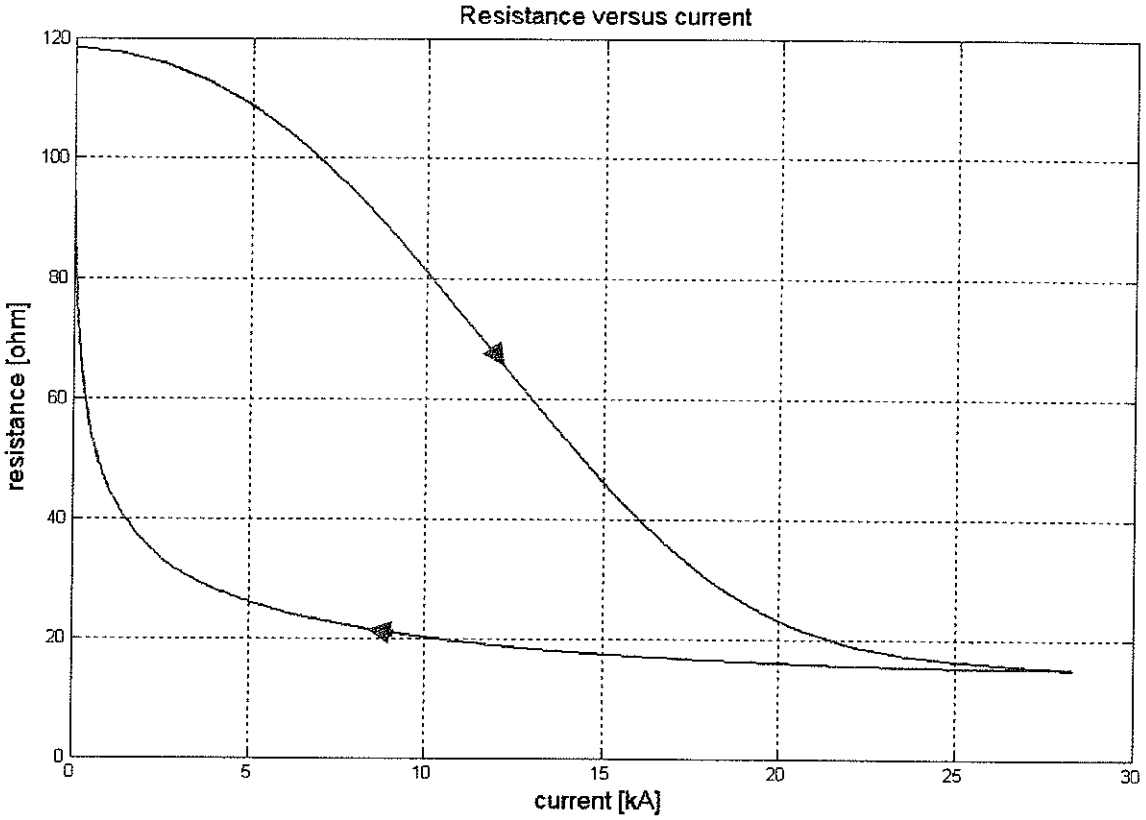

Fig. 6-5 Variation of ground resistance vs. current injected into sand and gravel having a resistivity of 31000 Ωcm, when the tower top is subjected to 1.5/51.75 μsec, 50 kA

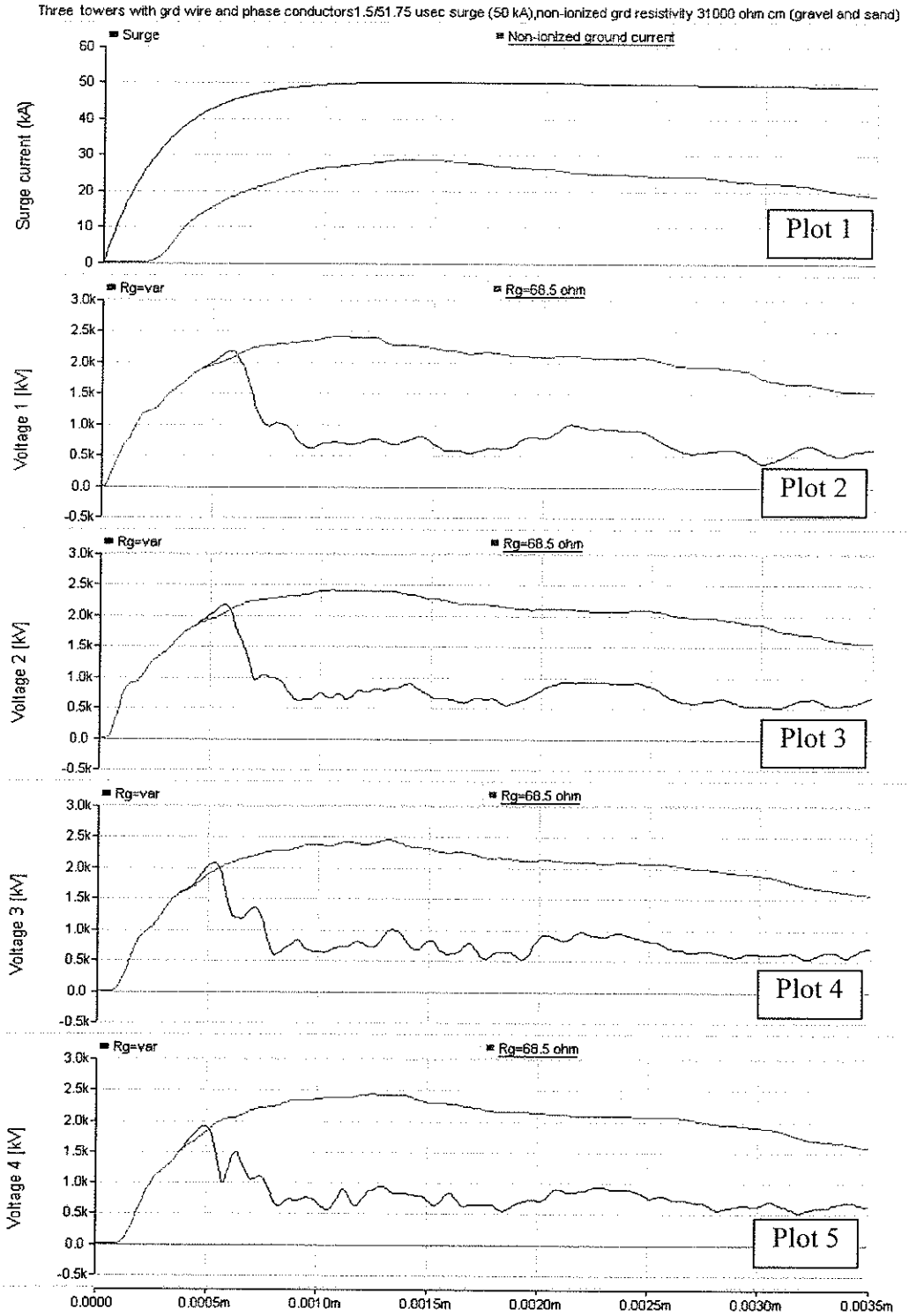

Fig. 6-6 The response of the transmission tower with two neighbouring towers equipped with ground wire and phase conductors to a 1.5/51.75 μsec (50 kA) surge waveform, non-ionized ground resistivity =31000 Ωcm (clay), R_g=var / R_g = 68.5Ω average value of the variable ground resistance

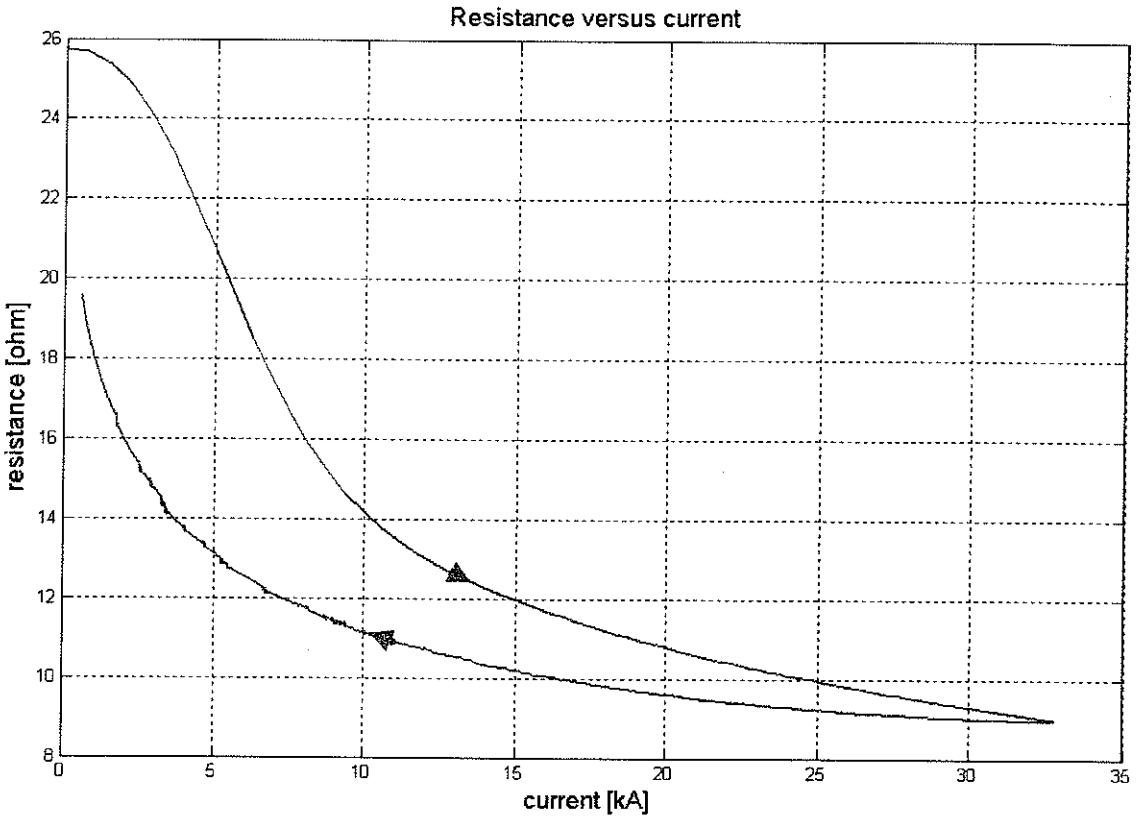

Fig. 6-7 Variation of ground resistance vs. current injected into clay having a resistivity of 8720 Ωcm, when the tower top is subjected to 8/20 μsec , 50 kA

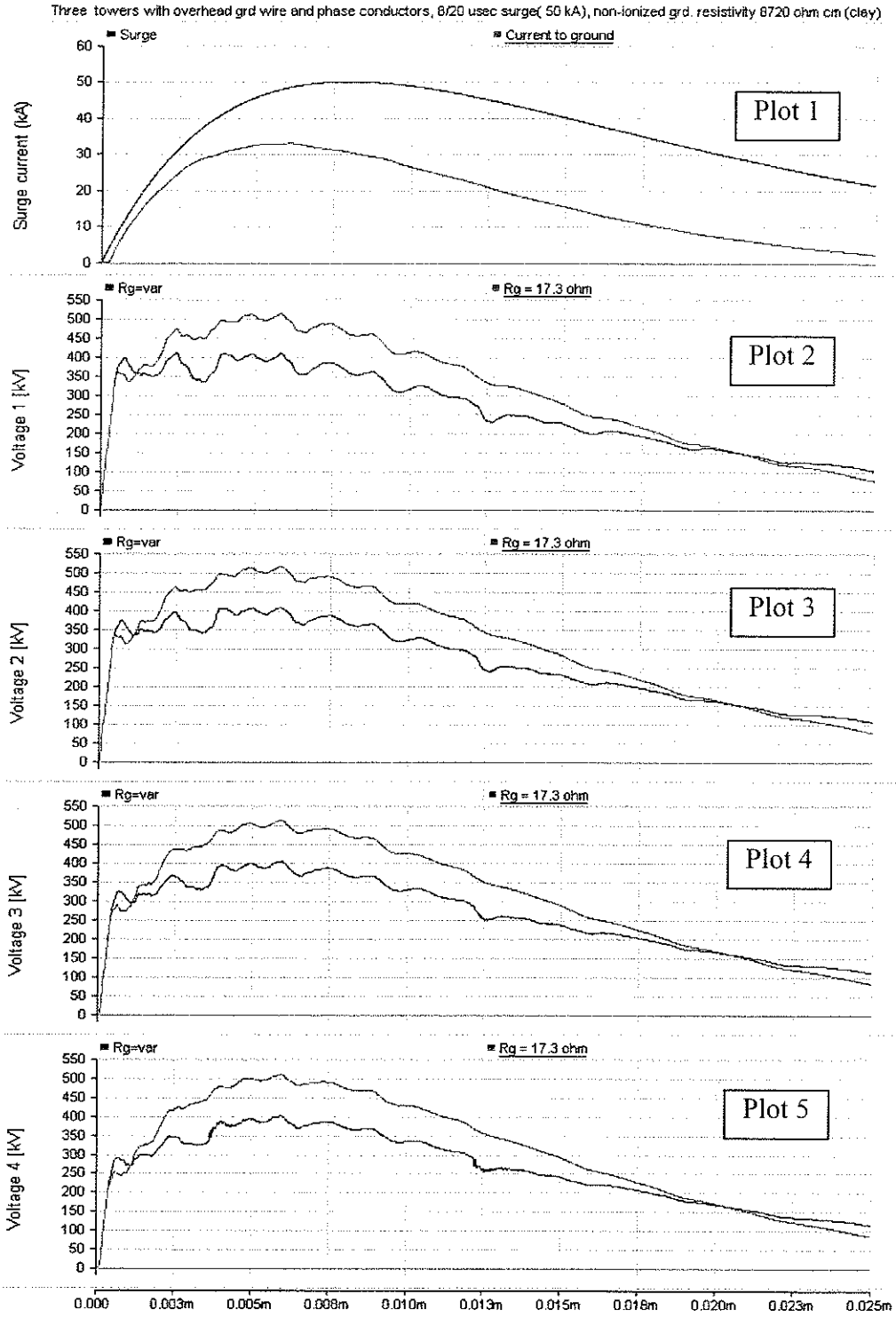

Fig. 6-8 The response of the transmission tower with two neighbouring towers equipped with ground wire and phase conductors to a 8/20 μsec (50 kA) surge waveform, non-ionized ground resistivity =8720 Ωcm (clay), R_g=var / R_g = 17.3 Ω average value of the variable ground resistance

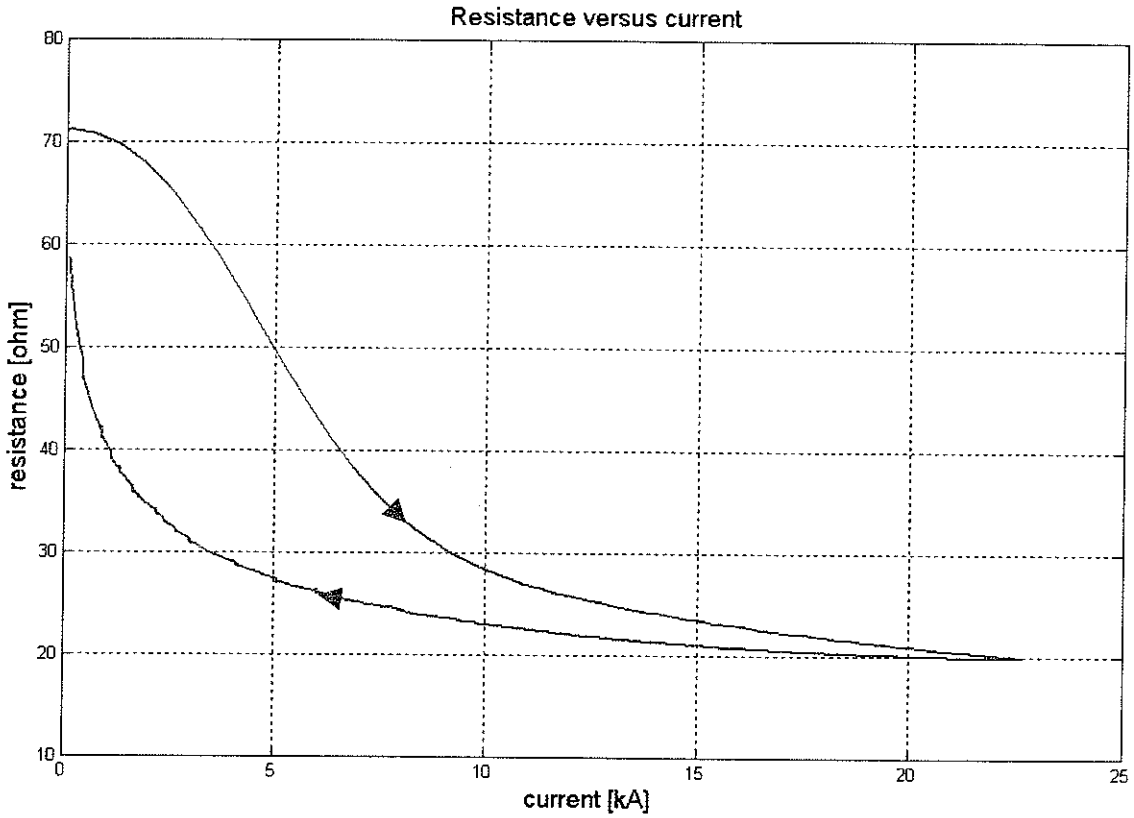

Fig. 6-9 Variation of ground resistance vs. current injected into sand having a resistivity of 15700 Ωcm, when the tower top is subjected to 8/20 μsec , 50 kA

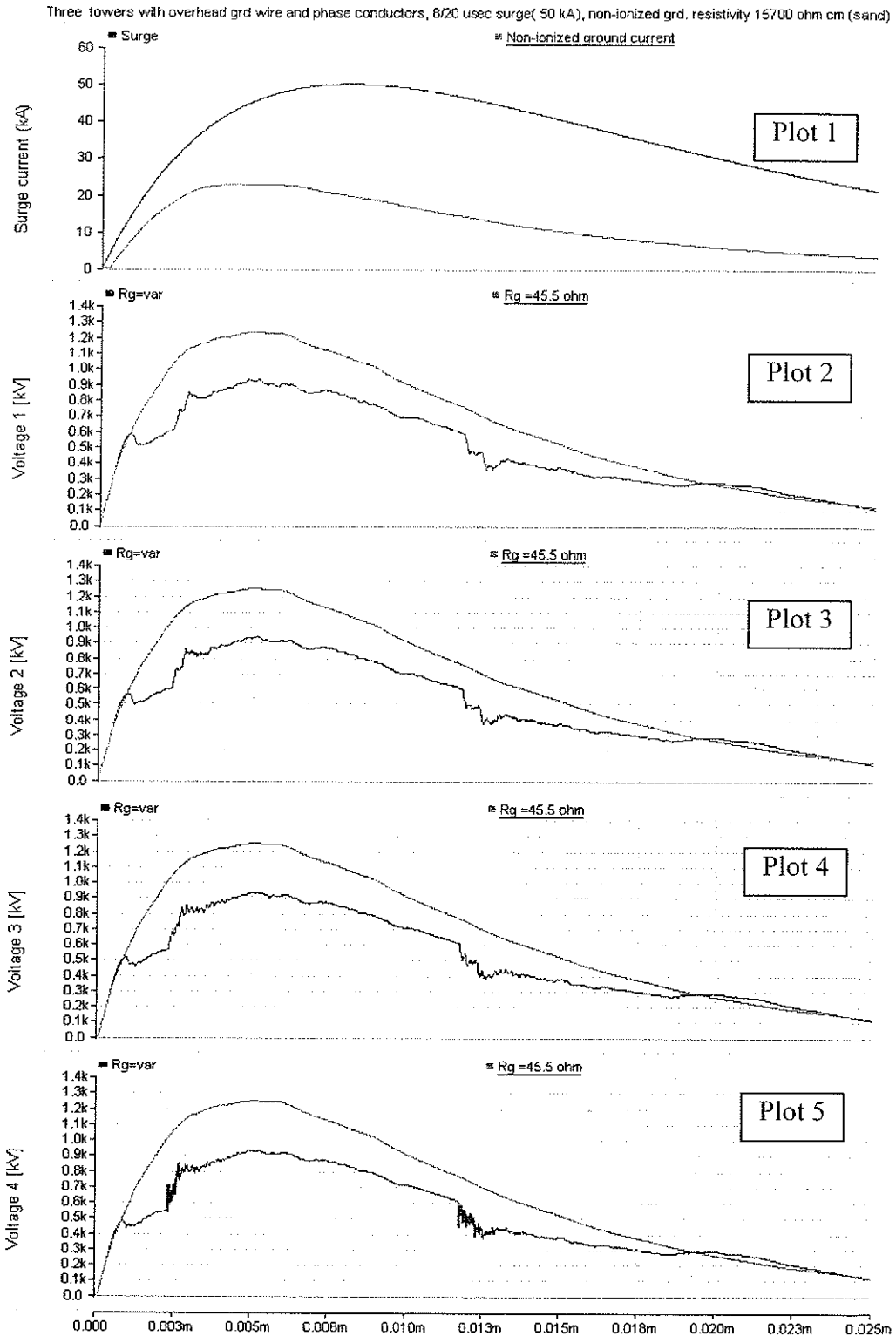

Fig. 6-10 The response of the transmission tower with two neighbouring towers equipped with ground wire and phase conductors to a 8/20 μsec (50 kA) surge waveform, non-ionized ground resistivity =15700 Ωcm (sand), R_g=var / R_g = 45.5 Ω average value of the variable ground resistance

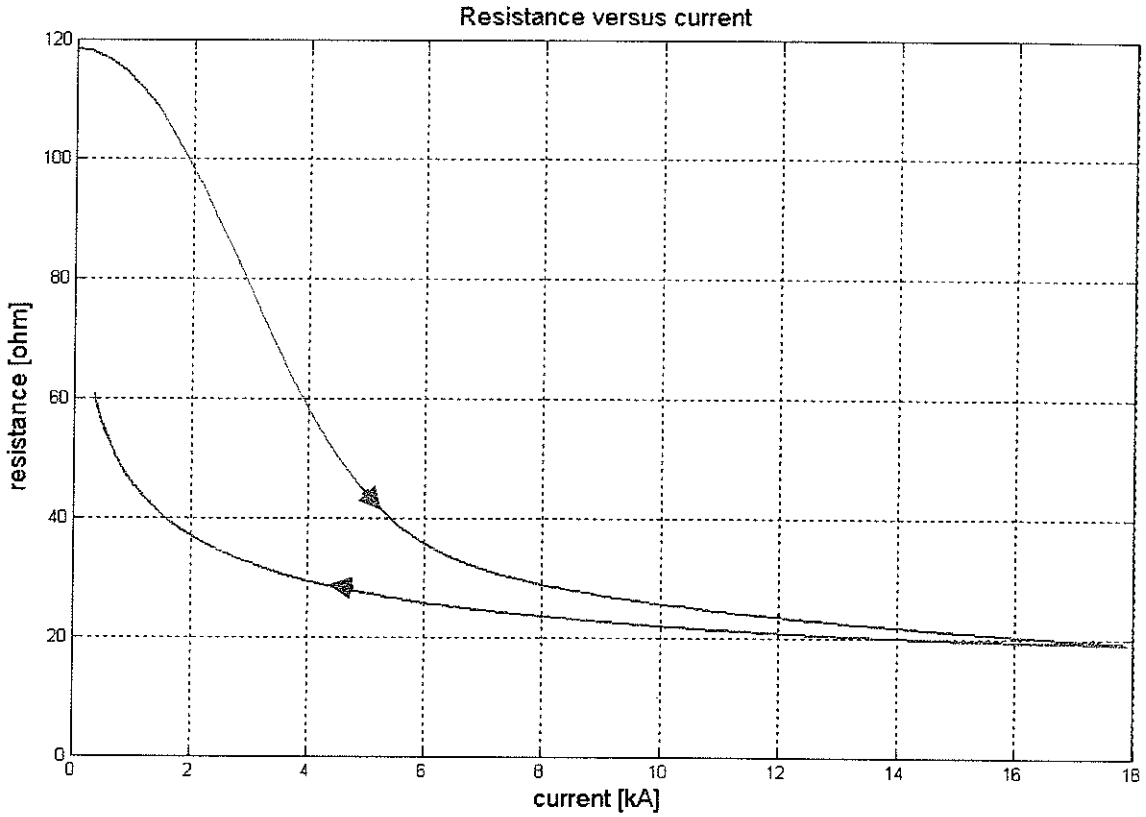

Fig. 6-11 Variation of ground resistance vs. current injected into sand and gravel having a resistivity of 31000 Ωcm, when the tower top is subjected to 8/20 μsec, 50 kA

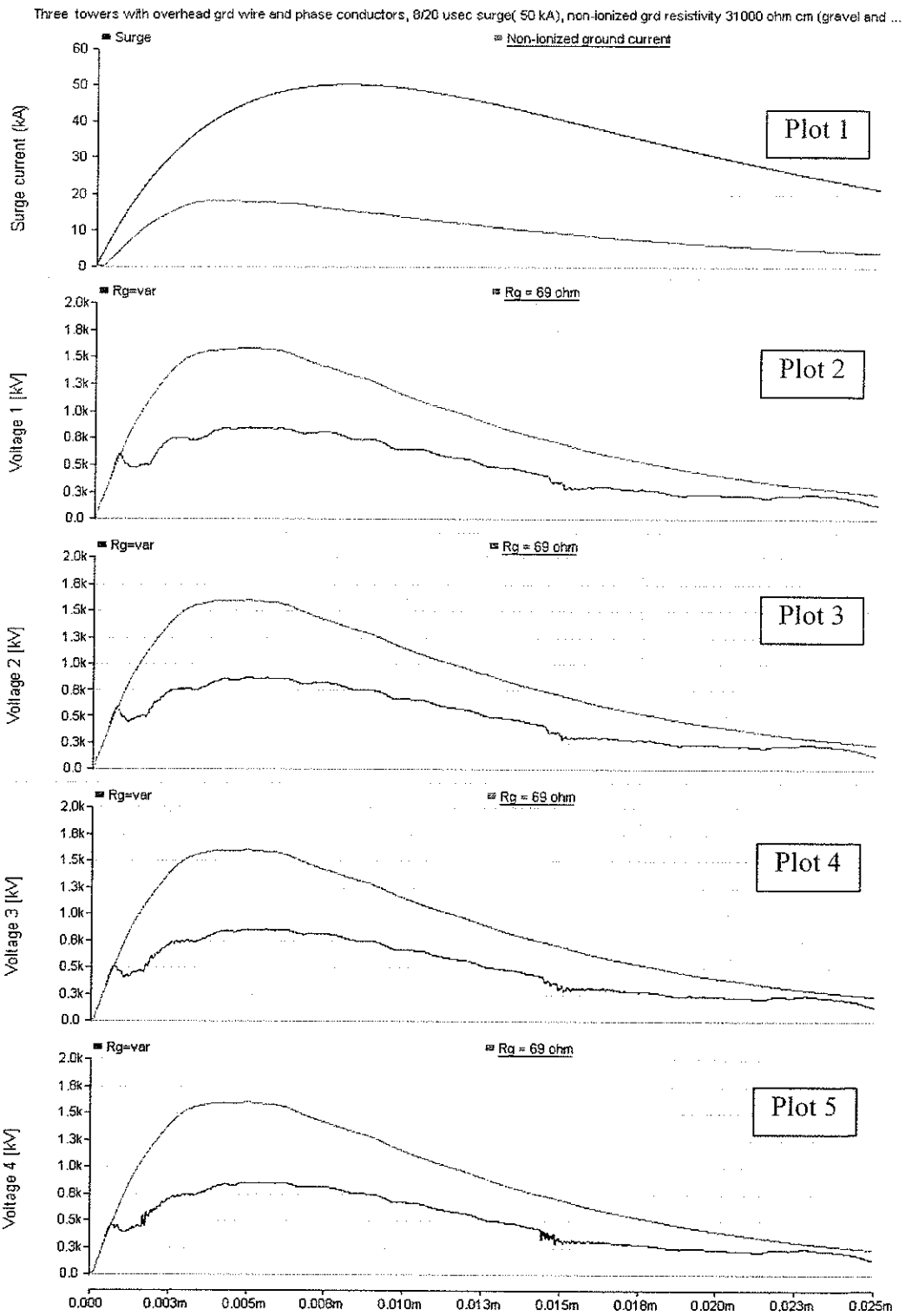

Fig. 6-12 The response of the transmission tower with two neighbouring towers equipped with ground wire and phase conductors to a 8/20 μsec (50 kA) surge waveform, non-ionized ground resistivity =31000 Ωcm (clay), R_g=var / R_g = 69 Ω average value of the variable ground resistance

It may be seen from Fig. 6-2, Fig. 6-4, Fig. 6-6, Fig. 6-8, Fig. 6-10 and Fig. 6-12 that the modeling technique of the ground as a constant or a variable resistance has a bigger effect on the magnitudes of the voltages induced at the tip of the tower cross-arms when the tower is subjected to a slow surge. In the case of fast surge, the effect of the dynamic behaviour of the ground resistance as a function of current becomes significant for soils with higher no-ionized resistivity (31000 Ωcm) (Fig. 6-6), but can be neglected for those with lower resistivity (8700 Ωcm and 15700 Ωcm) (Fig. 6-2, Fig. 6-4).

CHAPTER 7

CONCLUSIONS

In this thesis, a general model that includes both tower and ground effects is proposed for an accurate simulation of back-flashover waveforms.

In Chapters 3 and 4, different tower and ground models from literature were investigated separately in order to select the models that provide the most accurate representation of the transmission tower and ground respectively. In Chapters 5 and 6, by combining the previously selected models of tower and ground, the effect of the combined model on the response of the system to surge current was investigated. The relative sensitivity of tower and ground models has also analyzed in the thesis.

In Chapter 3, three tower models from literature were investigated using PSCad as a simulation tool: Conical Model (Sargent and Darveniza Model) [9], Multi Storey Model (Ihii Model) [6] and Distributed Constant Line Model (Hara Model) [13]. The field experiments from literature were simulated by employing the three tower models. Different cases have been investigated: Case 1: a stand alone tower with no ground wires and constant ground resistance, subjected to different double exponential surge current waveforms, Case 2: a stand alone tower with a ground wire of infinite length subjected to a piece wise surge current waveform and, Case 3: a tower with two neighbouring towers with ground wire and phase conductors, subjected to a piece wise surge current waveform and double exponential surge current waveforms. The double exponential surge currents considered were a fast surge current (1.5/51.75 μsec, 50 kA crest value) and a slow surge current (8/20 μsec, 50 kA crest value). The piece wise

linear surge current waveform was an approximation of a natural lightning employed in a field experiment. The comparison between the simulation results obtained using each model with the ones obtained from the field experiments gave the grade of reproductibility of the overvoltage at the tower top and / or at the tip of the tower arms, when the system is subjected to lightning. The Distributed Constant Line model (Hara model) was validated and selected to be used in further studies in this thesis.

At the same time, by analyzing the simulation results, one can conclude that in the case of a slow surge, the difference between the induced voltages at the top or at the crossarm tips of the tower obtained by employing the three tower models having the same ground resistance is not significant, which implies that in this case, the tower modelling technique does not have much of an effect on the results. The magnitude and the waveform of the induced voltage developed at each tower crossarm tip are more sensitive to the variation of ground resistance when the tower is contacted by a slow surge waveform. In the case of a fast surge waveform, the effect of variation of ground resistance on the induced voltages can be neglected for lower ground resistance values, while the tower model has a large effect on the induced voltages. A possible explanation is that for a slow impulse, the reflected waves from the tower footing have a higher impact on the voltage values recorded at tip of the tower arms.

Also, in the case of a transmission tower with two neighbouring towers equipped with phase and overhead ground wires, the simulation results have showed that the peak values of the induced voltages recorded on the middle tower are approximate 100 kV lower than in the case of a stand alone tower equipped with infinite overhead ground wires. This difference may be attributed to reflections from the adjacent towers.

The ground model considered for the study in Chapter 4 was the Soil Ionization Dynamic Model developed by Alemeida and Correia [18]. The model is based on the dynamic model of ground proposed by A.C. Liew and M. Darveniza [12] which describes the variation of ground resistance with the impulse current. A code in Matlab was written based on the algorithm proposed by Alemeida and Correia to reproduce the field experiments from literature regarding the dynamic behaviour of ground resistance of different type of soils when are contacted by different type of surge currents. The simulation and experimental results were in good agreement, and therefore this ground model was considered to be used in further study in the following chapters.

In Chapters 5 and 6, the effect of the combined model of tower and ground on the determination of the magnitudes and waveforms of the overvoltages induced by various types of fast and slow surge currents are investigated. Two configurations were considered: a stand alone tower equipped with an infinitely extending ground wire, and a tower with two neighbouring towers equipped with ground wire and phase conductors. For both configurations, the resistance of ground was modelled as either a variable resistance or a constant. The simulation results in the case of a stand alone transmission tower equipped with infinitely extended ground wire and a variable ground resistance which is subjected to various slow surge currents, showed similarities with the ones for which the same slow surge currents are injected directly into the ground, described in Chapter 4. This reconfirms the conclusion reached in Chapter 3 that the tower effect on the induced voltages is nonexistent when the tower is contacted by a slow surge current, and only the ground effect is important in this case. Also, the simulation results obtained by employing variable ground resistances were compared with the ones using constant

ground resistances. The modeling technique of the ground as a constant or a variable resistance has a larger effect on the magnitudes of the induced voltages when the tower is subjected to a slow surge. In the case of a fast surge, the effect of the dynamic behaviour of the ground resistance as a function of current becomes significant for soils with higher no-ionized resistivity (31000 Ωcm), while for those with lower resistivity (8700 Ωcm and 15700 Ωcm) can be neglected. A possible explanation is that for a fast surge current the ground effect is not as important as the tower effect on the induced voltages.

In conclusion, when a system is contacted by a fast surge and the ground resistivity is less than about 31000 Ωcm, the tower effect is more important and the ground effect is insignificant; when the system is contacted by a slow surge, the tower effect can be neglected, the ground model being the one which affects the induced voltages and this is the case when the dynamic behaviour of ground as a function of current has to be taken into account.

References

[1] Breuer, G.D. et al., "Field Studies of the Surge Response of a 345-Kv Transmission Tower and Ground Wire," Ibid., vol. 76, 1957 Feb. 1958 section, pp. 1392-1402.

[2] Caswell, R.W. et al., "Lightning performance of 138-kV twin-circuit transmission lines of Commonwealth Edison Company-operating experience and field studies," AIEE Trans. vol. PAS 76, pp. 1480-1491, 1957.

[3] Chisholm, W.A. et al., "Travel Time of Transmission Towers," IEEE Trans., vol. PAS-104, No. 10, 1985, pp. 2922-2928.

[4] Chisholm, W.A. et al., "Lightning Surge Response of Transmission Towers," IEEE Trans., vol. PAS-102, No. 9, 1983, pp. 3232-3242.

[5] Hara, T. and Yamamoto, O., "Modelling of a transmission tower for lightning-surge analysis," IEE Proc.-Fener. Transm. Distrib., Vol. 143, No. 3, May 1996, pp. 283-289

[6] Ishii, M. et al., "Multistory Transmission Tower Model for Lightning Surge Analysis," IEEE Trans PWRD Vol. 6, July 1991, pp. 1327-1335.

[7] Jordan, C.A., "Lightning Computations for Transmission Lines with Overhead Ground Wires Part III, G.E. Rev., 37, 1934.

[8] Kawai, M., "Studies of Surge Response on a Transmission Line Tower," IEEE Trans., PAS-83, 1964, pp. 30-34.

[9] Sargent, M.A. and Darveniza, M.A., "Tower Surge Impedance," IEEE Trans. Pas-88, No. 5, 1969, pp. 680-687.

[10] Wagner, C.F. and Hileman, A.R. "A New Approach to the Calculation of the Lightning Performance of Transmission Lines, III – A Simplified Method: Stroke to Tower," AIEE Trans. Vol. 79, 1960, pp. 589-603.

[11] Yamada, T. et al., "Experimental Evaluation of a UHV Tower Model for Lightning Surge Analysis," IEEE Trans. on Power Delivery, Vol. 10, No. 1, January 1995, pp. 393-402

[12] A.C. Liew and M. Darveniza "Dynamic model of impulse characteristics of concentrated earths", Proc. IEE, Vol. 121, No. 2, February 1974, pp. 123-134.

[13] T. Hara and O. Yamamoto, "Modelling of a transmission tower for lightning surge analysis", IEE Proc.- Gener. Transm. Distrib., Vol. 143, No. 3, May 1996, pp. 283-289.

[14] Y. Matsumoto et al., "Measurement of lightning surges on test transmission line equipped with arresters struck by natural and triggered lightning", IEEE Transactions on Power Delivery, Vol. 11, No. 2, April 1996, pp. 996-1002.

[15] H. Motoyama, K. Shinjo, Y. Matsumoto, N. Itamoto, "Observation and analysis of multiphase back flashover on the Okushishiku test transmission line caused by winter lightning, IEEE Transactions on Power Delivery, Vol. 13, No. 4, October 1998, pp. 1391-1398.

[16] M.R.Raghuveer, "High Voltage Techniques", University of Manitoba, Course Notes, 2002.

[17] A.C. Liew and M. Darveniza "A sensitivity analysis of lightning performance calculations for transmission lines", IEEE Summer Power Meeting and EHV Conference, July 1970, pp. 1443-1451.

[18] M. E. Almeida and M. T. Correia de Barros " Modelling the hysteresis behaviour of the transmission tower footing", Graz Convention Center Austria, Europe, August 28 – September 1, 1995, pp. 6799-1 – 6799-4.

[19] P. L. Bellaschi, R.E. Armington, A.E. Snowden "Impulse and 60-cycle characteristics of driven grounds Pt. II", ibid, 1942, 61, pp. 349-363.

[20] H.B. Dwight "Calculation of resistances to ground", Trans. Am. Inst. Elec. Eng., 1936, 55, pp. 1319-1328.

[21] E. C. Jordan, "Electromagnetic Waves and Radiating Systems", Second Edition, Prentice-Hall, Inc., New Jersey

[22] Transmission Line Reference Book, 345 kV and above, Second Edition, Electric Power Research Institute, Palo Alto, California, 1982

[23] IEC 61312 "Protection Against Lightning Electromagnetic Impulse"

APPENDIX A

Derivation of impedance formula for conical model of transmission tower proposed by Sargent and Darveniza

Faraday's law – integral form:

$$\oint_L \bar{E}_i d\bar{l} = -\frac{\partial}{\partial t}\int_S \bar{B}\cdot d\bar{S} \tag{A.1}$$

$$\bar{B} = \nabla \times \bar{A} \tag{A.2}$$

$$\int_S \bar{B}\cdot d\bar{S} = \int_S (\nabla \times \bar{A})\cdot d\bar{S} = \oint_L \bar{A}\cdot d\bar{l} \text{ conform Sokes' Theorem} \tag{A.3}$$

$$\Rightarrow \oint_L \bar{E}_i d\bar{l} = -\int_S \frac{\partial \bar{A}}{\partial t}\cdot d\bar{l} \tag{A.4}$$

where $\bar{E}_i$ - the electric field due to currents at a point at any instant

$\bar{A}$ - the potential magnetic vector

l - the distance along a curve through the point

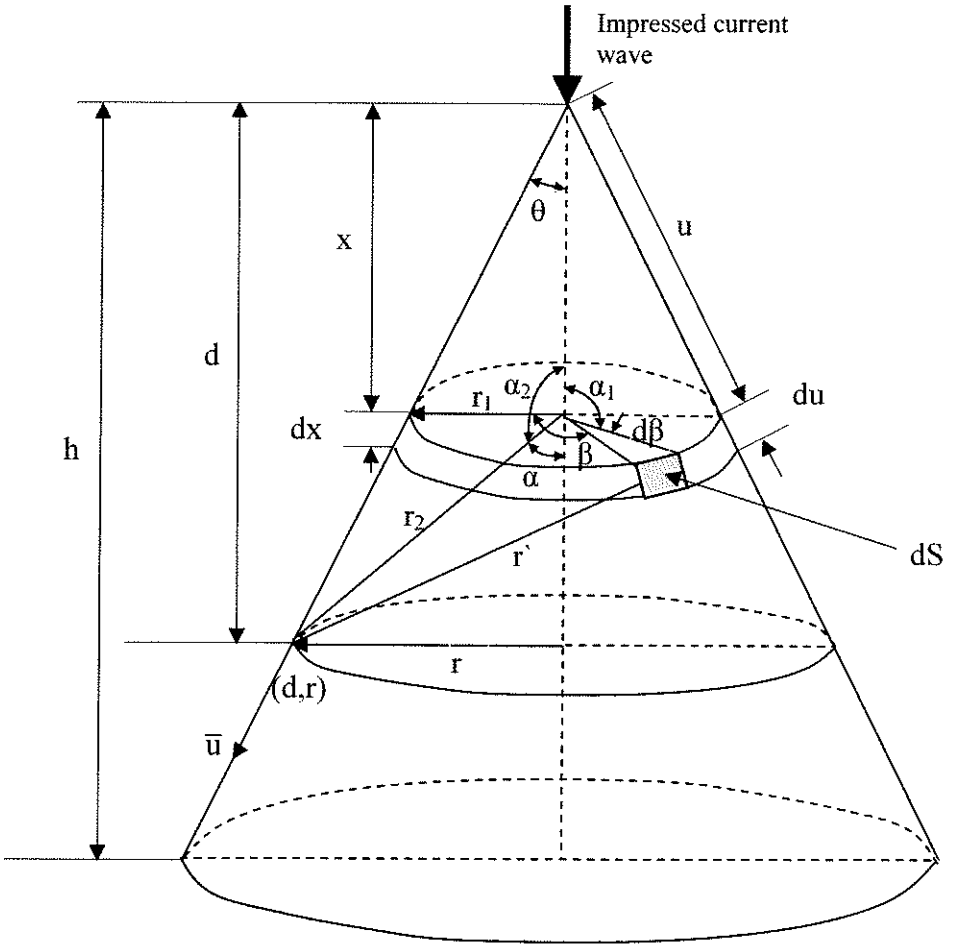

Fig. A-1 Conical tower used in field theory analyses [9]

A rectangular current wave is applied at the tower top (x=0 at t=0).

The source is an element (du, dβ) with spherical coordinates (r_1, α_1, β) – as part of the element dx at x from the tower top. The vector magnetic potential at a general point (d, r) has to be determined. The point has spherical coordinates (r_2, α_2, β`).

The vector magnetic potential at (d, r):

$$A = \frac{\mu_0}{4\pi} \iint \frac{J_s\left[x, t-\left(\frac{r}{c}\right)\right]}{r'} dS = \frac{\mu_0}{4\pi} \iint \frac{J_s\left[x, t-\left(\frac{r}{c}\right)\right]}{r'} r_1 du\, d\beta \qquad \text{(A.5)}$$

$$A = \frac{\mu_0}{4\pi} \iint \frac{J_s\left[x, t - \left(\frac{r}{c}\right)\right]}{r'} dS = \frac{\mu_0}{4\pi} \iint \frac{J_s\left[x, t - \left(\frac{r}{c}\right)\right]}{r'} r_1 du\, d\beta \qquad \text{(A.5)}$$

- the surface density of the current : $J_s = \frac{I}{2\,\pi\,r_1}$ where I is the current applied at the tower top

$$\Rightarrow A = \frac{\mu_0}{4\pi} \int_0^{2\pi} \int_0^{y} \frac{I}{2\pi} \frac{du\, d\beta}{r'} \qquad \text{(A.6)}$$

r` is the distance between the source and the point where A has to be calculated.

The distance between two points in spherical coordinates (in our case between two points of coordinates (r_1, α_1, β) and (r_2, α_2, β`):

$$r'^2 = r_2^2 + r_1^2 - 2r_1 r_2 \cos\alpha_1 \cos\alpha_2 - 2r_1 r_2 \sin\alpha_1 \sin\alpha_2 \cos(\beta - \beta') \qquad \text{(A.7)}$$

In our case:

$$\begin{aligned} r_1 &= x \tan\theta \\ r_2^2 &(d - x)^2 + d^2 \tan^2\theta \end{aligned} \qquad \text{(A.8)}$$

$$\alpha_1 = \frac{\pi}{2} \rightarrow \sin\frac{\pi}{2} = 1;\ \cos\frac{\pi}{2} = 0$$

$$\sin\alpha_2 = \sin(\pi - \alpha) = \sin\ \pi\ \cos\ \alpha - \sin\ \alpha\ \cos\ \pi = \sin\ \alpha = \frac{d\ \tan\ \theta}{r_2} \qquad \text{(A.9)}$$

$$\Rightarrow \sin\ \alpha_2 = \frac{d\ \tan\ \theta}{r_2}$$

$$\beta' = 0$$

$$\begin{aligned} r'^2 &= r_2^2 + r_1^2 - 2r_1 r_2 \frac{d\tan\theta}{r_2}\cos\beta = (d - x)^2 + d^2\tan^2\theta + x^2\tan^2\theta - 2dx\tan^2\theta\cos\beta \\ &= x^2 + d^2 - 2dx + (x^2 + d^2)\tan^2\theta - 2d\,x\tan^2\theta\cos\beta \\ &= (x^2 + d^2)(1 + \tan^2\theta) - 2d\,x\,(1 + \tan^2\theta\cos\beta) \\ &= \frac{1}{\cos^2\theta}\left[x^2 + d^2 - 2d\,x\cos^2\theta\,(1 + \tan^2\theta\cos\beta)\right] \end{aligned} \qquad \text{(A.10)}$$

We have the following constants:

$$m = \tan\theta$$

$$S = \sin\theta$$

$$K = \cos\theta$$

$$\begin{aligned} r'^2 &= \frac{1}{K^2}(x^2 + d^2 - 2bdx) \\ &\text{where } b = K^2(1 + m^2\cos\beta) \end{aligned} \qquad \text{(A.11)}$$

The vector magnetic potential at (d, r) in the direction of unit vector $\bar{u}$:

$$A_u = \frac{\mu_0}{4\pi}\frac{I}{2\pi}\int_0^{2\pi}\int_0^{y}\frac{Kb\ du\ d\beta}{\sqrt{x^2+d^2-2bdx}}\bar{u} = \frac{\mu_0}{4\pi}\frac{I}{2\pi}\int_0^{2\pi}\int_0^{x}\frac{b\ dx\ d\beta}{\sqrt{x^2+d^2-2bdx}} \tag{A.12}$$

y accounts for retardation effect.

$$t = \frac{y}{Kc} + \frac{\sqrt{y^2+d^2-2bdy}}{Kc} \tag{A.13}$$

$$A_u = \frac{\mu_0}{4\pi}\frac{I}{2\pi}\int_0^{2\pi} b\left[\ln(kct - bd) - \ln(1-b)d\right]d\beta \tag{A.14}$$

Faraday's law:
$$\left.\begin{aligned}\nabla\times\bar{E} &= -\frac{\partial\bar{B}}{\partial t}\\ B &= \nabla\times\bar{A}\end{aligned}\right\} \Rightarrow \frac{\partial\bar{A}_u}{\partial t} = -\bar{E}_{iu} \tag{A.15}$$

$$\frac{\partial\bar{A}_u}{\partial t} = \frac{\mu_0}{4\pi}\frac{I}{2\pi}\int_0^{2\pi}\frac{Kcb}{Kct-bd}d\beta = \frac{\mu_0}{4\pi}\frac{I}{2\pi}\int_0^{2\pi}\frac{cb}{ct-\frac{bd}{K}}d\beta \tag{A.16}$$

$$K = \cos\theta = \frac{d}{u} \Rightarrow u = \frac{d}{K} \tag{A.17}$$

$$\int_{u=0}^{u=ct}\overline{E_{iu}}\,du = -\frac{\mu_0}{4\pi}\frac{I}{2\pi}\int_0^{2\pi}\int_{u=0}^{u=ct}\frac{cb}{ct-bdu}du\,d\beta = -\frac{30I}{2\pi}\int_0^{2\pi}\ln\left[\frac{1}{\left[2S^2\sin^2\left(\beta/2\right)\right]}\right]d\beta$$

$$= -I\left[60\ln\left(\sqrt{2}/S\right)\right] = -ZI$$

$$\Rightarrow Z = 60\ln\left(\sqrt{2}/S\right) \tag{A.18}$$

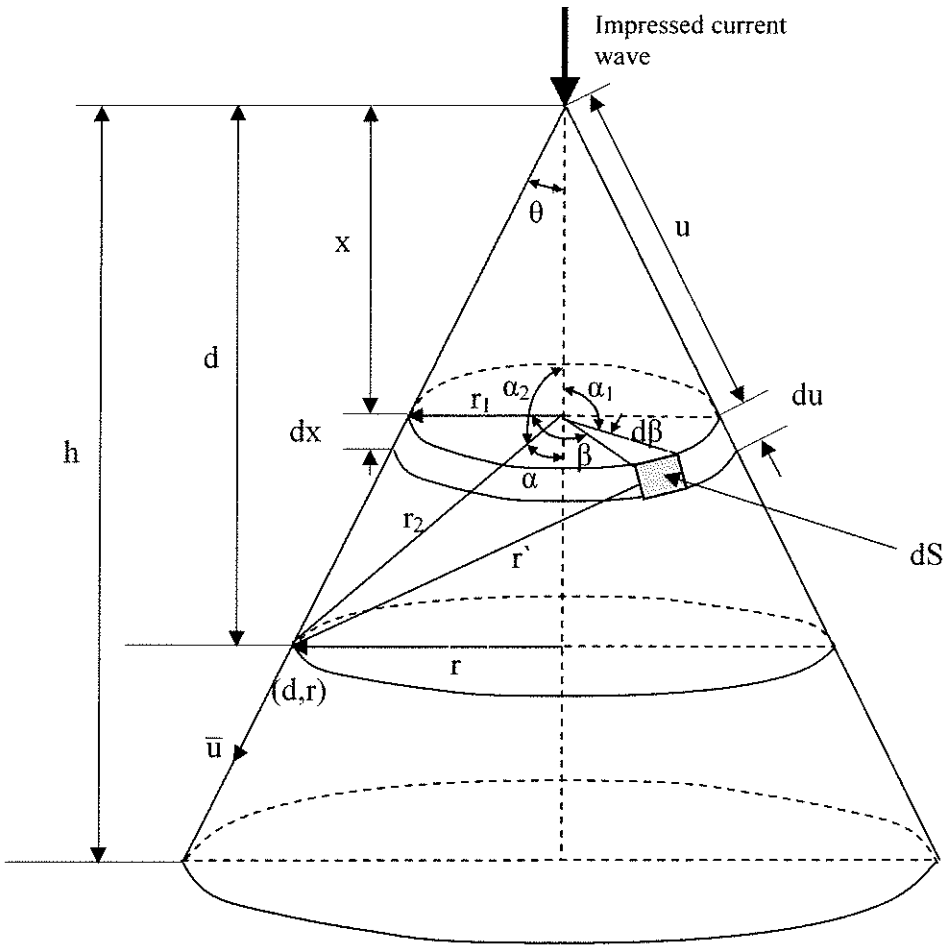

Fig. A-1 Conical tower used in field theory analyses [9]

A rectangular current wave is applied at the tower top (x=0 at t=0).

The source is an element (du, dβ) with spherical coordinates (r_1, α_1, β) – as part of the element dx at x from the tower top. The vector magnetic potential at a general point (d, r) has to be determined. The point has spherical coordinates (r_2, α_2, β`).

The vector magnetic potential at (d, r):

$$A = \frac{\mu_0}{4\pi} \iint \frac{J_s\left[x, t-\left(\frac{r}{c}\right)\right]}{r'} dS = \frac{\mu_0}{4\pi} \iint \frac{J_s\left[x, t-\left(\frac{r}{c}\right)\right]}{r'} r_1 du\, d\beta \qquad \text{(A.5)}$$

- the surface density of the current : $J_s = \frac{I}{2\,\pi\, r_1}$ where I is the current applied at the tower top

$$\Rightarrow A = \frac{\mu_0}{4\pi} \int_0^{2\pi} \int_0^{y} \frac{I}{2\pi} \frac{du\; d\beta}{r'} \tag{A.6}$$

r` is the distance between the source and the point where A has to be calculated.

The distance between two points in spherical coordinates (in our case between two points of coordinates (r_1, α_1, β) and (r_2, α_2, β`):

$$r'^2 = r_2^2 + r_1^2 - 2r_1 r_2 \cos\alpha_1 \cos\alpha_2 - 2r_1 r_2 \sin\alpha_1 \sin\alpha_2 \cos(\beta - \beta') \tag{A.7}$$

In our case:

$$\begin{aligned} r_1 &= x \tan\theta \\ r_2^2 &(d-x)^2 + d^2 \tan^2\theta \end{aligned} \tag{A.8}$$

$$\begin{aligned} &\alpha_1 = \frac{\pi}{2} \rightarrow \sin\frac{\pi}{2} = 1;\ \cos\frac{\pi}{2} = 0 \\ &\sin\alpha_2 = \sin(\pi - \alpha) = \sin\ \pi\ \cos\ \alpha - \sin\ \alpha\ \cos\ \pi = \sin\ \alpha = \frac{d\ \tan\ \theta}{r_2} \\ &\Rightarrow \sin\ \alpha_2 = \frac{d\ \tan\ \theta}{r_2} \end{aligned} \tag{A.9}$$

$$\beta' = 0$$

$$\begin{aligned} r'^2 &= r_2^2 + r_1^2 - 2r_1 r_2 \frac{d\tan\theta}{r_2}\cos\beta = (d-x)^2 + d^2\tan^2\theta + x^2\tan^2\theta - 2dx\tan^2\theta\cos\beta \\ &= x^2 + d^2 - 2dx + (x^2 + d^2)\tan^2\theta - 2d\,x\tan^2\theta\cos\beta \\ &= (x^2 + d^2)(1 + \tan^2\theta) - 2d\,x(1 + \tan^2\theta\cos\beta) \\ &= \frac{1}{\cos^2\theta}\left[x^2 + d^2 - 2d\,x\cos^2\theta(1 + \tan^2\theta\cos\beta)\right] \end{aligned} \tag{A.10}$$

We have the following constants:

$$m = \tan\theta$$

$$S = \sin\theta$$

$$K = \cos\theta$$

$$r'^2 = \frac{1}{K^2}\left(x^2 + d^2 - 2bdx\right) \qquad \text{(A.11)}$$
$$\text{where } b = K^2\left(1 + m^2\cos\beta\right)$$

The vector magnetic potential at (d, r) in the direction of unit vector $\bar{u}$:

$$A_u = \frac{\mu_0}{4\pi}\frac{I}{2\pi}\int_0^{2\pi}\int_0^{y}\frac{Kb\ du\ d\beta}{\sqrt{x^2 + d^2 - 2bdx}}\bar{u} = \frac{\mu_0}{4\pi}\frac{I}{2\pi}\int_0^{2\pi}\int_0^{x}\frac{b\ dx\ d\beta}{\sqrt{x^2 + d^2 - 2bdx}} \qquad \text{(A.12)}$$

y accounts for retardation effect.

$$t = \frac{y}{Kc} + \frac{\sqrt{y^2 + d^2 - 2bdy}}{Kc} \qquad \text{(A.13)}$$

$$A_u = \frac{\mu_0}{4\pi}\frac{I}{2\pi}\int_0^{2\pi} b\left[\ln\left(kct - bd\right) - \ln\left(1 - b\right)d\right]d\beta \qquad \text{(A.14)}$$

Faraday's law: $\left.\begin{aligned}\nabla\times\bar{E} &= -\frac{\partial\bar{B}}{\partial t}\\ B &= \nabla\times\bar{A}\end{aligned}\right\} \Rightarrow \frac{\partial\bar{A}_u}{\partial t} = -\bar{E}_{iu}$ (A.15)

$$\frac{\partial\bar{A}_u}{\partial t} = \frac{\mu_0}{4\pi}\frac{I}{2\pi}\int_0^{2\pi}\frac{Kcb}{Kct - bd}d\beta = \frac{\mu_0}{4\pi}\frac{I}{2\pi}\int_0^{2\pi}\frac{cb}{ct - \frac{bd}{K}}d\beta \qquad \text{(A.16)}$$

$$K = \cos\theta = \frac{d}{u} \Rightarrow u = \frac{d}{K} \qquad \text{(A.17)}$$

$$\int_{u=0}^{u=ct} \overline{E_{iu}}\, du = -\frac{\mu_0}{4\pi}\frac{I}{2\pi}\int_0^{2\pi}\int_{u=0}^{u=ct}\frac{cb}{ct-bdu}\, du\, d\beta = -\frac{30I}{2\pi}\int_0^{2\pi}\ln\left[\frac{1}{\left[2S^2\sin^2\left(\beta/2\right)\right]}\right]d\beta$$

$$= -I\left[60\ln\left(\sqrt{2}/S\right)\right] = -ZI$$

$$\Rightarrow Z = 60\ln\left(\sqrt{2}/S\right) \qquad \text{(A.18)}$$

APPENDIX B

Calculation of damping impedance for the multi-storey transmission tower model proposed by Ishii

General representation of a transmission line:

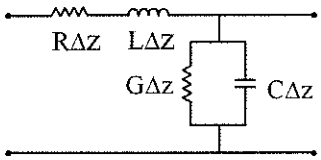

The propagation coefficient for a transmission line:

$$\gamma = \alpha + j\beta = \sqrt{(R + j\omega L)(G + j\omega C)} \qquad (B.1)$$

$\alpha = Re\ \{\gamma\}$ –attenuation coefficient

$\beta = Im\ \{\gamma\}$ – phase constant

In our case

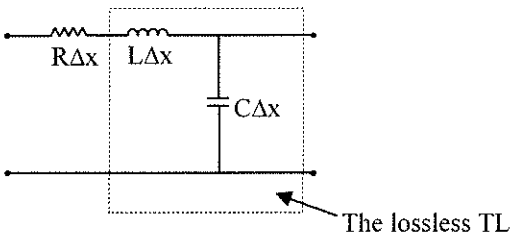

R is the damping resistance per unit length.

We have the case of a low-loss transmission line for which $R << \omega L$ [21]

$$\gamma = \sqrt{j^2\omega^2 \ LC\left(\frac{R}{j\omega \ L}+1\right)} = j\omega\sqrt{LC} \ \sqrt{\frac{R}{j\omega \ L}+1} \approx j\omega\sqrt{LC} \ \left(\frac{R}{2j\omega \ L}+1\right)$$
$$\approx \frac{R}{2\sqrt{L/C}} + j\omega\sqrt{LC} \qquad \text{(B.2)}$$

$$Z_t = \sqrt{L/C} \qquad \text{(B.3)}$$

$$\alpha = Re\{\gamma\} = \frac{R}{2\sqrt{L/C}} \qquad \text{(B.4)}$$

attenuation factor: $\gamma = e^{-\alpha x} = e^{-\frac{R}{2Z_t}x}$ where R is the series resistance per unit length

$$\Rightarrow R = -\frac{2Z_t \ln\gamma}{x} \quad [\Omega/m] \qquad \text{(B.5)}$$

APPENDIX C

Derivation of equivalent radius formula for n parallel conductors

Equivalent radius of a multi-conductor system is calculated using the formula of the total surge impedance of n parallel cylinders:

$$\frac{1}{Z_{T,n}} = \frac{1}{Z_1} + \frac{1}{Z_2} + \cdots + \frac{1}{Z_n} = \frac{n}{Z_1}; \quad (Z_1 = Z_2 = \cdots = Z_n) \tag{C.1}$$

$$Z_{T,n} = \frac{Z_1}{n} = \frac{1}{n}\left(Z_{T,11} + Z_{T,12} + \cdots + Z_{T,1n}\right) \tag{C.2}$$

where $Z_{T,kk} = 60\left(\ln\frac{2\sqrt{2}h}{r} - 2\right)$ - the self surge impedance of the k^{th} cylinder

$Z_{T,kl} = 60\left(\ln\frac{2\sqrt{2}h}{R_{kl}} - 2\right)$ - the mutual surge impedance between the k^{th} and l^{th} cylinder

The equivalent radius for two parallel conductors (n=2)

$$Z_{T,2} = \frac{1}{2}\left(Z_{T,11} + Z_{T,12}\right) \tag{C.3}$$

$$Z_{T,11} = 60\left(\ln\frac{2\sqrt{2}h}{r} - 2\right) \tag{C.4}$$

$$Z_{T,12} = 60\left(\ln\frac{2\sqrt{2}h}{R} - 2\right) \tag{C.5}$$

$$Z_{T,2} = \frac{60}{2}\left(\ln\frac{2\sqrt{2}h}{r} - 2 + \ln\frac{2\sqrt{2}h}{R} - 2\right) = \frac{60}{2}\left[\ln\frac{\left(2\sqrt{2}h\right)^2}{Rr} - 4\right]$$

$$= 60\left(\ln\frac{2\sqrt{2}h}{\sqrt{Rr}} - 2\right) = 60\left(\ln\frac{2\sqrt{2}h}{r_c} - 2\right) \Rightarrow r_{c2} = \sqrt{Rr}$$

(C.6)

The equivalent radius for three parallel conductors (n=3)

$$Z_{T,3} = \frac{1}{3}\left(Z_{T,11} + Z_{T,12} + Z_{T,13}\right) \tag{C.7}$$

$$Z_{T,11} = 60\left(\ln\frac{2\sqrt{2}h}{r} - 2\right) \tag{C.8}$$

$$Z_{T,12} = 60\left(\ln\frac{2\sqrt{2}h}{R_1} - 2\right) \tag{C.9}$$

$$Z_{T,13} = 60\left(\ln\frac{2\sqrt{2}h}{R_2} - 2\right); \quad R_1 = R_2 = R \tag{C.10}$$

$$Z_{T,3} = \frac{60}{3}\left[\ln\left(\frac{2\sqrt{2}h}{\sqrt[3]{rR_1R_2}}\right)^3 - 6\right] = 60\left(\ln\frac{2\sqrt{2}h}{r_c} - 2\right) \Rightarrow r_{c3} = \sqrt[3]{rR_1R_2} = r^{1/3}R^{2/3} \tag{C.11}$$

The equivalent radius for four parallel conductors (n=4)

$$Z_{T,4} = \frac{1}{4}\left(Z_{T,11} + Z_{T,12} + Z_{T,13} + Z_{T,14}\right) \tag{C.12}$$

$$Z_{T,11} = 60\left(\ln\frac{2\sqrt{2}h}{r} - 2\right) \tag{C.13}$$

$$Z_{T,12} = 60\left(\ln\frac{2\sqrt{2}h}{R_1} - 2\right) \tag{C.14}$$

$$Z_{T,13} = 60\left(\ln\frac{2\sqrt{2}h}{R_2} - 2\right); \quad R_2 = R\sqrt{2}$$

(C.15)

$$Z_{T,14} = 60\left(\ln\frac{2\sqrt{2}h}{R_3} - 2\right); \quad R_1 = R_3 = R \tag{C.16}$$

$$\begin{aligned} Z_{T,4} &= \frac{60}{4}\left[\ln\frac{\left(2\sqrt{2}h\right)^4}{rR_1R_2R_3} - 2\right] = 60\left[\frac{1}{4}\ln\frac{\left(2\sqrt{2}h\right)^4}{rR^3\sqrt{2}} - 2\right] \\ &= 60\left[\ln\frac{2\sqrt{2}h}{r^{1/4}R^{3/4}2^{1/8}} - 2\right] = 60\left(\ln\frac{2\sqrt{2}h}{r_c} - 2\right) \Rightarrow r_{c4} = 2^{1/8}r^{1/4}R^{3/4} \end{aligned} \tag{C.17}$$

The equivalent radius for n parallel conductors can be derived also from the equivalent bundle diameter formula:

$$d_{eq} = D\left(\frac{nd}{D}\right)^{1/n} \tag{C.18}$$

D is the bundle diameter and d is the conductor diameter.

In the case when the conductor and bundle radius varies, the expressions of r and R are:

$$r = r_T^{1/3}r_B^{2/3} \tag{C.19}$$

$$R = R_T^{1/3}R_B^{2/3} \tag{C.20}$$

r_T and r_B are the conductor radius at the top and base and R_T and R_B are the bundle radius at the top and base.

APPENDIX D

Impulse surge current generation

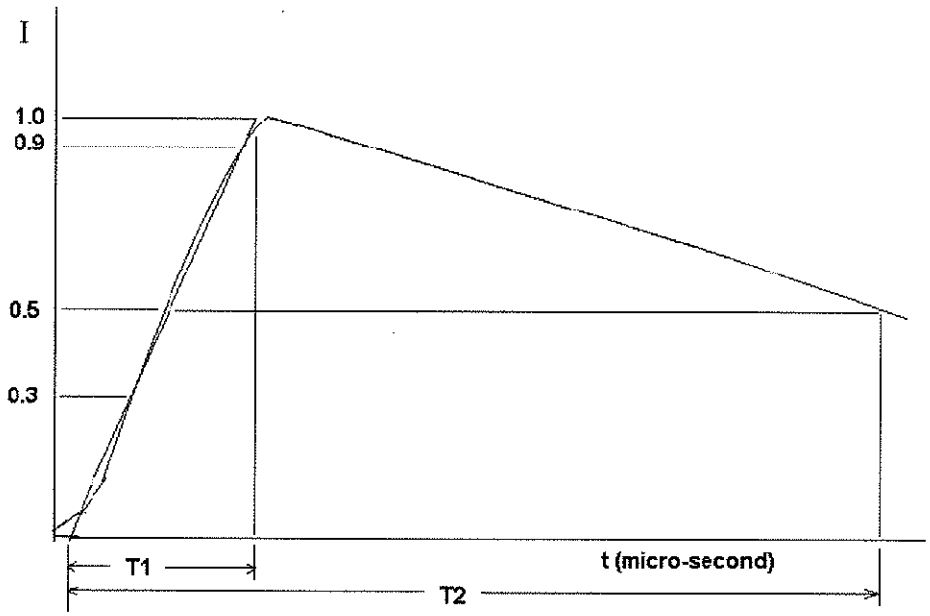

Fig. D-1 Standard impulse current waveform

The induced lightning surge is often represented by a double exponential impulse waveform. The impulse current is expressed as:

$$I(t)=I\left(e^{-at}-e^{-bt}\right) \qquad (D.1)$$

where a, b and I are constants.

The parameters characterizing the impulse wave shape are: front time, t_1, which is the time for the current to increase to the 0.9 of the peak value and tail time, t_2, which is the time from 0 to the time at which half of the peak value is reached on the wave tail.

The following formulas were used for calculating the impulse waveshape constants:

$$\frac{t_2}{t_1} = k - \frac{(k-1)\ln\left(\frac{k-1}{2}\right)}{\ln k} \qquad (D.2)$$

$$\text{where } k = \frac{b}{a}$$

$$a = \frac{1}{t_1}\frac{1}{k-1}\ln k \qquad (D.3)$$

$$b = ka = \frac{k}{t_1}\frac{1}{k-1}\ln k \qquad (D.4)$$

$$I = \frac{I_{max}}{k-1} k^{\frac{k}{k-1}} \qquad (D.5)$$

By choosing a particular double exponential surge waveform, I_{max} , t_1 and t_2 are known. K is determined from the plot of k versus t_2/ t_1 (D.2) and consequently, a, b and I are determined using (D.3), (D.4) and (D.5) and implemented in (D.1). [16]

The current impulse waveform characteristics used in the present study are presented in Table D-1.

Table D-1. The impulse current waveform characteristics

t_1/t_2 [μsec]	I_{max} [kA]	k	a	b	I [kA]
0.2/0.5	10	2.4	3126700	750400	32.03
1.5/51.75	50	270.16	13868	3746500	51.24
8/20	50	2.4	78167	187600	160

APPENDIX E

Simulation results of the field experiment presented by Hara in [5]

Simulation results of the field experiment presented by Hara in [5] at the tip of the four crossarm of the tower starting with the topmost one are shown in Plot 2, Plot 3, Plot 4 and Plot 5.

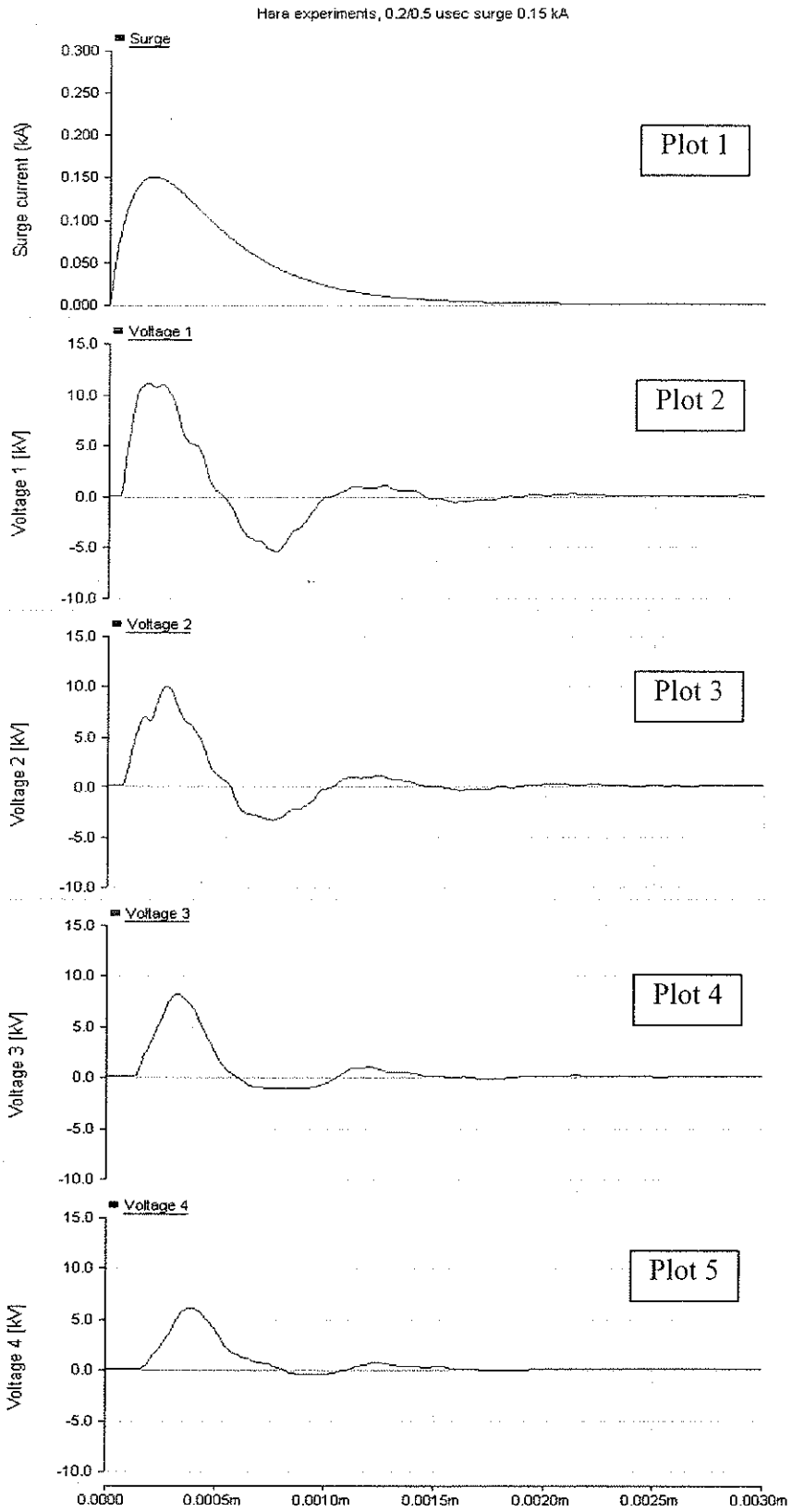

Fig. E-1 The response of a transmission tower to a 0.15 kA impulse current, with 200 nsec time to crest

APPENDIX F

The equivalent circuit for a transmission tower with two neighbouring towers equipped with phase and overhead ground wires

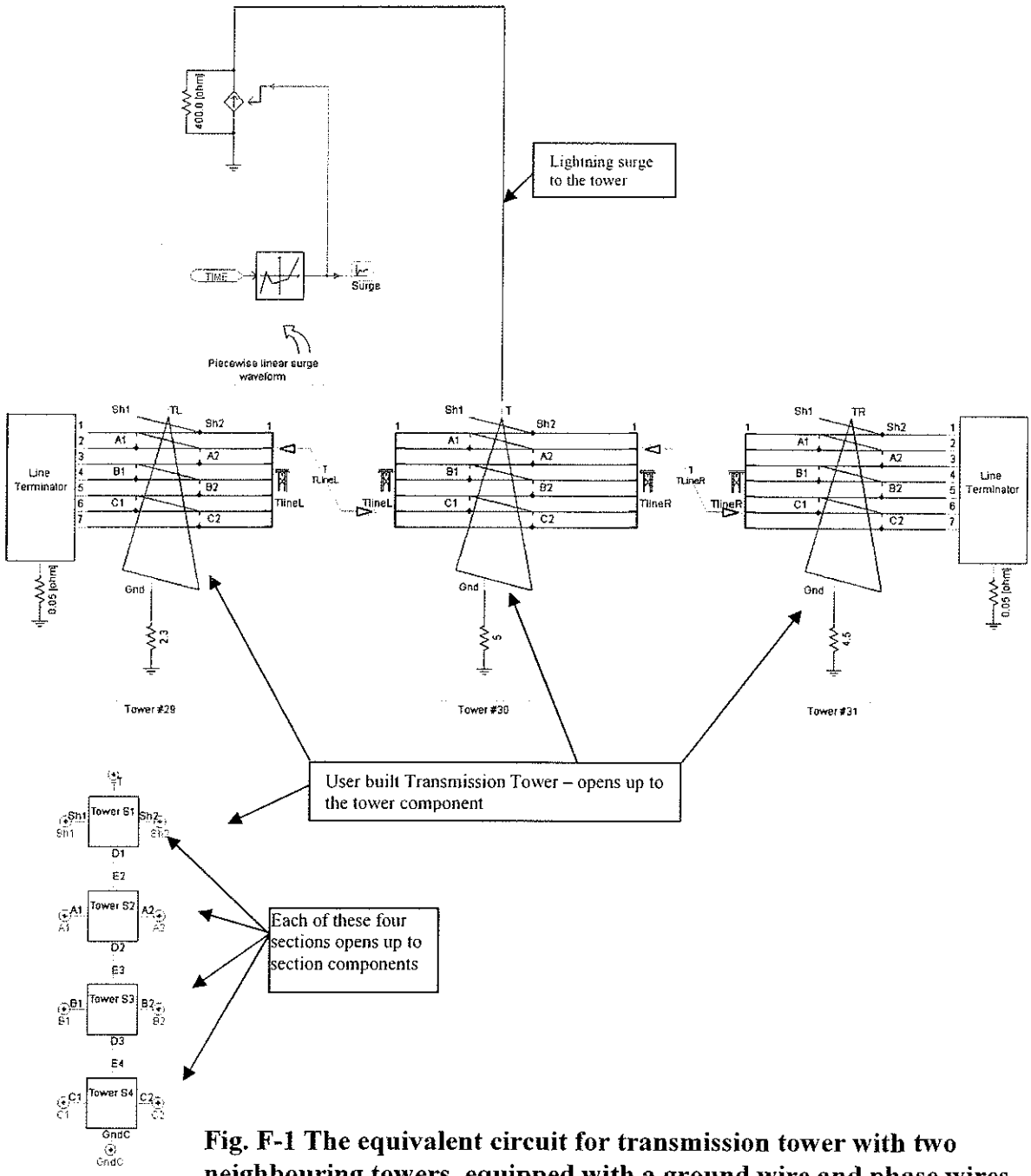

Fig. F-1 The equivalent circuit for transmission tower with two neighbouring towers, equipped with a ground wire and phase wires

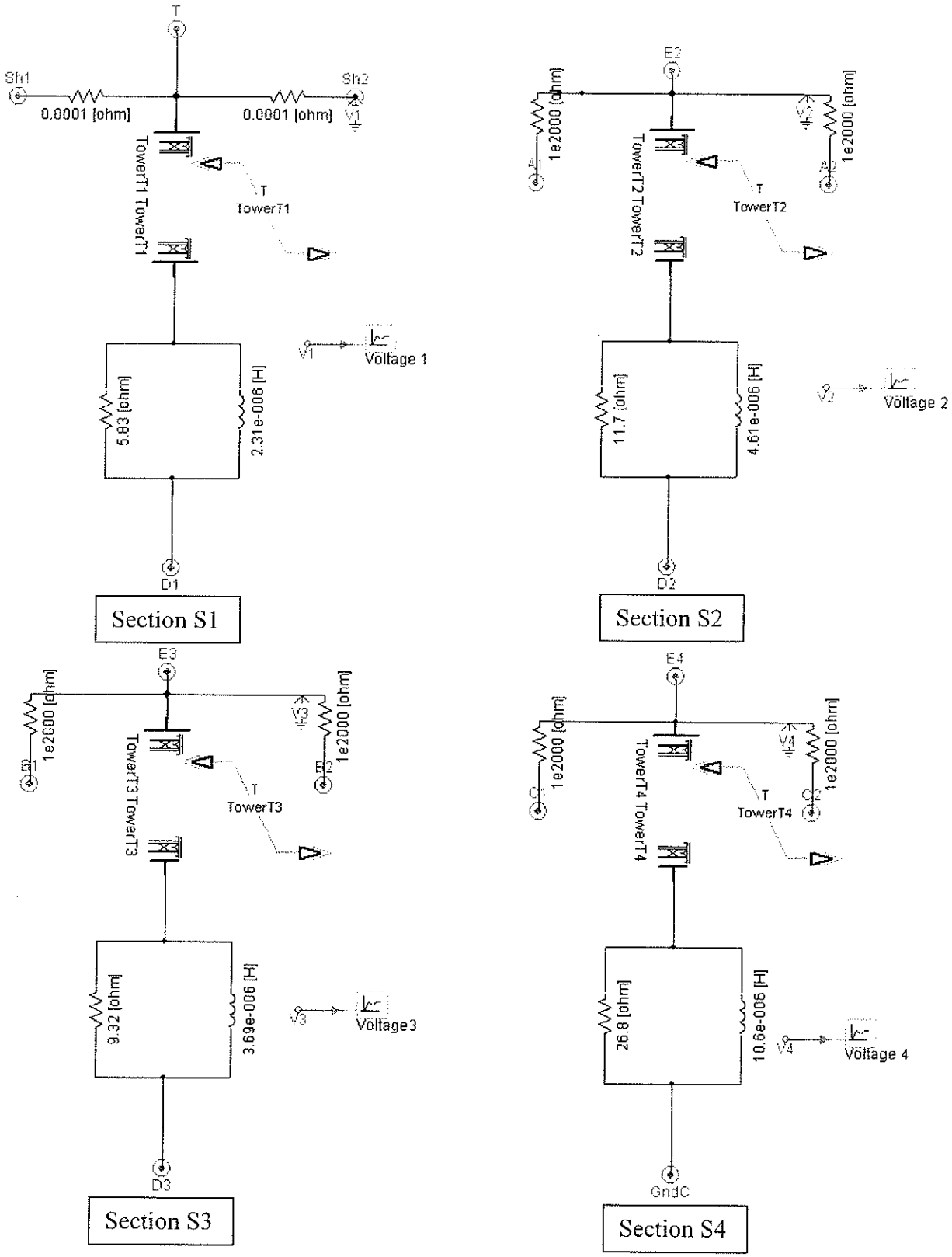

Fig. F-2 The four section components for Multi Storey model (Ishii model) transmission tower

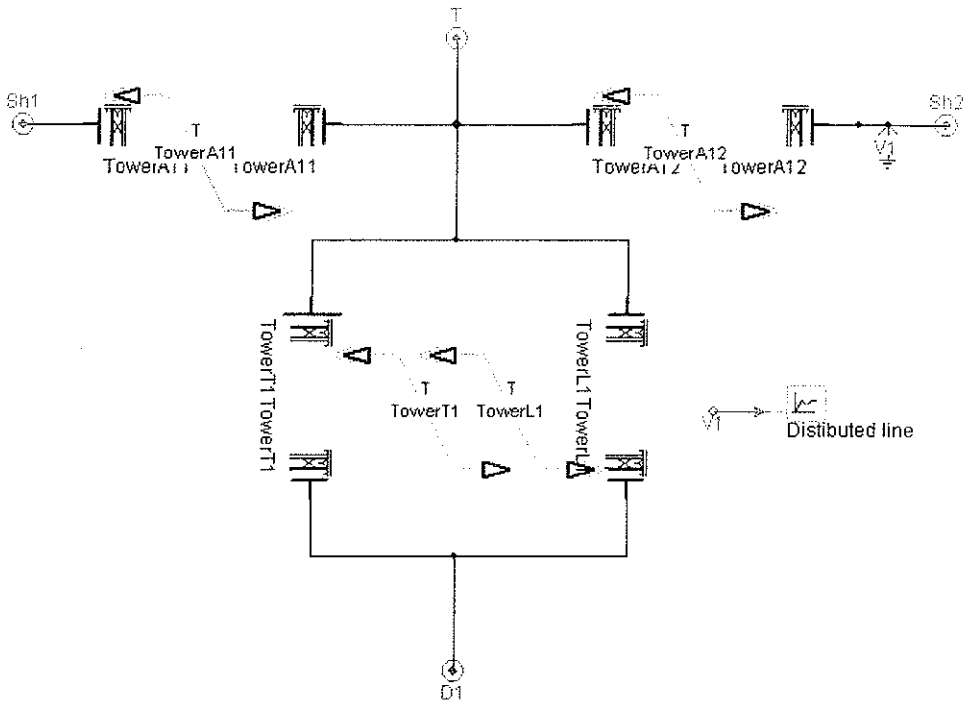

Section S1

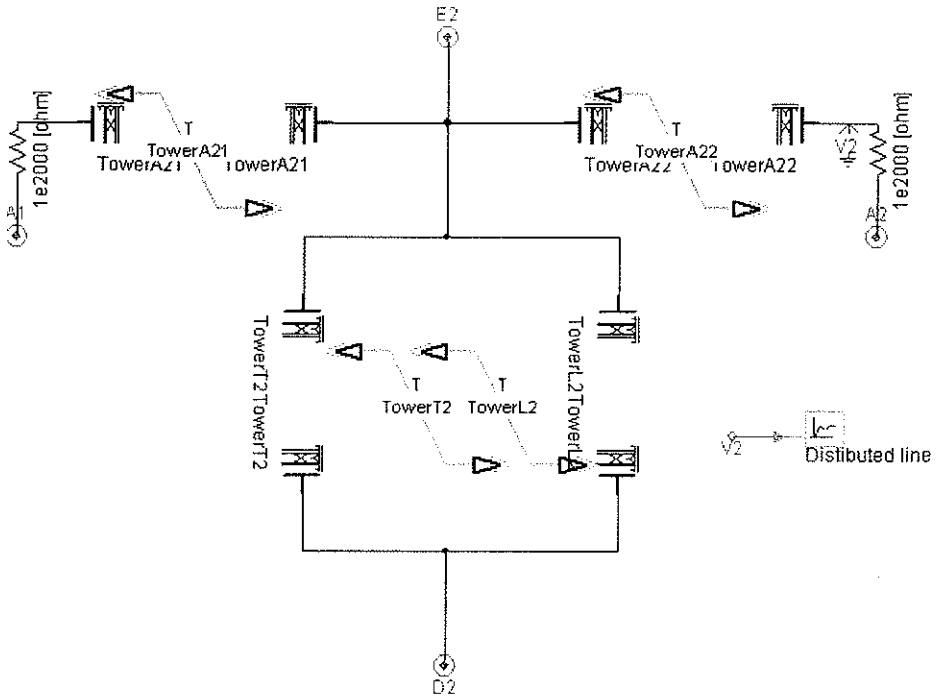

Section S2

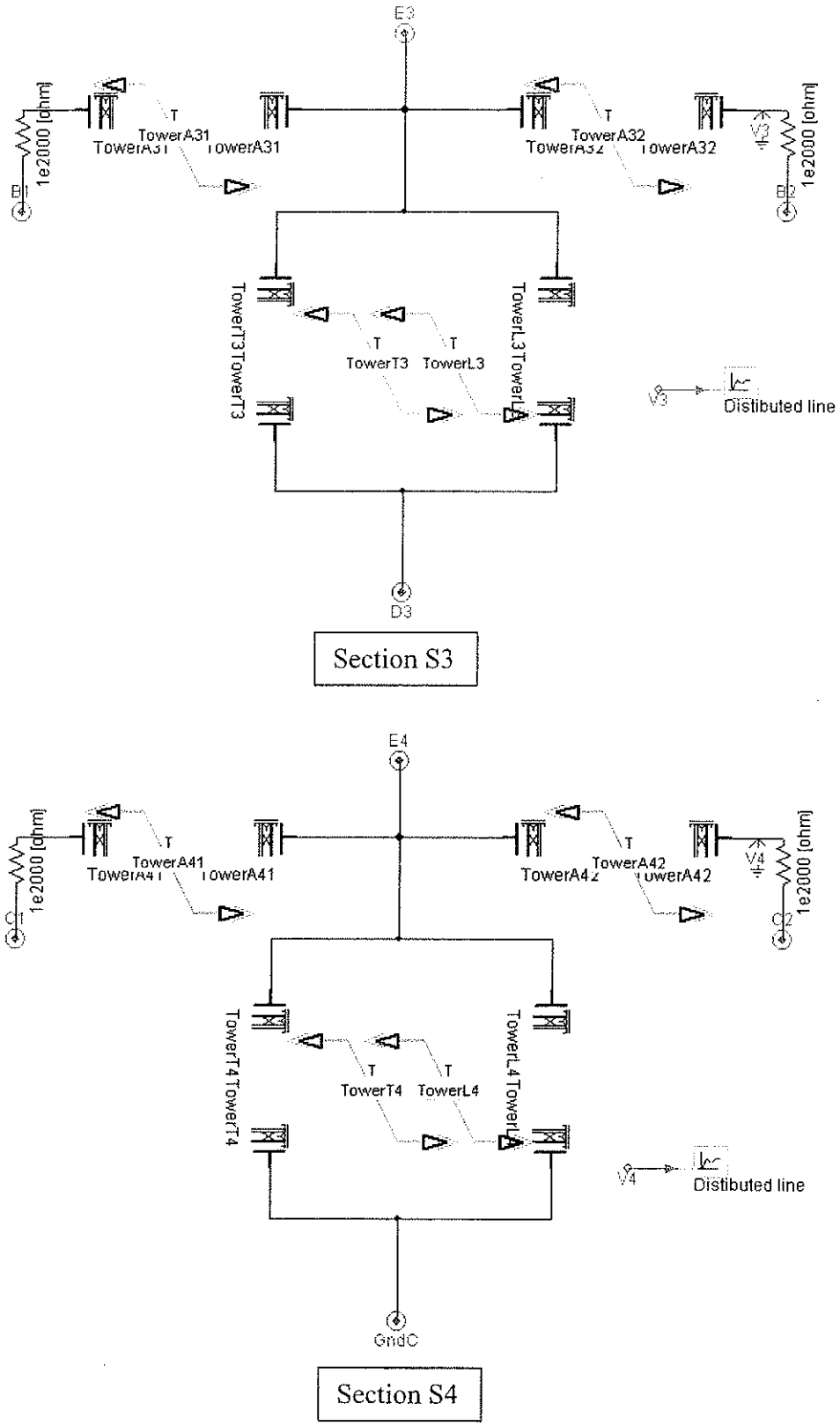

Fig. F-3 The four section components for Distributed Constant Line model (Hara model) transmission tower